# SPSD II

# SILICA RETENTION IN THE SCHELDT CONTINUUM AND ITS IMPACT ON COASTAL EUTROPHICATION (SISCO)

L. CHOU, W. VYVERMAN, P. REGNIER

ATMOSPHERE AND CLIMATE

**MARINE ECOSYSTEMS AND BIODIVERSITY**

TERRESTRIAL ECOSYSTEMS AND BIODIVERSITY

**NORTH SEA**
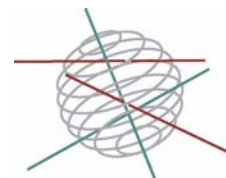
ANTARCTICA

BIODIVERSITY

**PART 2**
**GLOBAL CHANGE, ECOSYSTEMS AND BIODIVERSITY**

.be

Part 2:
Global change, Ecosystems and Biodiversity

FINAL REPORT

**SILICA RETENTION IN THE SCHELDT CONTINUUM AND
ITS IMPACT ON COASTAL EUTROPHICATION**

**(SISCO)**

**EV/17**

Lei Chou[1], Vincent Carbonnel[1], Laura Rebreanu[1], Jean-Pierre Vanderborght[1],
Nathalie Roevros[1], Michael Tsagaris[1], Claar van der Zee[1]

Marie Lionard[2], Koenraad Muylaert[2], Renaat Dasseville[2], Wim Vyverman[2]

Sandra Arndt[3], David Aguilera[3], Pierre Regnier[3]


[1]Université Libre de Bruxelles, Laboratoire d'Océanographie Chimique
et Géochimie des Eaux
Campus Plaine – CP 208, Bd du Triomphe, B-1050 Brussels, Belgium

[2]Universiteit Gent, Protistologie & Aquatische Ecologie
Krijgslaan 281 - S8, B-9000 Gent, Belgium

[3]Utrecht University, Faculty of Geosciences, Department of Earth Sciences  -
Geochemistry
P.O. Box 80.021, 3508 TA Utrecht, The Netherlands

BELGIAN SCIENCE POLICY    ULB    UNIVERSITEIT GENT    Universiteit Utrecht

## TABLE OF CONTENTS

## 1.    ABSTRACT

SISCO (Silica retention in the Scheldt continuum and its impact on coastal eutrophication) was an interdisciplinary consortium consisting of biologists, (bio)geochemists and hydrodynamic-biogeochemical modellers. The overall objective was to elucidate the biogeochemical cycling of silicon (Si) and its anthropogenic perturbation in the Scheldt continuum river-estuary-coastal zone. We aimed specifically at 1) identifying the sources and sinks of Si in the aquatic continuum, 2) quantifying the major processes controlling the biogeochemical behaviour of Si in the water column, 3) evaluating the early diagenesis of Si in order to determine the burial fluxes and internal recycling rates within the sediments, and 4) developing a Si module within an existing transport-reaction model to assess the Si fluxes carried by the Scheldt to the Southern Bight of the North Sea.  To achieve the aims, we applied an integrated approach combining 1) analyses of historical data, 2) field surveys and laboratory investigations, and 3) model development.

Analysis of historical chlorophyll a data (1995-2006) in the upper Scheldt estuary exhibited a high inter-annual variability of the phytoplankton biomass in summer, which could be attributed primarily to the flushing rates of the freshwater in the upper estuary. This points towards a strong hydrodynamic control on phytoplankton development in the upper estuary.

The intensive phytoplankton monitoring survey in 2003 showed that phytoplankton biomass not only differed between the tidal Rupel and Scheldt branches but also in their tributaries. The difference was ascribed to the smaller cross-section of the rivers in the Rupel basin, resulting in a higher water velocity and lower retention time of the water, which would limit phytoplankton development.

Study of the phytoplankton community composition along the river-estuarine-coastal zone continuum of the Scheldt revealed a succession from a riverine to a marine phytoplankton community. There is no single estuarine phytoplankton community but rather a succession of estuarine species along the salinity gradient.

Monthly monitoring survey of phytoplankton in 2003 in the Belgian coastal zone exhibited a pronounced spatio-temporal variability in the timing and magnitude of the spring bloom. The spring bloom started earlier in the western part of the Belgian coastal zone probably due to a more favourable mixing depth to photic depth ratio. The magnitude of the spring bloom was higher in the eastern part of the coastal zone, probably because of higher nitrogen (N) and phosphorus (P) inputs from the Scheldt.

Temporal evolution of dissolved and biogenic silica concentrations along the Scheldt freshwater estuary and in its tributaries was investigated during one year in 2003. In

the tributaries, dissolved silica (DSi) concentrations remained high and biogenic silica (BSi) concentrations were low throughout the year. In the freshwater estuary during summer however, DSi was completely consumed and BSi concentration increased. Mass balance calculations showed that silica consumption and retention in the freshwater estuary were important at a seasonal time-scale: from May to September, one third of the total amount of riverine silica was retained. The consumption and retention were high when discharge was low (and inversely), suggesting that silica retention would be of much less significance when annual fluxes were considered.

The longitudinal distribution of DSi and BSi along the salinity gradient in the Scheldt estuary was determined. The 1D-CONTRAST model was used to simulate the conservative mixing in the brackish estuary of DSi from the freshwater and the seawater end-members; existing datasets of DSi and salinity was used as inputs for boundary conditions. Comparison of the observed DSi profiles with the model outputs indicated a consumption of DSi in the brackish estuary in spring-summer and a conservative transport in winter. BSi were found to be closely linked with SPM in the brackish estuary, suggesting a mixing of marine particles with those of freshwater origin having different BSi contents.

The longitudinal distribution of BSi in surface sediments, as well as the vertical BSi and DSi profiles did not show clear seasonal trends. There was however a correlation between the type of sediment and the BSi content, suggesting a strong influence of the particle transport. BSi appeared in general to accumulate in the superficial layers of the sediments following the spring/summer diatom blooms.

Benthic DSi fluxes across the sediment–water interface were assessed based on the pore water DSi profiles, indicating generally low values, but in agreement with the existing data in the literature. Incubation of sediment cores yielded higher DSi fluxes towards the water column.

Silica dissolution kinetics was studied during long-term laboratory experiments using sediments from the Scheldt continuum. The dissolution rates of Si were relatively low for surface sediments and at depth, but increased in the first few centimetres. Our results showed that only a small fraction of the total BSi present in the sediments had dissolved even after several months.

A fully coupled two-dimensional, hydrodynamic and reactive transport model was developed within the MIKE 21-ECOLab simulation environment to describe the pelagic silica dynamics along the Scheldt continuum. The model extended from the upper tidal river and its tributaries to the southern Bight of the North Sea. A transient, vertically resolved, analytical model for the early diagenesis of Si was in addition developed to quantify the importance of benthic-pelagic coupling in estuarine and coastal biogeochemical silica cycling.

Model simulations showed that the area-integrated deposition of biogenic silica in the tidal freshwater reaches of the Scheldt estuary was driven by the combined influence of pelagic production and river discharge. Overall, the riverine input exceeded the diffusive silica flux by about two orders of magnitude. The benthic recycling of silica would sustain only a small fraction (<1%) of the total pelagic primary production in the Scheldt estuary and the benthic-pelagic coupling would thus be of minor importance on the system scale.

Key words: Diatoms, dissolved Si, biogenic Si, biogeochemical cycling of Si, phytoplankton dynamics, pigments, Scheldt estuary, Belgian coastal zone, freshwater estuary, diagenesis of Si, reactive transport modelling

## 2. INTRODUCTION

Diatoms (Bacillariophyta) are the major component of the spring phytoplankton blooms in both freshwater and marine ecosystems. They are responsible for about half the primary production in the world's oceans (Tréguer & Pondaven, 2000). Diatoms tend to dominate the 'new production' in marine ecosystems. Due to their large size, they are grazed upon by the macrozooplankton, which in turn serve as a direct food source for higher trophic levels such as commercially exploitable fish species. Diatom production is also closely linked to the formation of fast sinking particles which play a major role in exporting organic carbon to deep ocean waters and thus in sequestering anthropogenic $CO_2$ (Smetacek, 1998; Tréguer & Pondaven, 2000). The "regenerated production" is dominated by the pico- and nano-phytoplankton, which form the base of a longer food chain. Contrary to the new production, this regenerated production is less efficiently transferred through the food web and contributes little to export of organic carbon to the ocean's interior.

Unlike other algae, diatom growth requires, in addition to the essential nutrients such as nitrogen (N) and phosphorus (P), large amounts of dissolved silicates (DSi) which forms the rigid algal cell wall or frustule, accounting for half the cell's dry weight. The biogeochemical cycling of DSi in aquatic systems is thus of environmental importance in structuring biological communities. The essential difference in the behaviour between N, P and Si is their rate of regeneration and recycling. Silicon (Si) is released back to the water column via the dissolution of biogenic silica (BSi), which is a considerably slower process compared to the remineralisation of N and P.

Nutrients (N, P and Si) are introduced into the aquatic ecosystems via surface runoff by soil leaching and erosion and via atmospheric deposition. Before reaching the coastal zone, nutrients from land sources make their way through the aquatic continuum, consisting of rivers, lakes, wetlands and estuaries, where intense physico-chemical and biological processes occur. As a consequence, nutrients are transformed, immobilized or removed during their transit before entering the marine environment. The various components along the aquatic continuum may thus act as a series of efficient, selective and adaptive filters resulting in nutrient retention (Billen et al., 1991). The degree of retention varies from one nutrient to the other and depends on their recycling efficiency and their ability to be transferred to the sediments or to the atmosphere.

Estuaries, interfacing the terrestrial and the oceanic realms, are thus key transitional zones where intense biogeochemical processes take place, modifying nutrient fluxes from land to the sea. Not only dissolved, but also particulate matter undergoes changes within the freshwater-estuarine continuum.

The Scheldt is one of the major rivers entering the Southern Bight of the North Sea (SBNS). Its estuary, situated in a heavily populated and highly industrialised zone, is among the most perturbed ones in the world with extremely high nutrient and organic loadings. The concentration of N and P nutrients reflects the strong anthropogenic perturbations with present-day mean freshwater values up to 600 µM of total dissolved N ($NO_3$ + $NO_2$ + $NH_4$) and 8 µM of $PO_4$. These values are more than one order of magnitude larger than the natural concentrations in unpolluted rivers. In contrast, the concentration values of DSi in freshwater during the winter (250 µM) are comparable to those observed in similar rivers of the temperate region (Chou and Wollast, 2006) .

The increase of N and P inputs by the various estuaries bordering the North Sea, and the decrease of DSi due to eutrophication of the river system, have significantly modified the phytoplankton succession in the adjacent coastal zone (Lancelot et al., 1987; Cadée and Hegeman, 1991a,b; Billen et al., 1991; Rousseau et al., 2002). The early spring diatom bloom in the SBNS has been drastically reduced and replaced by the excessive development of flagellates (Phaeocystis sp.). As a consequence, the food web is considerably reduced and the Phaeocystis residues form anaesthetic foams on the beaches, causing environmental concern (Lancelot, 1995).

According to Redfield et al. (1963), diatom growth requires Si:N and Si:P molar ratios of 1 and 16, respectively. Analysis of long term trends of the ratio of nutrients, delivered annually by the Scheldt basin at the entrance of the estuarine zone, indicated values of Si:N ratio below 1 since the mid 1960's (Billen et al., 2005). The Si:P ratio also declined rapidly since the 1950's reaching values below the Redfield ratio by the late 1960's, and began to increase again since the 1990's due to the decreased P loading (Billen et al., 2005).

Billen et al. (2005) evaluated the nutrient fluxes and water quality in the drainage network of the Scheldt basin during the past five decades. Analysis of data on DSi concentrations available for a station, situated at about km 60 to the sea, showed a distinct decreasing trend at least during the last 30 years. The authors interpreted this trend as the result of higher Si retention due to increased diatom production in the cleaner drainage network upstream.

The change in the relative delivery of nutrients in river discharge leading to the modification of phytoplankton species composition has also been reported for the Baltic and Black Seas (Humborg et al., 2000), and other aquatic environments (Conley et al., 1993). There is furthermore a growing concern that large-scale alterations on land, such as river damming and river diversion, could lead to severe reductions of DSi input to the sea and cause dramatic impact on aquatic food webs in coastal marine environments (Ittekot et al., 2000). The biogeochemical fluxes of Si

deserve thus a better quantification in order to understand its role in coastal eutrophication.

Within this context, an interdisciplinary consortium composed of biologists, geochemists and modellers was formed to carry out the SISCO (Silica retention in the Scheldt continuum and its impact on coastal eutrophication) project. The overall objective was to elucidate the biogeochemical cycling of Si and its anthropogenic perturbation in the Scheldt continuum river-estuary-coastal zone. We aimed specifically at 1) identifying the sources and sinks of Si in the aquatic continuum, 2) quantifying the major processes controlling the biogeochemical behaviour of Si in the water column, 3) evaluating the early diagenesis of Si in order to determine the burial fluxes and internal recycling rates within the sediments, and 4) developing a Si module within an existing transport-reaction model to assess the Si fluxes carried by the Scheldt to the Southern Bight of the North Sea. To achieve the aims, our approach combined 1) analyses of historical data, 2) field surveys and laboratory investigations, and 3) model development.

The present report presents and discusses the main results obtained by the SISCO project. It focuses on the pelagic and benthic processes and their coupling, which affect the silicon dynamics in the Scheldt continuum river-estuary-coastal zone. Biogeochemical fluxes of Si are evaluated based on field observations and model simulations. The model developed within SISCO is tested for its applicability to quantify fully transient nutrient fluxes along the continuum as a support for marine sustainable development policy makers.

## 3. MATERIAL AND METHODS

### 3.1 Field study area : The Scheldt continuum river-estuary-coastal zone

The Scheldt River and its tributaries drain an area of 21 580 km$^2$ in northern France, western Belgium and the southwestern Netherlands. Its estuary is a strong tidal estuary with a mean annual river discharge of 3.8 km$^3$ yr$^{-1}$ (Wollast, 1988). There are very large seasonal fluctuations of the freshwater discharge with mean minimal values of 20 m$^3$ s$^{-1}$ to maximal values exceeding 350 m$^3$ s$^{-1}$. The tidal amplitude at the mouth is about 4 m allowing an input of 1 x 10$^9$ m$^3$ per tide. During the same tidal period, the volume of freshwater leaving the estuary is only 6 x 10$^3$ m$^3$ per tide. The salt intrusion covers a distance of about 100 km from the mouth at Vlissingen and the tide is still close to 2 m at 160 km from the mouth, where tidal changes are blocked by a sluice near the city of Ghent (Figure 1). High water velocities and bottom friction are sufficient to mix efficiently the water column and little or no vertical stratification can be observed.
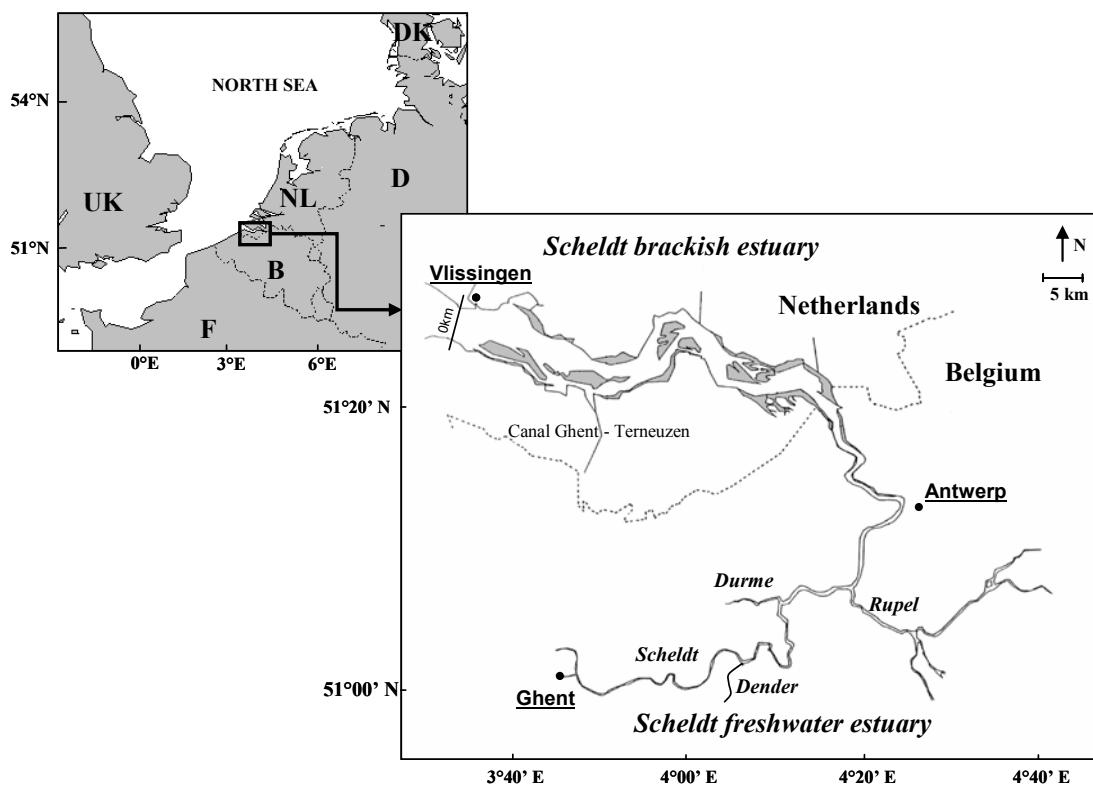


**Figure 1**. Map of the Scheldt estuary where its tributaries. The major cities are underlined and indicated by the black dots.

In the case of the Scheldt, the residence time of freshwater in the mixing zone may reach 2 to 3 months during the summer and is still about 1 month during the high flood period in winter and early spring. The turbidity is elevated in the freshwater present in the upper tidal estuary with a marked cycle of deposition and resuspension of particulate matter linked to tides. Beyond the turbidity maximum in the vicinity of salinity 5 psu, the suspended particulate matter content decreases progressively with increasing salinity.

The hydrographical basin of the Scheldt includes one of the most heavily populated regions of Europe, where highly diversified industrial activity has developed. As a result, the whole catchment has been heavily polluted until the mid 1970's, when degradation of water quality reached its peak due to the continuous increase of nutrient and organic matter inputs. The lack of wastewater treatment, especially in the upstream zones, was an important factor contributing to this degradation. The estuary was particularly affected by domestic and industrial inputs from Brussels, Antwerp and Ghent areas. Since then, better management of industrial and domestic wastewater point sources has led to a progressive improvement of the environmental conditions in the estuary. Billen et al. (2005) and Soetaert et al. (2006) provide two recent comprehensive reviews of this long-term evolution.

The Scheldt estuary comprises important freshwater reaches where the highest (diatom-dominated) phytoplankton biomass and production of the estuary were observed (Muylaert et al., 2005; Van Damme et al., 2005). This suggests significant DSi consumption, possibly down to limiting DSi levels in summer (Muylaert et al., 2001). The Scheldt discharges in the Southern Bight of the North Sea where DSi is possibly limiting in spring/summer (Van der Zee and Chou, 2005). There, DSi drives the extent of the early spring diatom bloom, while the excess of dissolved inorganic nitrogen (DIN) stimulates a subsequent massive development of flagellates (Phaeocystis sp.) that alters both the food web and the environment (Lancelot, 1995).

During the SISCO project, we conducted field studies from the freshwater tidal reaches through the brackish estuary to the coastal plume zone to investigate the biogeochemistry of silicon and associated elements. Intensive monitoring surveys were conducted during one year in the freshwater tidal estuary and seasonal campaigns on board the RV Belgica were carried out in the brackish estuary and the Belgian coastal zone.

### 3.1.1  Sampling in the freshwater tidal estuary

The freshwater tidal Scheldt estuary stretches from near Antwerp to Ghent. It also includes the River Rupel and the downstream parts of its four tributaries where the tidal influence decreases naturally (Figure 2). Weekly to monthly sampling in the freshwater reaches were carried at 9 stations during one year from March 2003 to February 2004. Measurements of DSi, BSi and other related parameters were carried out.
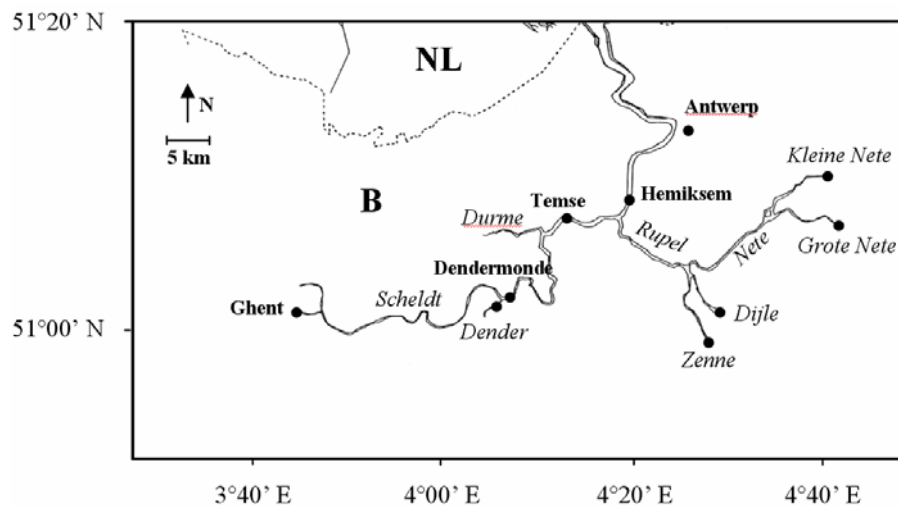


**Figure 2**. Sampling area of the Scheldt freshwater tidal estuary.
The sampling points are indicated by the black dots. The names of the rivers are indicated in italics. The sampling stations at Ghent, Dender, Zenne, Dijle, Grote Nete and Kleine Nete correspond to the tidal limits of the estuary.

### 3.1.2  Sampling in the brackish estuary and the Belgian coastal zone

#### 3.1.2.1  Water column

Seasonal campaigns were conducted on board the RV Belgica during 3 years (2003-2005) in the brackish estuary and the Belgian coastal zone (BCZ) to investigate the temporal and spatial evolution along the salinity gradient of DSi, BSi and associated elements in the water column. The fixed sampling stations are indicated in Figure 3. Additional stations were sampled depending on the salinity.

During the year of 2003, monthly sampling of water samples at 10 stations in the BCZ was also carried out on board the RV Zeeleeuw to investigate the seasonal cycling of nutrients and phytoplankton dynamics in the Southern Bight of the North Sea (Figure 3). This part of the North Sea is highly influenced by the eutrophied rivers Scheldt and Rhine/Meuse, and by oceanic water flowing from the Atlantic through the Channel into the North Sea. The 10 stations can be grouped along three

near shore-offshore transects: one located close to the mouth of the Scheldt (stations 700, B07, 710 and 780), a second one near the city of Oostende (stations 130, 230 and 330) and the third most southern transect near Nieuwpoort (stations 120, 215 and ZG02).
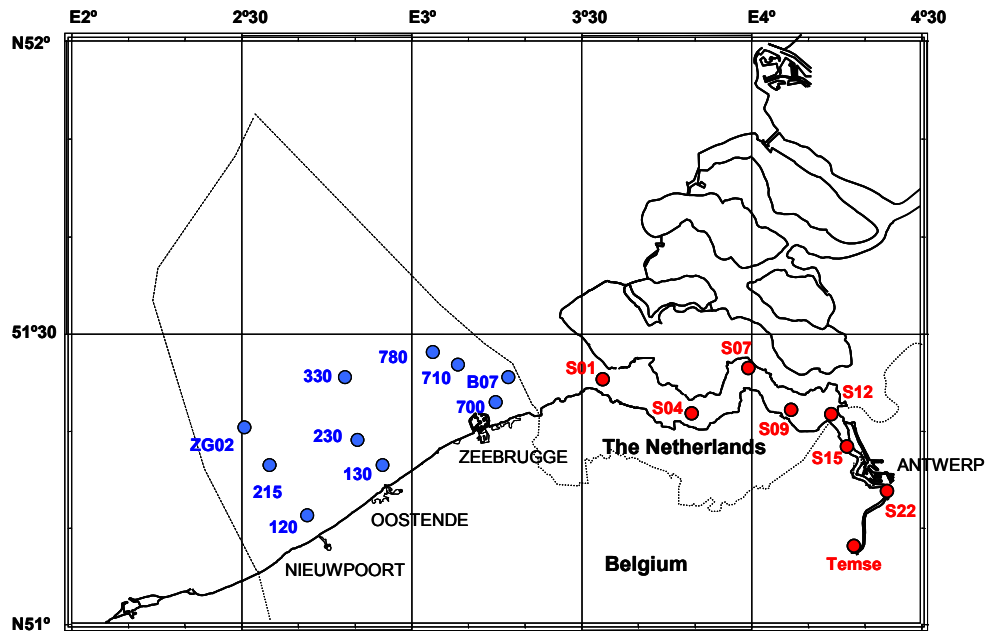


**Figure 3**. Sampling stations in the Scheldt brackish estuary (red dots) and in the Belgian coastal zone (blue dots).

### 3.1.2.2  Sediments

During the Belgica cruises, in addition to water samples, sediments were collected seasonally in 2004, 2005 and 2006 at a range of sites (Figure 3). Box cores were obtained at four stations located respectively, in the upper, less saline part of the estuary (station S22), in the maximum turbidity zone (station S15), at the mouth of the estuary (station S01), and in the coastal zone (station 230).

The Boxcorer was sub-sampled using Plexiglas tubes of 4.5 cm diameter and 30 cm height. These samples were either analysed for their content in BSi and DSi or used for direct measurements of the DSi fluxes across the sediment–water interface via incubation experiments. Surface sediments were also collected along a salinity transect across the estuary by means of a Reineck corer and only the first 3 to 5 mm were sampled.

## 3.2 Laboratory studies

### 3.2.1 Incubation experiments of sediment cores

In order to measure the fluxes of DSi across the sediment–water interface incubation experiments were carried out using the entire sediment cores collected in 2005 and 2006. The experiments were either conducted on board the ship, on freshly sampled cores, for up to 72 hours, or in the laboratory on previously frozen cores, for longer periods of time (up to 3 months) and the release of DSi to the overlying water was followed as function of time.
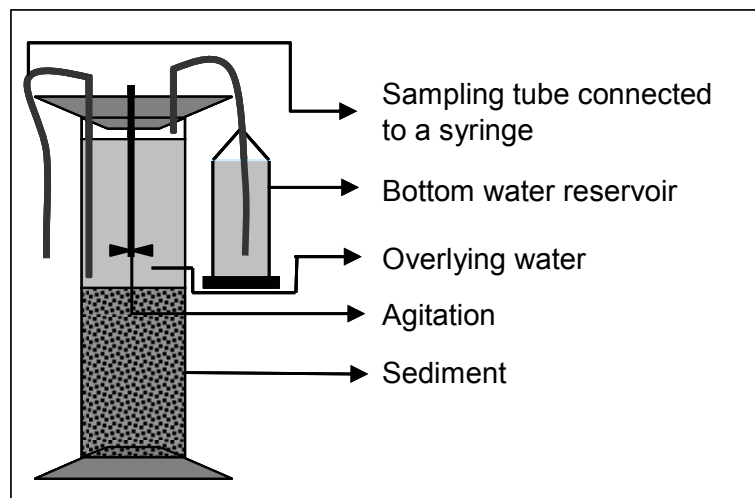


**Figure 4**. Schematic diagramme showing the set-up of the incubation experiments of sediment cores.

The experimental set-up is shown in Figure 4. The sealed cores were placed in the dark, at the in-situ temperature for a given period of time. The overlying water was continuously stirred, in order to ensure the homogeneity of the water column and to avoid the formation of an important diffusive layer at the sediment–water interface. The stirring rate was carefully controlled to avoid the re-suspension of the sediments. Water samples were taken at regular time intervals, with a higher frequency at the beginning of the experiment. The samples were directly filtered on 0.2 μm filter (cellulose acetate) and the volume withdrawn was automatically replaced by bottom water (Figure 4), to keep the total volume constant throughout the experience. The bottom water was collected at the same time or immediately after the boxcorer, and it was filtered on 0.45 μm filter (cellulose acetate or nitrate) prior to the experiment. Sub-samples were analysed for DSi according to the method described in §3.3.4.

### 3.2.2 Dissolution experiments

Experiments on dissolution kinetics of BSi were carried out in batch reactors on a reference material, diatomaceous earth, and on sediments collected in 2004 from three different locations and at several depths, for four salinity values (Table 1). The solid to solution ratio was of 2.5 g $l^{-1}$, and the temperature was kept constant at 25 ± 0.5 °C. The solutions used were either Milli-Q water (0 salinity) or artificial seawater (NaCl, $MgSO_4$), and the pH was maintained at 8 ± 0.2 by means of a $NaHCO_3$ buffer. During the first 9 days of each experiment, the tubes were continuously agitated, and afterwards they were hand-shaken daily. Samples were taken at different time intervals, filtered on 0.2 μm filters and analysed for DSi and Al respectively by the molybdate-blue colorimetric method and by ICP-OES (§3.3.4).

**Table 1**. Locations and depths of the sediments used for the dissolution experiments. Sampling dates of the cores are also given, as well as the working salinity values, which correspond to those characteristic of the site.

| Station | Location | Depth (cm) | Salinity (psu) | Month in 2004 |
|---------|----------|------------|----------------|----------------|
| 230 | Belgian coastal zone | 0.5, 1.5, 6.0 | 35 | September |
| S01 | Mouth of the estuary | 0.5, 4.5, 9.0, 13.0 | 35 | September |
| S15 | Zone of maximum turbidity | 0.5, 1.5, 13.0 | 0, 5, 15 | September |
| S01 | Mouth of the estuary | 0.5, 2.5, 4.5, 5.5, 13.0 | 35 | May |

## 3.3 Analytical

### 3.3.1 Phytoplankton

For identification and enumartion of phytoplankton, water samples were fixed in the field with Lugol's solution and post-fixed for long-term storage with formalin. Phytoplankton were identified up to species level and enumerated using an inverted microscope. A fixed number of 100 cells or colonies were counted per sample. For each month, the biovolume of at least 15 "units" of each species was measured in different samples. The phytoplankton biovolume was converted to carbon biomass using published conversion factors (Menden-Deuer & Lessard, 2000).

### 3.3.2 Pigments

For pigment analyses, a known volume of water was filtered over a GF/F filter. The filter was stored at -80°C until analysis. Pigments were identified and quantified using HPLC according to the protocol of Wright et al. (1991). The software CHEMTAX was used to estimate the contribution of major algal groups to total chlorophyll a from concentrations of accessory pigments (Mackey et al., 1996). Input ratios of accessory pigment to chlorophyll a for the major algal groups were obtained from the literature and from monospecific cultures of representatives of these algal groups in the Scheldt continuum.

### 3.3.3 Particulate organic carbon

Particulate organic carbon (POC) measurements were performed on particulate matter collected by filtration of seawater on precombusted (4 h, 500°C) GF/F filters. POC was measured using a Fisions NA-1500 elemental analyser after carbonate removal from the filters by strong acid fumes overnight. Certified reference stream sediment (STSD-2) from the Geological Survey of Canada was used for the calibration.

### 3.3.4 DSi, SPM and BSi in the water column

A known volume of water was vacuum filtered on a pre-weighed polycarbonate filter (Whatman Nuclepore, Ø 47 mm, 0.4 µm porosity). The filtrate was acidified with 2 M HCl (200 µl per 50 ml sample) and kept in the dark at 4°C until analysis. The samples were measured colorimetrically for DSi on a Skalar Auto-analyser following a method adapted from Grasshoff et al. (1983). The SPM collected on the filter was rinsed with Milli-Q water and dried overnight at 50°C. The filter was weighed again for the SPM determination by weight difference and the filter was kept for BSi analysis.

BSi was determined by a wet-alkaline method according to the scheme shown in Figure 5, modified from Ragueneau et al. (2005a). High amounts of lithogenic silica are present in the SPM of the freshwater Scheldt estuary (Bouezmarni and Wollast 2005). Thus, the aluminium released was used to correct for the concomitant dissolution of Si from lithogenic material (Ragueneau et al., 2005a). In addition, four steps were performed instead of two to increase the precision of the correction, and the SPM was not rinsed between the steps to reduce the time necessary for the digestion.
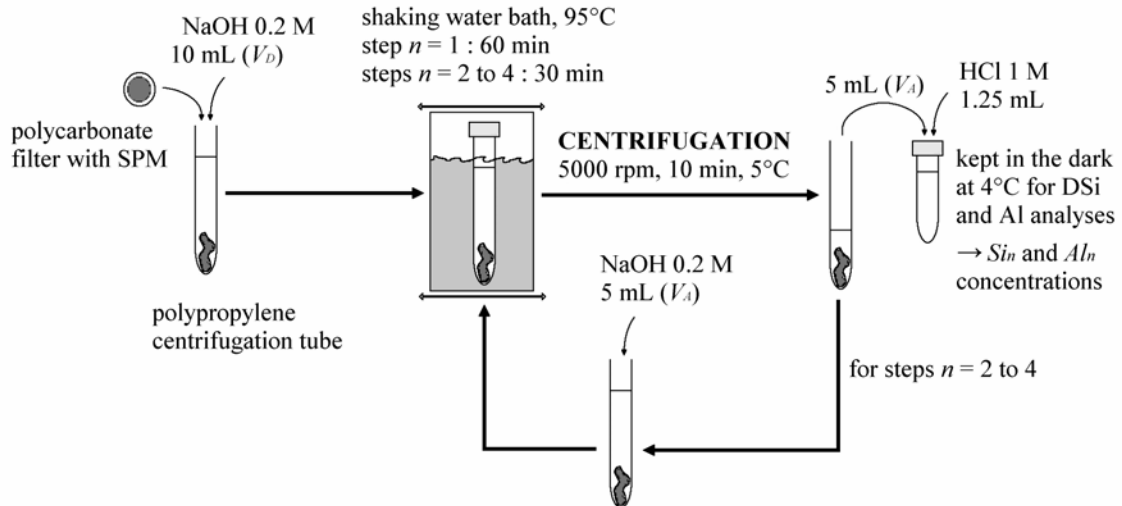
**Figure 5**. Scheme of the BSi digestion protocol.

The four aliquots were analysed for DSi and Al concentrations ($Si_n$ and $Al_n$, in µM), either both by ICP-OES (Inductively Coupled Plasma – Optic Emission Spectroscopy), or by colorimetry using a Skalar Auto-analyser for DSi as described previously and manually for dissolved Al following Dougan and Wilson (1974). The differences between the analytical methods were insignificant compared to the precision of the BSi determination. The following common assumptions are made: 1) all the BSi is dissolved during the first step, 2) all the Al measured is from the digestion of lithogenic material and 3) this latter material dissolves with a constant Si/Al ratio (designated here k) (Kamatani and Oku, 2000; Ragueneau et al., 2005a). Then the DSi and Al concentrations measured in the aliquots of each step n follow Eqn. 1:

$$Si_n = c_n \cdot \frac{BSi}{V_D \cdot d} + k \cdot Al_n \qquad \text{(Eqn. 1)}$$

With

$$c_n = \left( \frac{V_D - V_A}{V_D} \right)^{n-1} \qquad \text{(Eqn. 2)}$$

where BSi is the amount of BSi on the filter (in µmol), $V_D$ and $V_A$ the volumes (in liter) as defined in Figure 5 and d the dilution factor due to the addition of HCl (here 1.25). BSi (as well as k) can be calculated by a least-squares multiple regression on $Si_n$:

$$BSi = V_D \cdot d \cdot \frac{\left(\sum_{n=1}^{4} Al_n^2\right) \cdot \left(\sum_{n=1}^{4} c_n \cdot Si_n\right) - \left(\sum_{n=1}^{4} c_n \cdot Al_n\right) \cdot \left(\sum_{n=1}^{4} Si_n \cdot Al_n\right)}{\left(\sum_{n=1}^{4} c_n^2\right) \cdot \left(\sum_{n=1}^{4} Al_n^2\right) - \left(\sum_{n=1}^{4} c_n \cdot Al_n\right)^2} \qquad \text{(Eqn. 3)}$$

The three assumptions can be verified for natural samples; the recalculation of $Si_n$ following Eqn. 1 generally deviated by less than 1% from the measured value. The method has also been validated by tests using pure lithogenic (English kaolinite in Milli-Q or filtered seawater) and biogenic (diatom cultures) silica suspensions, and known mixtures of the two.

The concomitant variations between BSi and the chlorophyll a associated with diatoms (DiaChla) concentrations in the Dijle, Grote and Kleine Nete showed that the method for BSi determination allowed still the estimation of the very low concentrations of BSi in the water column and its low contents in the SPM. In the three rivers, the annual average BSi content in the SPM ranged only from 1.3% to 3.2% (expressed as mass percentages of $SiO_2$ containing 10% of water). However, the method was not applicable to the Zenne because in most cases BSi concentrations could not be determined, as negative values were retrieved from Eqn. 3 (data not shown). Kamatani and Oku (2000) attributed such apparent negative results to the dissolution of allophane minerals. In the Zenne, however, this apparent negative value might be due to the presence of particulate material brought by the untreated sewage waters from the city of Brussels.

### 3.3.5  BSi in the sediment and DSi in pore waters

All the sediment cores used for the BSi determination were treated on board, under nitrogen atmosphere. Before treatment they were stored at the sampling in-situ temperature, in the dark. The cores were cut into 1 to 2 cm slices and centrifuged in order to collect the interstitial waters, which were directly filtered on 0.2 μm Nucleopore filters.

The particulate phase as well as the surface sediments were oven-dried (50°C) for 24h to 72h and then homogenised with a mortar and a pestle, before analysis for their BSi content by a modified version of DeMaster's (1981) alkaline digestion technique. The digestion solution used was 0.2M NaOH, and the extraction was performed at 95°C, for 5 hours; sub-samples were collected after 2, 3, 4 and 5 hours. The observed extraction kinetics is interpreted as a result from a combination of rapidly dissolving amorphous Si, assimilated to biogenic silica, and more slowly dissolving crystalline silicates. The tangent to the released silica concentration vs.

time function is extrapolated to time zero and the concentration thus obtained – the y intercept – is used to estimate the mass of the most reactive silica phases responsible for the initial rapid release of Si on sediment exposure to the alkaline solution. Digestion sub-samples were analysed for dissolved silica by the molybdate-blue spectrophotometric method (Grasshoff et al., 1983), which is the method used for all DSi determinations (§3.3.4).

### 3.3.6 Si:C ratio in diatoms

In order to determine the Si:C ratios in diatoms of the Scheldt, cultures of two Cyclotella meneghiniana isolated from the Scheldt were performed in WC medium (Guillard and Lorenzen, 1972) at about 100 µE m$^{-2}$ s$^{-1}$ in incubators with a 14h:10h light:dark cycle at 13°C. Si/C ratios were determined twice, and each time triplicate cultures were performed. Cultures were filtered in parallel on Nuclepore polycarbonate 0.4 µm porosity filters for BSi and on precombusted Whatman GF/F filters for POC. BSi was measured with a method adapted from the one used for the natural waters (see §3.3.4): only the first digestion step was performed, during a longer time (about 3 hours) and no aluminium correction was done as there was no lithogenic silica in our culture medium. POC was measured according to the method described in §3.3.3.

## 3.4 Model description

### 3.4.1 Pelagic model

The estuarine hydrodynamics is described using the nested hydrodynamic model MIKE 21 NHD$^{©}$ (DHI). The model simulates unsteady two-dimensional flows in a vertically homogeneous water column. It solves simultaneously the depth-averaged Saint-Venant equations for barotropic flow. Figure 6 shows that three dynamically nested grids are used to cover the whole of the Scheldt estuary (Arndt et al., 2007; Arndt and Regnier, 2007). The model extension includes all major tributaries of the Scheldt, where reliable hydrodynamic boundary conditions can be specified. The spatial resolution is 33x33 m for the riverine estuary and the channel bend close to Antwerp, while the saline and brackish zones of the estuary are resolved with a grid spacing of 100x100 m. Flooding and drying of intertidal flats (ca. 11000 ha) is also taken into account. Boundary elevations which include all tidal harmonic constituents with amplitude larger than 3 cm (Regnier et al., 1998) are imposed at the estuarine mouth. Daily river discharge data (source: Flanders Hydraulic Research) are specified for all tributaries at the upstream limit of tidal propagation.
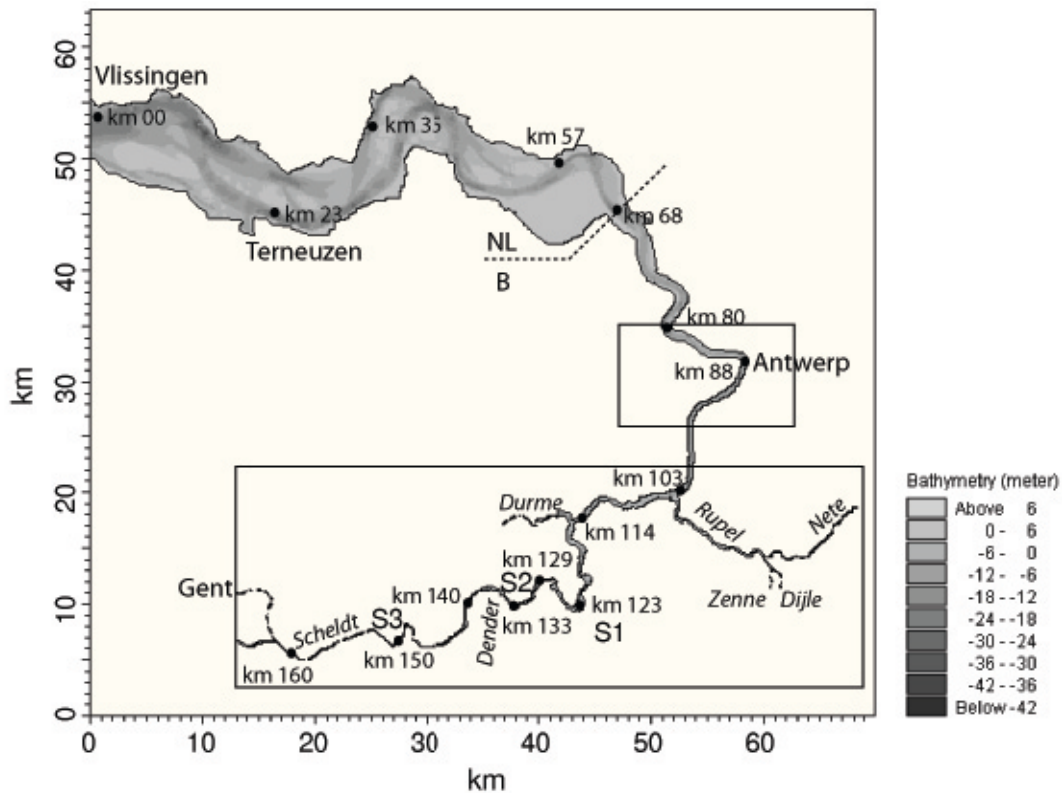
**Figure 6**. Map of the Scheldt estuary. From Arndt and Regnier (2007).

The model includes a fully-formulated suspended particulate matter (SPM) transport algorithm (Arndt et al., 2007). SPM is subject to advective and dispersive transport, as well as local mass exchange with the estuarine bed. The erosion and deposition fluxes are expressed according to the formulations of Ariathurai (1974), Partheniades (1962), and Einstein and Krone (1962). The deposition flux is proportional to the settling velocity, which depends directly on the diameter of suspended particles. The dynamic adaptation of the SPM diameter to processes such as deposition and erosion is calculated using the effective variable approach proposed by Wirtz and Eckhardt (1996) and Wirtz (1997).
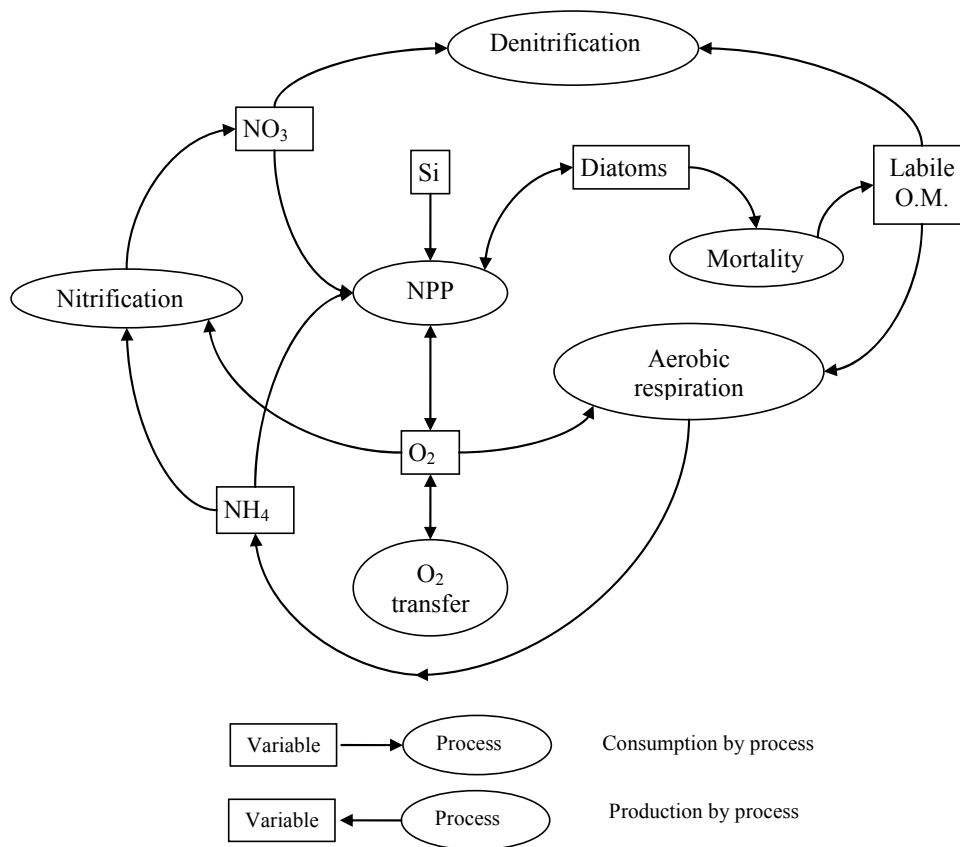
**Figure 7**. Sketch of the reaction network implemented in the model.
From Vanderborght et al. (2007).

The biogeochemical model is implemented within the ECOLab$^{©}$ environmental modelling tool and includes the following state variables: salinity, organic matter, oxygen, ammonium, nitrate, dissolved silica and diatom biomass. Figure 7 summarizes the reaction network built into the model. The kinetic formulations of the biogeochemical processes considered are similar to those implemented in the most recent version of the 1D-CONTRASTE model (Regnier and Steefel, 1999; Vanderborght et al., 2002). Major improvements consist in the incorporation of silica as an explicit model variable and the coupling between SPM dynamics, light penetration and primary production. Details on this coupling can be found in Vanderborght et al. (2007) and Arndt et al. (2007).

### 3.4.2 Benthic model

To cope with the full complexity of benthic processes, a transient, vertically resolved, numerical diagenetic model of silica is implemented within the knowledge-based biogeochemical reaction network simulator (Aguilera et al., 2005). In addition, for system-scale simulations, a robust, analytical and, therefore, cost-efficient method is developed as an alternative (Arndt and Regnier, 2007). It is a vertically resolved model which captures the transient dynamics of benthic dissolved silica (BDSI) and benthic biogenic silica (BBSI) and allows investigating the dynamics of benthic silica cycling on a seasonal time scale in response to a pelagic diatom bloom.

The processes considered in the analytical model are the dissolution, bioturbation, deposition, erosion and burial of biogenic silica. The model is based on the assumption that the depth profile of BBSI in the sediment follows an exponential decrease, which is cut off at a maximum depth in the sediment and normalized to the depth integrated biogenic silica content. The dissolution of BBSI leads to a build up of BDSI, which migrates in the sediment column. The simulation of BDSI depth profiles is based on the transient diagenetic equation for solute species (e.g. Berner, 1980).

### 3.4.3 Benthic-pelagic coupling

The benthic model is coupled to the two-dimensional pelagic model, and the total number of grid points for which vertically resolved benthic silica profiles is determined amounts to 56000. The deposition, resuspension and burial fluxes of BBSI are directly coupled to the local SPM dynamics. The release of dissolved silica through the sediment-water interface directly depends on the dynamic evolution of local concentration gradients between pelagic and benthic silica concentration. A complete description of both benthic and fully-coupled models is given in Arndt and Regnier (2007).

## 4. RESULTS AND DISCUSSION

### 4.1 Analysis of historical data

Chlorophyll a data collected between 1995 to 2006 in the upper Scheldt estuary were analysed to evaluate the factors that determine inter-annual variability in phytoplankton biomass in the upper Scheldt estuary. The chlorophyll a data for this analysis were collected in the framework of the OMES project ("Onderzoek naar Milieu-Effecten van het Sigma-plan"), coordinated by Prof. Meire (University Antwerp).

Two blooms were observed each year in the upper estuary: a spring bloom and a summer bloom (Figure 8). In general, the chlorophyll a maximum of the spring bloom was situated more upstream in the estuary than the summer bloom. This is in agreement with a previous study on phytoplankton seasonal succession in the upper Scheldt estuary carried out in 1996 (Muylaert et al., 2000, 2005). In these previous studies, it was demonstrated that the spring bloom was imported from the river Scheldt while the summer bloom developed within the estuary. Comparison of chlorophyll concentrations between the river and the estuary throughout the period 1995-2006 indicated that this is an annually recurring phenomenon.

Maximum chlorophyll a concentrations tended to be higher during the summer bloom than during the spring bloom. Chlorophyll a measurements of up to 700 µg were recorded (in 2003). This is very high for estuarine ecosystems and more than an order of magnitude higher than the maximum chlorophyll a concentrations being reported for the brackish reaches of the Scheldt estuary (Soetaert et al., 1994). Chlorophyll a concentration during summer was not always that high and the mean summer chlorophyll a concentration displayed a strong inter-annual variability. Chlorophyll a concentrations were particularly high in 1997, 2003 and 2004. This interannual variability was primarily correlated with the flushing rate of the water in the upper estuary. Higher flushing rates in summer were associated with lower chlorophyll a concentrations (Pearson correlation coefficient: $r = -0.69$, $n = 8$). This points to a strong hydrodynamical control on phytoplankton development in the upper estuary. The consequence of this is that future climate-related changes in rainfall (e.g. reduced rainfall in summer due to global warming) or human alterations in the hydrology of the Scheldt basin (e.g. diversion of water from the Scheldt River to Terneuzen) may have important consequences for the intensity of algal blooms in the upper Scheldt estuary.
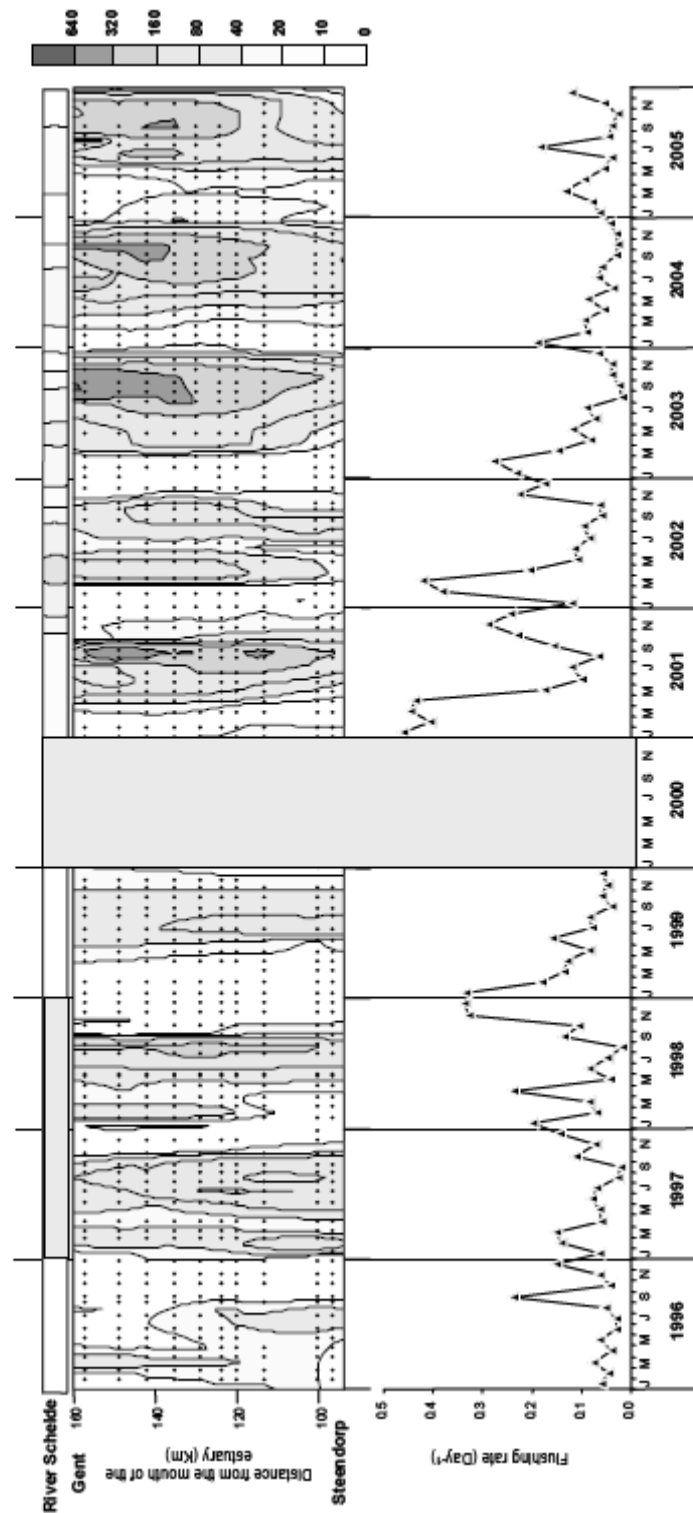
**Figure 8**. Left: spatio-temporal evolution of chlorophyll a concentration in the upper Scheldt estuary between 1995 and 2006 (X-axis represents time, Y-axis represents distance from the mouth of the estuary, grey-scale level is equivalent with chlorophyll
a concentration and black dots represent sampling events in space and time).
Right: temporal evolution of the flushing rate of the freshwater tidal zone between 1995 and 2006 (flushing rate was calculated as discharge/volume).

No relation was observed between the mean summer chlorophyll a concentration in the upper estuary and the temperature, irradiance or water turbidity (as indicated by SPM or suspended particulate matter concentrations). SPM concentrations even tended to be higher during years with high chlorophyll a concentrations. The mean summer mean summer chlorophyll a concentration in the upper estuary was also not correlated with the mean summer DSi concentration, nor with the minimum summer DSi concentration. This indicates that the intensity of the phytoplankton summer bloom in the upper estuary not necessarily influences DSi transport through the estuary.

## 4.2    Phytoplankton dynamics

### 4.2.1 The use of pigments as a proxy for phytoplankton biomass and community composition in the upper Scheldt estuary

In 2002, phytoplankton biomass and community composition were assessed using microscopy and HPLC-CHEMTAX in a set of 160 samples. The samples were collected monthly along a longitudinal transect in the upper Scheldt estuary, between Gent and the Dutch-Belgian border. Sampling was carried out in cooperation with the OMES study.

Both methods revealed the same general spatio-temporal trends in phytoplankton biomass and community composition. Both methods revealed the occurrence of two phytoplankton blooms: a spring bloom and a summer bloom (Figure 9). The spring bloom was situated more upstream in the estuary than the summer bloom.  Diatoms were dominant throughout the year although chlorophytes attained a high biomass in the most upstream stations in summer. These observations are in agreement with a previous study in the upper Scheldt estuary (Muylaert et al., 2000).

Despite the same general trends in the microscopical and the HPLC-CHEMTAX data, two marked discrepancies were observed. First, when phytoplankton biomass was low, the carbon-to-chlorophyll a ratio was unrealistically low (<10). Such a low ratio has never been reported from laboratory or field studies (Geider 1987, Thompson 1999). Second, in contrast to diatom biomass, chlorophyte biomass estimated by microscopy was very weakly correlated with biomass estimated using HPLC-CHEMTAX (Figure 10). HPLC-CHEMTAX pointed to an important contribution of chlorophytes to total chlorophyll a in winter, when very few chlorophytes were detected during the microscopical analyses.
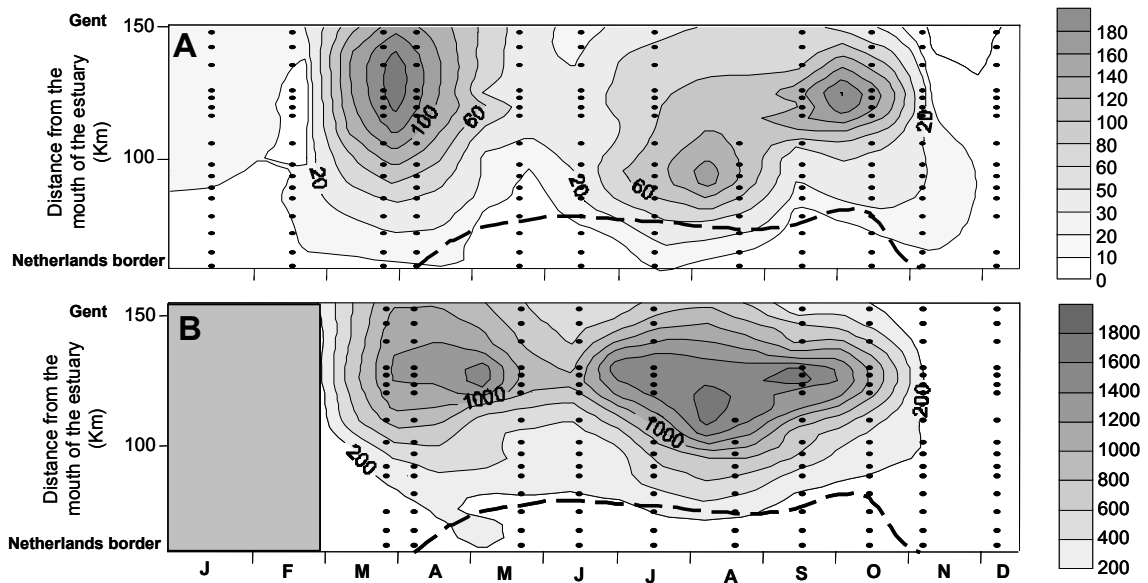
**Figure 9**. Spatio-temporal evolution of chlorophyll a concentration (above) and phytoplankton biomass estimated from microscopical cell counts (below) in the upper Scheldt estuary in 2002 (X-axis represents time, Y-axis represents distance from the mouth of the estuary, gray-scale level is equivalent with chlorophyll a concentration and black dots represent sampling events in space and time).
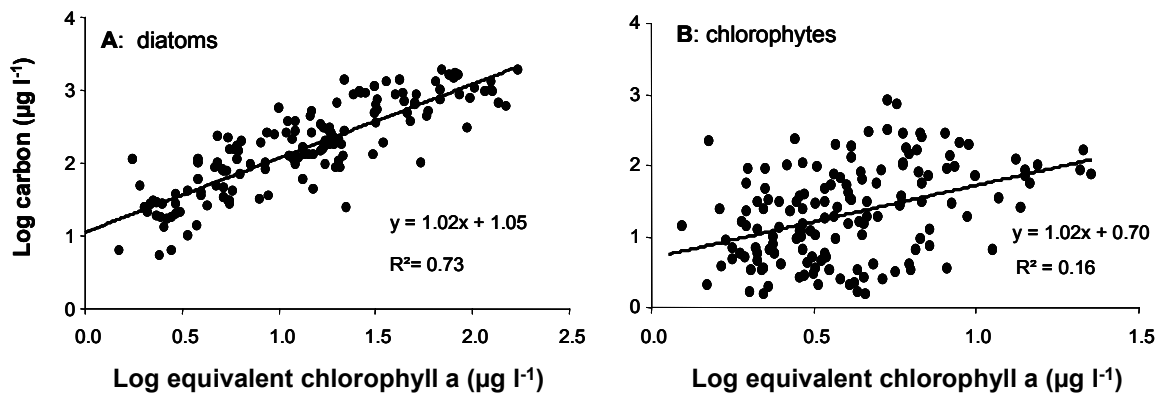


**Figure 10**. Correlation between equivalents in chlorophyll a (estimated using HPLC-CHEMTAX) and biomass (estimated using microscopical cell counts) for diatoms (left) and chlorophytes (right).

A close relation was found between the carbon-to-chlorophyll a ratio and the residuals of the regression of chlorophyte biomass estimated by microscopy versus the same biomass estimated by HPLC-CHEMTAX. This suggested that the two discrepancies had a common cause. Apparently, when phytoplankton biomass was low, HPLC analysis detected more chlorophyll a and pigments typical of chlorophytes than would be expected. It was hypothesized that these excess pigments were

derived terrestrial plant detritus. Inputs of terrestrial plant detritus from the intertidal marshes can be expected to be quite high in the upper estuary, as the vegetation on these intertidal marshes is highly productive (Soetaert et al., 2004; Struyf et al., 2006). Pigments in this detritus degrade relatively slowly (Bianchi and Findlay, 1991; Luo et al., 2002) and this may result in non-negligible quantities of macrophyte pigments in the water column. When phytoplankton biomass is low, these detrital pigments result in an overestimation of phytoplankton biomass from chlorophyll a and an overestimation of chlorophyte biomass by HPLC-CHEMTAX.

It was concluded that HPLC-CHEMTAX may slightly overestimate phytoplankton biomass in general and chlorophyte biomass in particular. This error is probably negligible during phytoplankton blooms, when phytoplankton biomass is relatively high, but the error may become important when phytoplankton biomass is low (e.g. in winter or in the brackish reaches).

### 4.2.2 Phytoplankton dynamics in the Scheldt and Rupel basins and their tributaries in the year 2003

In a joint sampling campaign for the SISCO project, the two major sub-basins of the upper Scheldt estuary (Rupel and Scheldt) as well their tributaries were sampled weekly in 2003 and phytoplankton biomass and community composition was assessed using HPLC-CHEMTAX analyses (Figure 11).

The main goal of this phytoplankton monitoring was to provide an estimate of diatom biomass for an integrated study of diatom and BSi production and DSi consumption. However, this study also compared for the first time phytoplankton development in the Scheldt and Rupel branches of the estuary and their tributaries. Phytoplankton biomass was substantially lower in the Rupel branch of the estuary when compared to the Scheldt branch. This was ascribed to the low water retention time of the Rupel branch. Water retention time in the Rupel branch is low compared to that of the Scheldt branch because its volume is > 4 times lower and discharge is about 50% higher than in the Scheldt branch. This observation is in line with the close correlation between mean summer phytoplankton biomass and discharge (see above) and points to an important role of hydrodynamics in regulating phytoplankton development in the upper reaches of the Scheldt estuary. The difference in water retention time between the Scheldt and Rupel branches, and therefore probably also the difference in phytoplankton biomass, is at least partly due to human alterations of the ecosystem. Discharge into the Scheldt branch of the estuary is artificially low because water is diverted towards the canal Gent-Terneuzen. On an annual average, about 50% of the discharge of the Scheldt and Leie rivers (two major tributaries to the Scheldt branch of the estuary) is diverted to Terneuzen to feed the locks on the canal. During summer, the fraction of water that is diverted is even more important,

resulting in a more pronounced difference in water retention time between the Scheldt and Rupel branches. Without this diversion of water, the constraints on phytoplankton development in the Scheldt branch of the estuary would probably be more severe and phytoplankton production might be substantially lower.
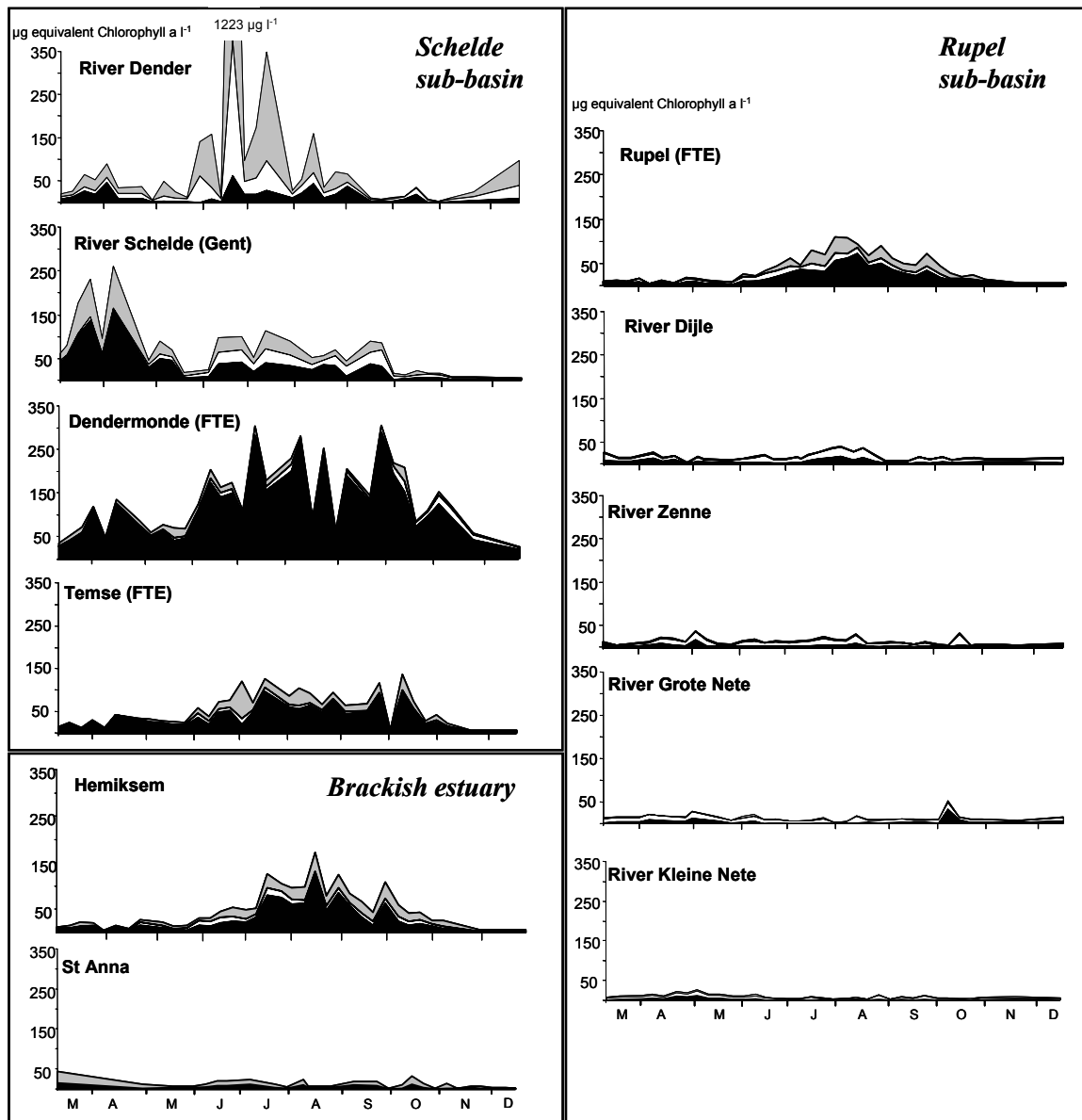


**Figure 11**. Seasonal succession in chlorophyll a concentration (in µg l⁻¹) at several stations in the upper Scheldt estuary as well as in the tributary rivers. The contribution of major algal groups to total chlorophyll a as estimated from concentrations of accessory pigments using CHEMTAX is shown (black: diatoms: white: chlorophytes, grey: other algal groups).

Despite the short retention of the water in the Rupel branch of the estuary (estimated to be on average only 2.3 days, without considering tidal flushing), phytoplankton biomass in the Rupel branch was still substantial. Phytoplankton biomass and community composition in the Rupel basin were strongly correlated with those in the

Scheldt basin. It was estimated that the amount of water from the main channel of the Scheldt estuary that is imported into the Rupel branch by the flood tide during each tidal cycle is comparable to the mean volume of the Rupel branch. Therefore, we assume that most of the phytoplankton observed in the Rupel branh was imported from the Scheldt branch by tidal mixing.

Phytoplankton biomass not only differed between the tidal Rupel and Scheldt brnaches but also in their tributaries, with phytoplankton biomass being substantially lower in the tributaries of the Rupel basin when compared to those of the Scheldt basin. This difference was ascribed to the smaller cross-section of the rivers in the Rupel basin. The smaller cross-section would result in a higher water velocity and lower retention time of the water, which would limit phytoplankton development. The lower import of phytoplankton biomass from the tributaries into the Rupel estuarine branch compared to the Scheldt estuarine branch probably contributed to the differences in phytoplankton biomass between the two branches. In summer, however, import of phytoplankton from the tributaries added only a small contribution to total phytoplankton biomass in the Scheldt branch.

The seasonal development of phytoplankton biomass and community composition in the tributaries was very different in the tributary rivers and in the estuary. In the rivers, phytoplankton biomass peaked in spring and was lower in summer. The spring bloom in the rivers was dominated by the diatom Stephanodiscus while chlorophytes like Scenedesmus and Pediastrum were the dominant algal group in summer. A succession from diatoms in spring to chlorophytes in summer is characteristic for many large lowland rivers (e.g. Garnier et al., 1995). In the estuary, on the contrary, phytoplankton biomass peaked in summer. Moreover, the phytoplankton community in the estuary was dominated by diatoms throughout the year. In spring, the phytoplankton community in the estuary was dominated by the diatom Stephanodiscus, which was mainly imported from the tributary rivers Scheldt and Dender. In summer, the phytoplankton community in the upper estuary was dominated by the diatom Cyclotella scaldensis, whose populations developed in the estuary. In summer, chlorophytes imported from the rivers contributed to the phytoplankton community in the estuary but were only of secondary importance.

The difference in phytoplankton community composition between the rivers and estuary in summer was probably related to differences in turbulence and light climate. In the tributary rivers in summer, light levels were relatively high due to a shallow depth and low SPM concentration and turbulence was relatively low due to a low discharge and the lack of tidal currents. Such conditions would favour chlorophytes, which are adapted to relatively high light levels and are resistant to sedimentation (Köhler et al., 2002). At the same time, these conditions would not be beneficial to diatoms, which suffer significant sedimentation losses due to their heavy

silica frustules. In the estuary in summer, light levels were much lower due to a deeper water column and higher SPM concentrations while turbulence was higher due to the presence of tidal currents. These conditions would favour diatoms, which are adapted to low light conditions and require turbulent water to avoid sedimentation. At the same time, chlorophytes would be at a disadvantage due to the low light levels.

The fact that, in summer, phytoplankton biomass was lower in the tributary rivers than in the estuary was surprising because light levels were higher in the river and nutrient concentrations were comparable. It is unlikely that this difference is due to zooplankton grazing as during summer zooplankton abundance was comparable in the river and the estuary and the grazing impact was comparable (Lionard et al., 2005). A possible explanation for the lower biomass in the river compared to the estuary might be higher sedimentation losses in the rivers due to low turbulence.

### 4.2.3   Phytoplankton zonation along the Scheldt continuum

During summer 2003, phytoplankton community composition was studied monthly along the river-estuarine-coastal zone continuum of the Scheldt to investigate which diatom communities were present in the different estuarine zones during the most productive season. Phytoplankton was sampled at 10 stations distributed evenly along the estuarine salinity gradient as well as in the two major riverine tributaries and at two stations in the coastal zone. For the species that were observed in at least 4 samples, the distribution along the estuarine salinity gradient was determined using general additive modelling (GAM) regression. According to their distribution patterns, species were grouped into different communities.

Textbooks on estuarine ecology predict for many groups of organisms a succession in estuaries from a freshwater community in the upper estuary to a marine community near the mouth of the estuary, with a typical and distinct estuarine community in between near the salinity gradient. In our study of phytoplankton succession along the Scheldt continuum we indeed observed a succession from a riverine to a marine phytoplankton community. The riverine community was dominated by many chlorophyte species (e.g. Scenedesmus) and a few typical freshwater diatoms (e.g. Nitzschia spp.). The marine community contained many marine diatoms typical of coastal waters (e.g. Chaetoceros, Rhizosolenia, Guinardia, Paralia). These species from the riverine or coastal communities were imported into the estuary through river discharge (riverine community) or tidal mixing (coastal community) and were often found quite far down- or upstream in the estuary. These riverine and coastal communities had an important contribution to phytoplankton diversity in the estuary (Figure 12). About half of the species observed in the estuarine samples were either imported from the river or from the sea.
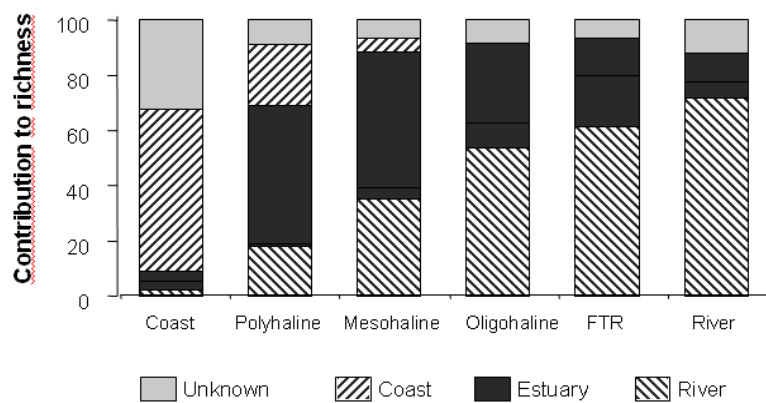
**Figure 12**. Contribution of phytoplankton species of riverine, estuarine or coastal origin to
total diversity (as richness or the number of species per sample)
in different salinity zones of the Scheldt estuary.
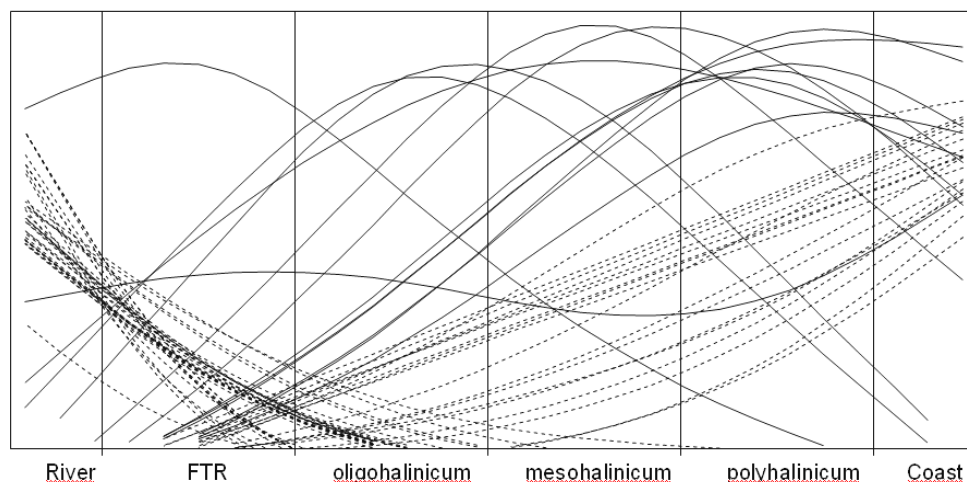


**Figure 13**. Distribution patterns of phytoplankton species found in the Scheldt estuary in
summer 2003 modelled using GAM regression. Distribution of species that
have their population maximum outside the estuary (river or coastal zone)
is shown as broken lines. For the species that have their population maximum within the
estuary, the distribution patterns are shown as a full line.

About one third of the phytoplankton species that were observed in the estuarine
samples attained their population maximum within the estuary. These species were
classified as typical estuarine species. However, these estuarine species did not form
a homogeneous community of species with a similar distribution pattern and a similar
position of their population maximum. Instead, the estuarine species had population
maxima that were spread evenly along the estuarine salinity gradient (Figure 13).
There is no single estuarine phytoplankton community but rather a succession of
estuarine species along the salinity gradient. Some of these species occur mainly in
the freshwater tidal zone (e.g. Cyclotella scaldensis), others near the steepest part of

the salinity gradient (oligo-mesohaline zones, Melosira nummuloides, Actinocyclus normannii, Cheatoceros subtilis) and still others downstream of the major salinity gradient (polyhaline zone, e.g. Rhizosolenia pungens, Melosira varians).

### 4.2.4 Phytoplankton seasonal succession in the Belgian coastal zone of the North Sea

While ample information is available for phytoplankton succession at fixed sites in the Belgian coastal zone (BCZ) of the North Sea (cf. Lancelot et al., 2005), little is known about the spatial variability in phytoplankton biomass and community composition in the BCZ. Therefore, during the course of 2003, samples were collected at 10 fixed monitoring stations in the BCZ of the North Sea. Phytoplankton was studied by means of microscopical cell counts and using HPLC pigment analysis followed by processing of the pigment data using CHEMTAX. In addition, underway chlorophyll a fluorescence recordings collected during spring by the RV Zeeleeuw were investigated.

Monthly monitoring of phytoplankton community composition at five stations revealed a succession of three distinct diatom communities. This succession started with a community of bentho-pelagic diatoms and relatively small pelagic diatoms (Actinoptychus senarius, Paralia sulcata, Plagiogrammopsis vanheurckii, Rhaphoneis amphiceros, Odontella aurita, Thalassiosira spp. <20 µm and >20 µm, Thalassionema nitzschioides). The second community was dominated by Chaetoceros spp. as well as Lithodesmium undulatum, Leptocylindricus danicus and Skeletonema costatum and appeared only shortly in the plankton in spring. The third community was dominated by rhizosolenid diatoms and Pseudonitzschia spp. and was dominant during summer. In autumn, the same succession occurred in reversed order (Figure 14). Similar diatom communities have previously been observed in the BCZ of the North Sea (Rousseau et al., 2002) and in Dutch coastal waters (e.g. Philippart et al., 2000).
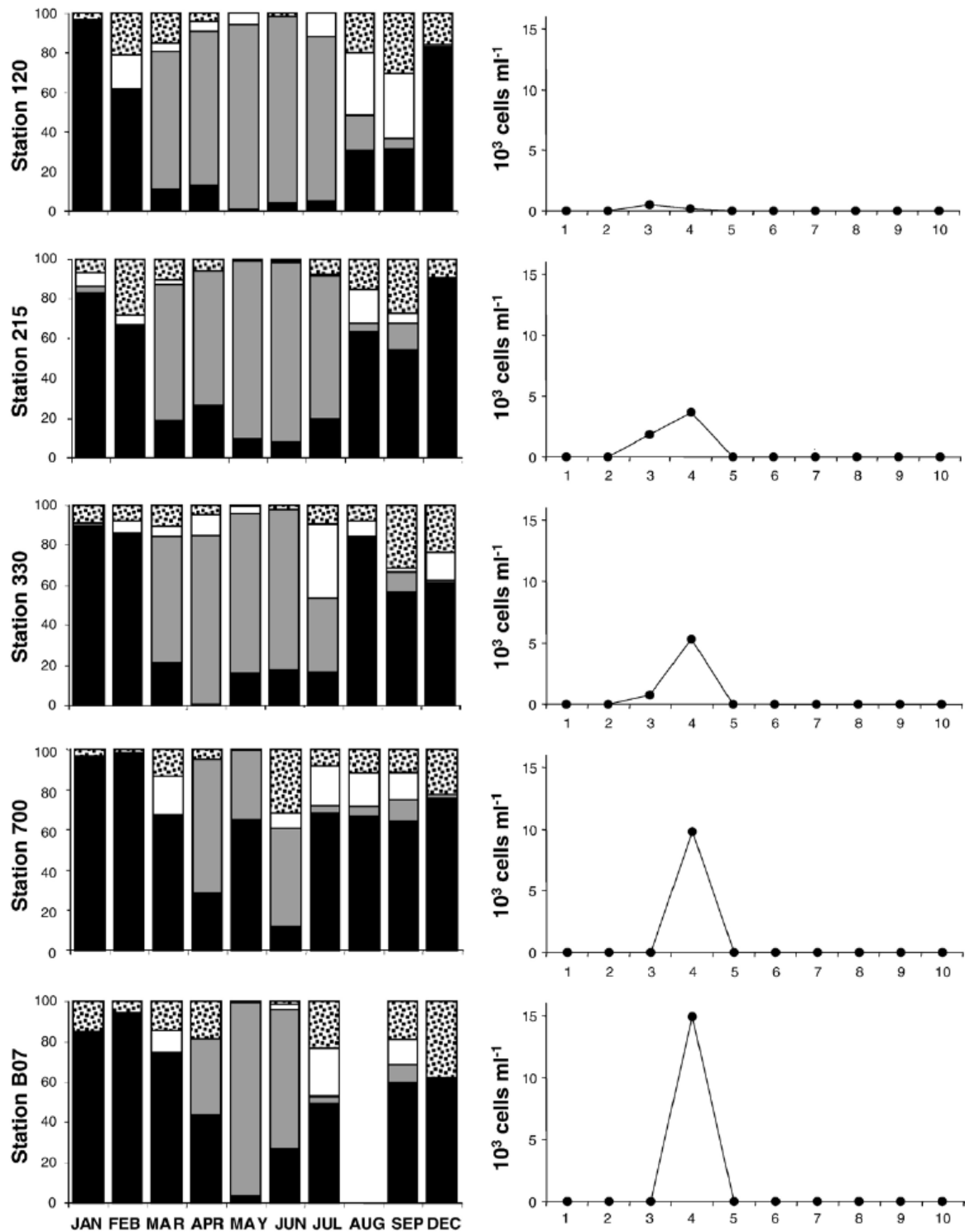
**Figure 14.** Left: contribution of taxa belonging to each of the 3 diatom communities described in the text to total diatom abundance (black: first community, white: second community, grey: third community, speckled: other taxa). Right: abundance of Phaeocystis at the same sites. From Muylaert et al. (2006).

The succession of these three communities was the same at each site, but the succession from the winter-spring to the summer community occurred one month earlier and the succession from the summer to the autumn community one month later at the SW than at the NE stations of the BCZ. Monthly monitoring of chlorophyll a at ten fixed sites and inspection of in vivo fluorescence recordings during various cruises of RV Zeeleeuw indicated that the spring bloom started about one month earlier in the SW part of the BCZ than in the NE part (see Muylaert et al., 2006). The spatial difference in the onset of the spring bloom was ascribed to the higher water column turbidity at the NE coast compared to the SW coast. The higher water turbidity at the NE versus the SW coast is probably related to the Scheldt estuarine plume.

Although a Phaeocystis bloom occurred at all monitoring stations, a clear spatial variation in the magnitude of such blooms was observed, with more intense blooms at the NE coast than at the SW coast. A close relation was observed between the intensity of the Phaeocystis bloom and the availability of inorganic nutrients (N and P) before the onset of the bloom (Figure 15). Availability of inorganic nutrients was higher closer to the Scheldt estuarine plume at the NE coast compared to the SW coast, which is situated further away from the estuarine plume.
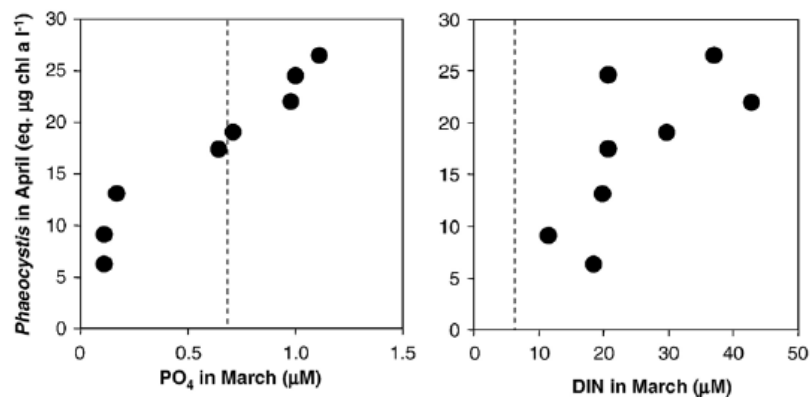


**Figure 15**. Relation between dissolved inorganic phosphate ($PO_4$) and dissolved inorganic nitrogen (DIN) concentrations in the water column in March and Phaeocystis biomass attained at the same stations one month later in April. The vertical broken line corresponds to the half-saturation constant of colonial Phaeocystis for uptake of phosphate and nitrate (Schoemann et al., 2005).

The use of HPLC pigment analyses to reconstruct phytoplankton community composition in coastal waters of the North Sea is complicated by the fact that the two dominant phytoplankton groups – diatoms and Phaeocystis – have a very similar pigment composition (Antajan et al. 2004). Analysis of pure cultures indicated that Phaeocystis from the North Sea differed only from diatoms in possessing chlorophyll $c_3$ in stead of chlorophyll $c_1$ or $c_2$. Using chlorophyll $c_3$ as an indicator for Phaeocystis

in CHEMTAX, we attempted to estimate the contribution of Phaeocystis to total chlorophyll a. Comparison of microscopical cell counts and CHEMTAX analysis of accessory pigment data indicated that HPLC analysis is a promising tool for monitoring Phaeocystis in the North Sea (Figure 16). The presence of chlorophyll $c_3$ containing diatoms, however, probably resulted in the detection of small quantities of Phaeocystis by HPLC-CHEMTAX analysis when microscopical analyses showed that the species was absent. Therefore, estimates of Phaeocystis biomass based on HPLC pigment analysis should always be interpreted with caution.
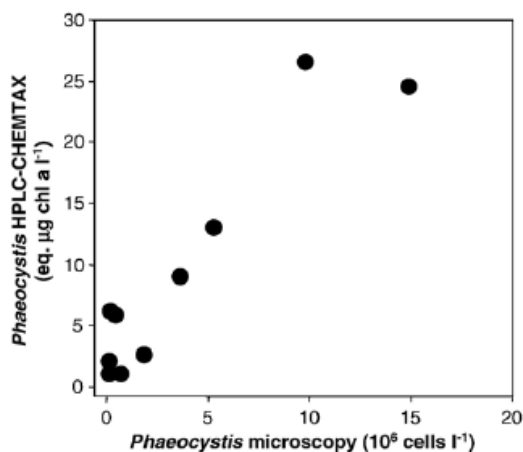


**Figure 16**. Comparison of Phaeocystis abundance estimated by means of microscopical cell counts and using CHEMTAX analysis of HPLC pigment data in April.

### 4.2.5 Si-limited growth of Cyclotella meneghiniana strains isolated from the upper Scheldt estuary and other aquatic systems

The dominant diatom genus in the upper reaches of the Scheldt estuary is Cyclotella. In order to determine at which DSi concentration Cyclotella from the Scheldt estuary would be Si-limited, two Cyclotella strains were isolated from the upper Scheldt estuary and their Si-limited growth kinetics were determined. The Si-limited growth kinetics of the two Scheldt Cyclotella strains were compared with those of three other Cyclotella strains isolated from different geographic locations (Ukrain, Malawi, Falklands).

The morphology of one of the two Scheldt strains and the three strains from other locations was studied in detail using light and SEM microscopy. Although morphological differences were observed between the strains, these were due to the different size of the cells. The size-differences between the strains were due to the fact the strains were in different phase of the cell size reduction cycle. According to morphological criteria, all strains could be assigned to the species Cyclotella meneghiniana, one of the commonest freshwater diatoms in the world.

The 28S rRNA of each of the five strains was sequenced and sequences were compared with sequences of 54 other C. meneghiniana strains from different geographic locations (obtained from Beszteri et al., 2005). The two Scheldt strains as well as the Ukrain strain had identical sequences and clustered with strains from two North-German estuaries (Geeste and Ems). The Falkland and Malawi strains had different sequences and did not cluster closely with any other strain. This observation confirmed previous conclusions that Cyclotella meneghiniana consists of several genetically distinct taxa which cannot be distinguished using the morphological criteria that are used to identify the species.

Si-limited growth kinetics were determined for all strains by monitoring diatom growth rate in medium with variable DSi concentrations. Growth rate as a function of DSi concentration followed Monod kinetics. The half-saturation constant for Si-limited growth varied strongly between the strains. The variability observed among the five 'C. meneghiniana' strains corresponded to the variability in Si-limited growth kinetics reported from previously studied freshwater diatoms (Martin-Jezequel et al., 2000). The strains from the Scheldt estuary and Uktrain had the highest half-saturation constant for Si-limited growth while the strains from Falklands and Malawi had a much lower half-saturation constant.

## 4.3 Pelagic silica dynamics of the upper estuary of the Scheldt continuum

### 4.3.1 Temporal distribution of DSi and BSi in the upper Scheldt estuary

In the rivers discharging in the Scheldt estuary in 2003, dissolved silica (DSi) concentrations remained high throughout the year with mean annual concentrations ranging from 154 µM in the Kleine Nete to 288 µM in the Dijle (Figure 17). Biogenic silica (BSi) concentrations were lower with mean annual concentrations ranging from 2.9 µM in the Dijle to 18.2 µM in the River Scheldt. Small riverine diatom growths were however observed by concomitant increases in BSi and in DiatChla (defined as chlorophyll a associated with diatoms based on HPLC pigment measurement) in spring in all rivers and in summer in the River Scheldt, in the Dender and in the Dijle. DSi concentrations also fluctuated during both seasons in the River Scheldt and in the Dender.
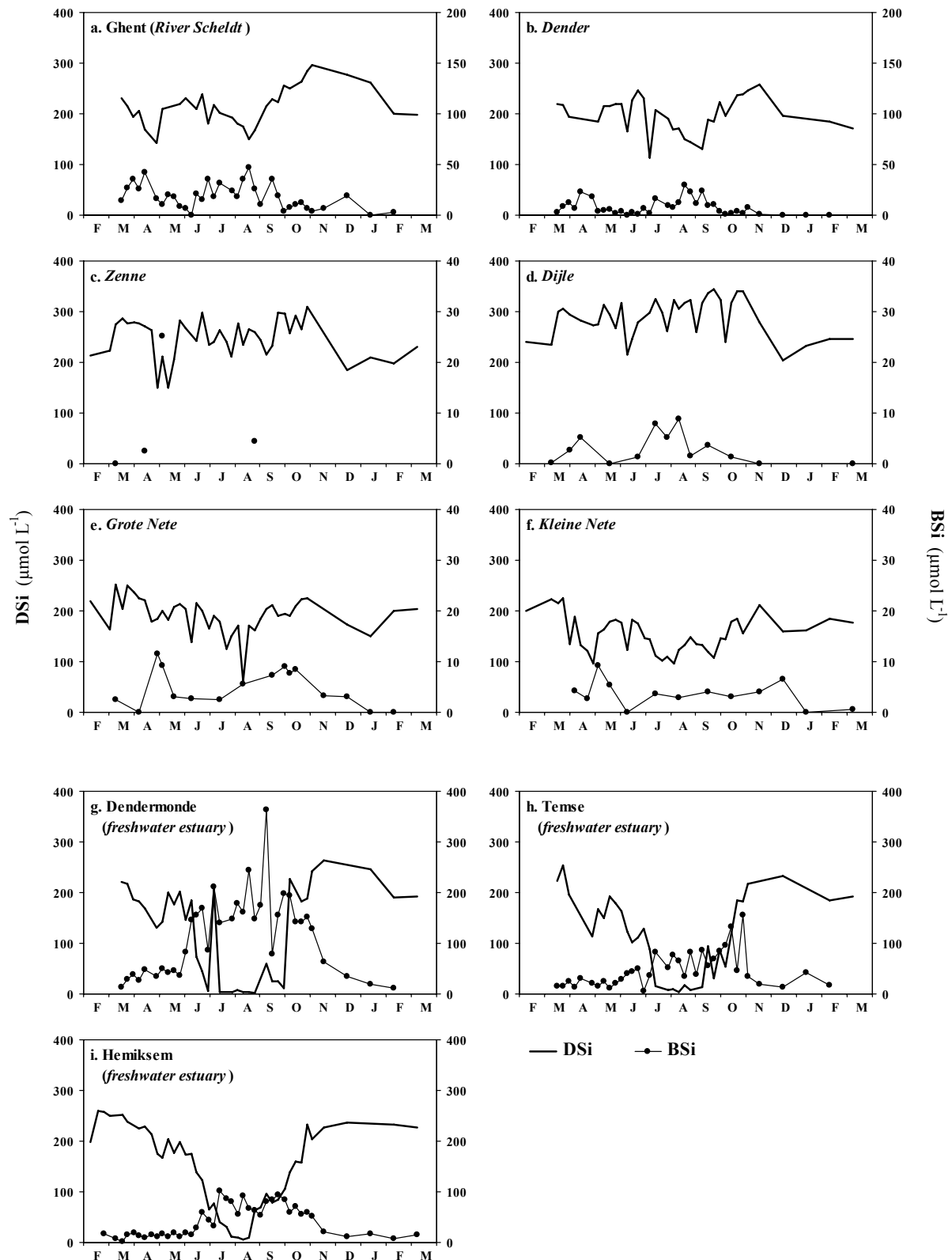
**Figure 17**. DSi (left scales) and BSi also (right scales) concentrations in tributaries (a. to f.) and along the freshwater estuary (g. to i.).

At all three stations along the freshwater estuary, DSi concentrations ranged from 150 µM to 250 µM in early spring and in autumn/winter. During the summer diatom bloom however, BSi concentration increased and DSi was completely consumed down to concentrations of a few µM, which may potentially limit the diatom growth. DSi was consumed for a longer period at Dendermonde than at Temse or at Hemiksem, and higher BSi concentrations were reached at Dendermonde compared to Temse and Hemiksem.

### 4.3.2 Temporal evolution of DSi consumption and BSi production in the freshwater tidal estuary

Fluxes of silica species can be computed as the product of concentrations and the weekly averaged discharge. Comparisons between adjacent stations provided estimations of the net DSi consumption and BSi production in the zones delimited by our sampling stations. DSi consumption and BSi production in the freshwater estuary occurred in two distinct diatom productivity zones related to two main sources of water: 1) the zone upstream of Dendermonde station, and 2) the zone comprised between Temse, Hemiksem and the tidal limits on the tributaries of the Rupel (zone 2) (Figure 18).
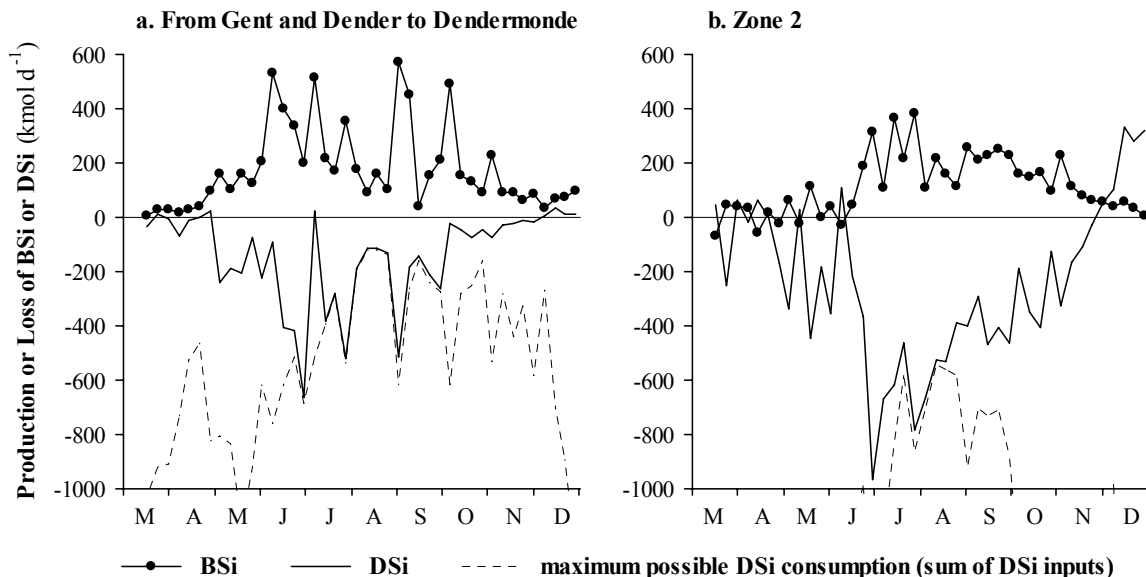


**Figure 18**. Production (positive values) or consumption (or loss, negative values) of DSi and BSi calculated as differences between output and input fluxes of DSi and BSi, (a) from Ghent and Dender to Dendermonde, and (b) in the zone 2.
The dash line represents the DSi consumption if all the DSi was consumed; it corresponds to the sum of the DSi input fluxes into the considered area with a negative sign.

In the zone upstream of Dendermonde, BSi production was maximum in June, July, September and October (Figure 18a). From the end of June to the end of September,

the DSi consumption and consequently the BSi production corresponded to the riverine DSi flux. Thus the overall rate of DSi consumption/BSi production was mainly driven by the freshwater discharge as the DSi concentration was nearly constant throughout the year in the rivers Scheldt and Dender. Even though the BSi concentrations were also high in August, the production reached a minimum in August because of the low discharge in the River Scheldt and the deviation of its water to feed the Ghent – Terneuzen canal. The productive periods were clearly restricted to June-July and the beginning of September, i.e. when DSi was provided by sufficient water discharge.

A summer diatom bloom also occurred in zone 2 as DSi was consumed and BSi produced. More DSi was consumed than BSi produced indicating presumably concomitant settling of BSi. The diatom production was thus estimated by the DSi consumption. It increased rapidly in June and subsequently decreased until October. All the DSi brought to zone 2 was consumed in late July and beginning of August. Compared to the zone upstream than Dendermonde, in zone 2 1) the DSi consumption started later but reached a higher rate and 2) the complete consumption of the DSi inputs occurred during a much shorter period. The higher water discharges in zone 2 prevented a decline in the DSi consumption as observed in August in zone 1 comprised between Temse station and the tidal limits on the rivers Scheldt and Dender.

Diatom growth is generally unexpected in zone 2 because of the short water residence times in the Nete and the Rupel, and the low light conditions in the area of the confluence due to the high suspended matter concentrations and the deepening of the water. However in 2003, it might have occurred in the Scheldt between Temse and the mouth of the Rupel, where the water tidal mixing provided DSi from the Rupel River, but also in the Nete due to 1) better light penetration because of the shallow waters of the Nete and 2) the exceptionally low discharge rates in the summer 2003 (<30 $m^3$ $s^{-1}$).

### 4.3.3  Silica budget of the freshwater estuary during the productive period

A silica budget was constructed for the productive period (May to September, 153 days) to estimate the amounts of BSi produced or settled (Figure 19).

In zone 1, most of inputs of silica were as DSi (Figure 19). Half of this amount of DSi was consumed before Dendermonde and entirely transformed to BSi. No significant net settling of BSi occurred in this section. Between Dendermonde and Temse, no net DSi consumption occurred but there was a settling of 75% of the BSi produced in the previous section.

The tributaries of the Rupel accounted for 75% of the DSi inputs to zone 2 but the BSi inputs from these tributaries (weekly values recalculated from DiatChla concentrations) did not contribute significantly to the BSi pool. There was both a production and a loss of BSi in zone 2 and the loss of BSi corresponded to 63% of what had been produced.

The silica fluxes normalized to the water surface area yield a DSi consumption rate of 34 and 62 mmol $m^{-2}$ $d^{-1}$ in zones 1 and 2 respectively, suggesting a higher productivity in zone 2. This could be explained by the low riverine DSi flux in summer in zone 1 leading to DSi limited production.
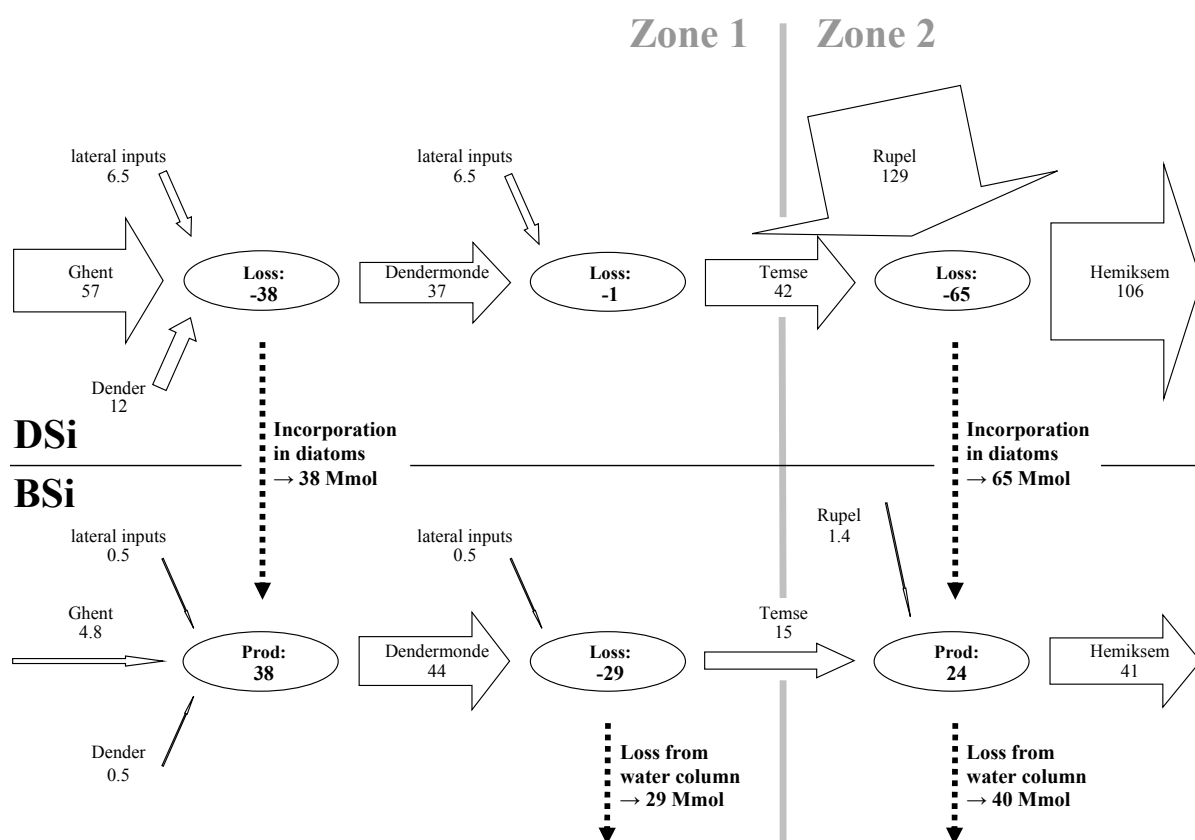


**Figure 19**. Integrated fluxes (white arrows) and calculated productions and losses (in ovals) of DSi and BSi in the Scheldt freshwater estuary expressed in Mmol for the two zones during the productive period (May to September, 153 days). The white arrows are drawn proportionally to the fluxes, and the dashed arrows represent the main processes (incorporation of DSi and losses of BSi) deduced from the mass-balances calculations.

Overall, the DSi consumption during the productive period in the freshwater estuary accounted for 49% of the received DSi and 67% of the produced BSi settled. This corresponded to a 32% retention of the total amount of silica (96% as DSi) brought to

the estuary during the productive period. The tributaries of the Rupel accounted for 60% of this amount and about 60% of the BSi production and settling occurred in zone 2.

### 4.3.4 Si:C ratio in living diatoms and in culture experiments

Particulate organic carbon (POC) data could not be used for the calculation of Si:C ratios due to the abundant presence of detrital material (Hellings et al., 1999). Si:C ratios were thus estimated from BSi/DiatChla ratios using the POC/chlorophyll a mass ratio of 30 found for phytoplankton in the freshwater Scheldt estuary (Muylaert et al., 2001).

Si:C and/or POC/chlorophyll a contents in diatoms are dependant on nutrient, temperature and light conditions (Geider, 1987, Ragueneau et al., 2000; Hildebrand, 2002). However, at Dendermonde from May to July, the in-situ BSi and DiatChla concentrations were linearly correlated with a constant BSi/DiatChla ratio of 0.88 $\mu$mol $\mu g^{-1}$ (Figure 20) although during this period DSi decreased from 200 $\mu$M to 4 $\mu$M (Figure 17) and light and temperature increased (IRMB 2003-2004). The fraction of BSi from dead diatoms was expected to be minimal as the period corresponded to the beginning and the peak of the bloom. The resulting Si:C molar ratio of 0.35 was thus assumed to be typical of living diatoms.

Our Si:C molar ratio of 0.35 is low compared to the value of 0.78 (Conley and Kilham, 1989) commonly used for freshwater diatoms. However, direct measurements of Si:C ratios were also performed on cultures of Cyclotella meneghiniana isolated from the Scheldt. The diatom community in the freshwater estuary was indeed dominated by this diatom species. Lower ratios varying between 0.118 and 0.30 were found. This variability could be due to the differences between in-situ and laboratory conditions, such as, most probably, the light availability. The growth of diatoms is thought to be light limited in the Scheldt as, following the water movement, they spend a significant time in the dark below the thin photic zone (Desmit et al., 2005). So it is possible that, due to higher light levels in the incubator, their growth in cultures was higher than in-situ production. The different silica contents could then be expected as this parameter is known to decrease with increasing growth rate (Hildebrand, 2002). However, taking into account the variability in the culture experiments, our indirect in-situ ratio is in accordance with the direct measurements performed on these mono-specific cultures. Additionally, Sicko-Goad et al. (1984) also found a similarly low molar ratio of 0.38 for C. meneghiniana. Similar in-situ Si:C molar ratios of 0.37 and 0.27 were calculated for the Rhine from the POC/chlorophyll a (Admiraal et al., 1992) and BSi/chlorophyll a ratios (Admiraal et al., 1990).
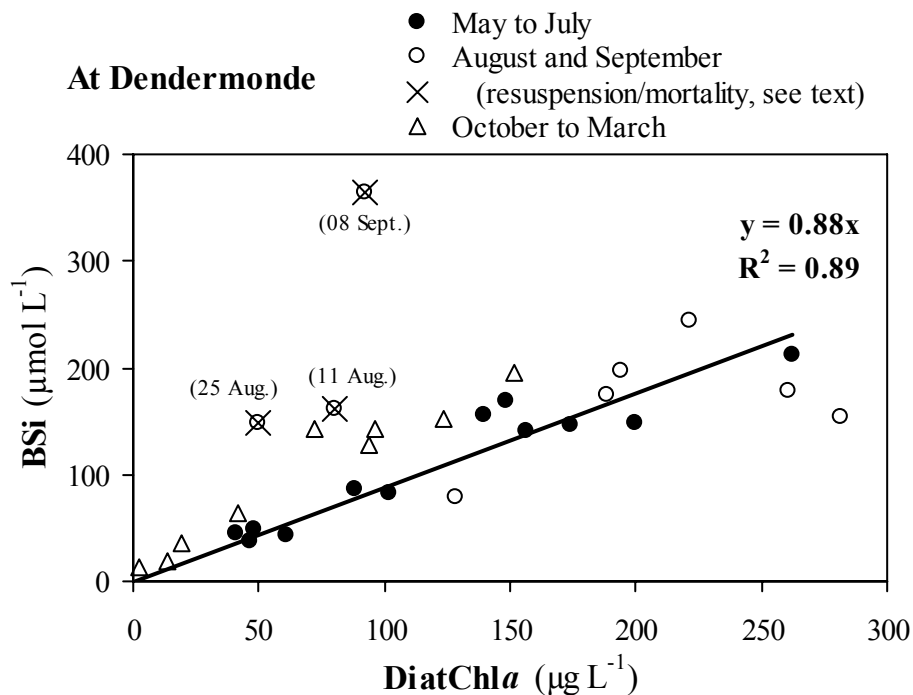
**Figure 20**. BSi versus DiatChla concentrations at Dendermonde for spring/summer, late summer and autumn/winter periods.
A regression of 0.88 µmol µg⁻¹ was obtained for the period from May to July.

### 4.3.5 Diatom mortality and resuspension after the productive period

The fractions of BSi associated and not associated with living diatoms (BSi-living and BSi-dead respectively) were assessed in summer and autumn/winter at all estuarine stations, assuming a BSi/DiatChla ratio of 0.88 µmol µg⁻¹ for living diatoms, and zero chlorophyll a content in dead diatoms. At Dendermonde in August and September, the BSi determined was regarded as BSi-living considering that the BSi/DiatChla ratio at Dendermonde did not appear to deviate significantly from the ratio measured from May to July (Figure 20). There were exceptions however at three sampling dates (11 and 25 August 2003 and 8 September 2003, dates discarded in Figure 20) when abnormally high BSi/DiatChla ratios were observed, presumably indicating mortality and/or resuspension. During the productive period at Temse, the BSi measured was mostly BSi-living although a large amount of BSi settled between Dendermonde and Temse. At Hemiksem however, a significant mortality was observed, consistent with the fact that between Temse and Hemiksem, the phytoplankton had spent more time in the dark due to the deepening of the water and the presence of a turbidity maximum in the area of the confluence with the Rupel (Chen et al., 2005; Arndt et al., 2007). BSi-dead accounted for 28% on average from May to August and this fraction increased to 66% in September. From October onwards, mortality was observed at all three stations: on average, BSi-dead

accounted for 45% of the total BSi at Dendermonde, 66% at Temse and 78% at Hemiksem.

The maximum amount of resuspended BSi and the minimum amount of BSi from diatom production in autumn/winter could be assessed in terms of the increases in the BSi-dead and BSi-living pools respectively. These are maximum and minimum estimates as the dead fraction may not only be due to resuspension of diatoms deposited during the productive period, but also to diatoms that had grown further upstream and had died while being transported downstream.

The highest BSi increase occurred in the Ghent – Dendermonde section, with more than half being BSi-living. As shown by a higher suspended matter concentration at Dendermonde compared to the adjacent stations, suspended particles may have been held in the vicinity of Dendermonde, leading also to the possible presence of persistent BSi from the productive period. Although a large amount of BSi settled between Dendermonde and Temse during the productive period, there was no significant BSi resuspension between October and February, but rather a diatom mortality as shown by the exchange from the BSi-living to the BSi-dead pools. In zone 2, most of the increase was ascribed to BSi-dead.

In the entire freshwater estuary from October to February, at least 12 Mmol of BSi were additionally produced and at most 13 Mmol were resuspended. The latter amount accounted for only 18% of the amount of BSi that settled between May and September. Together with the consideration that dissolution is not expected to be important in the freshwater estuary, it appears at first sight that most of the BSi deposited during the productive period in the Scheldt freshwater estuary was retained on an annual time-scale.

## 4.4 Pelagic silica dynamics of the brackish estuary towards the Belgian coastal zone

### 4.4.1 Influence of freshwater discharge on DSi concentrations in the end-members

Daily end-member DSi concentrations were obtained from several datasets (see legend in Figure 21b). Values were averaged if several DSi concentrations were available for a same day, or calculated by interpolation if no measurement was performed that day (Figure 21b). There was a general good agreement between the different datasets. Both the DSi concentration and the salinity at Vlissingen strongly vary with the state of the tide and interpolation was performed only for values recorded at high tide at Vlissingen (Figure 21c and 21d). They are indeed the best estimates for the salinity and the DSi concentration of the water which enters the Scheldt at each tide. There was a good agreement between the two datasets. The state of the tide at which the samples were taken was estimated by comparison with hydraulic outputs of the 1D-CONTRASTE model (Regnier et al., 1997; Vanderborght et al., 2002).

Daily salinity and DSi boundary input data were correlated to the freshwater discharge (Figure 22). Daily data were monthly averaged as the frequency of data available for DSi concentrations and salinity was in general of one per month.

Despite the fact that the years 2003-2005 could be considered as rather dry ones (except for the 2002-2003 winter however), the variation of discharge between the November-April and May-October periods was about two- to three-fold (Figure 23). Significant increasing patterns could be observed when plotting DSi concentrations at Vlissingen and in the freshwater end-member against freshwater discharge. However the interpretation should be done cautiously, as DSi could be strongly influenced by diatom consumption in the freshwater estuary, brackish estuary and the coastal zone.

Nevertheless, the variations in salinity could only be ascribed to mixing of freshwater and seawater. Thus, freshwater discharge had a strong influence on the salinity at Vlissingen (Figure 22) and as expected, salinity decreased with increasing freshwater discharge as a general pattern. In addition, plotting the averages for each month of the year revealed the hysteresis as observed by Baeyens et al. (1998), exhibiting the importance of the history of the hydraulic regime in the establishment of the salinity pattern. This stresses the fact that, in the Scheldt, steady-state is not established instantaneously. Indeed, the water residence time in the brackish estuary (1 to 3 months; Soetaert and Herman, 1995) is of the order of magnitude of the characteristic time of seasonal variation. If we assume the salinity of the seawater to

be 35 psu, the fraction of freshwater in the water at the outlet of the estuary would vary from about 5% in summer to 30% at high tide in winter for the period 2003-2005.
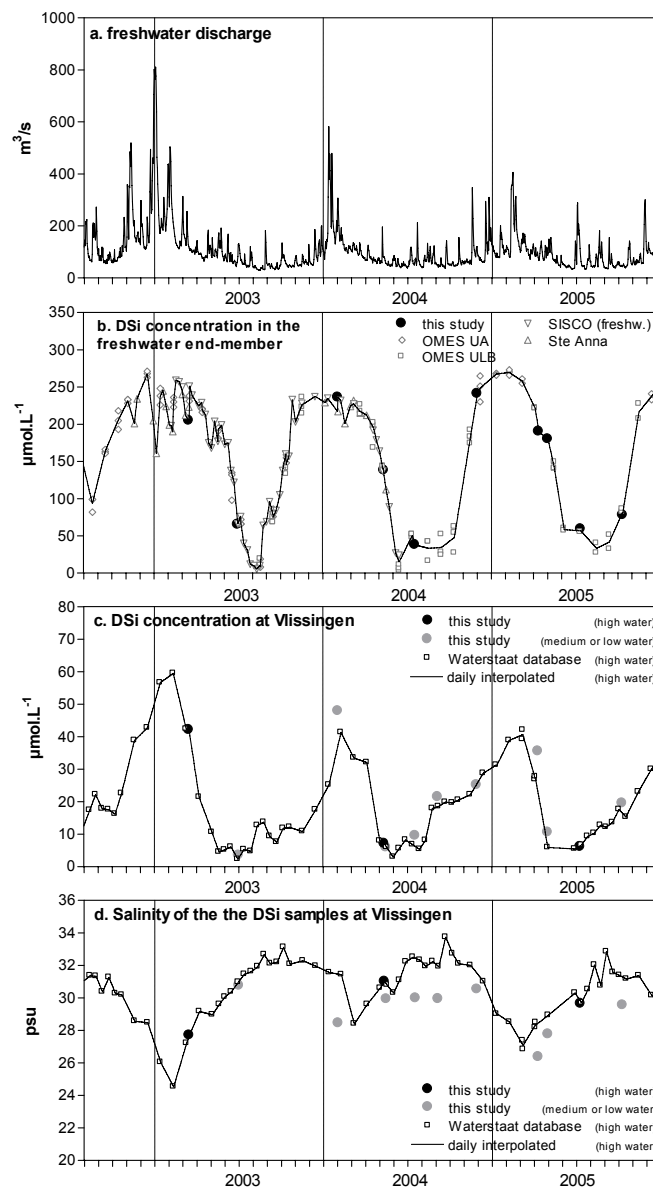


**Figure 21**. (a) Freshwater discharge estimated after the confluence with the Rupel (data provided by the Flemish Community (Afdeling Maritieme Toegang). (b) DSi concentrations from 5 different datasets measured between the confluence with the Rupel and Antwerp. The legend "this study" corresponds to the measured concentrations during the SISCO campaigns In the Scheldt brackish estuary. As well as for "Ste Anna" values, only samples for which the salinity was below 2 psu were taken into account. (c) DSi concentrations measured at high tide at Vlissingen (data from Waterstaat database, available online at www.waterbase.nl). Data for Vlissingen measured during our field campaigns in the Scheldt brackish estuary are also shown. (d) Salinity of the samples for which the DSi concentration is shown in Figure 21c.
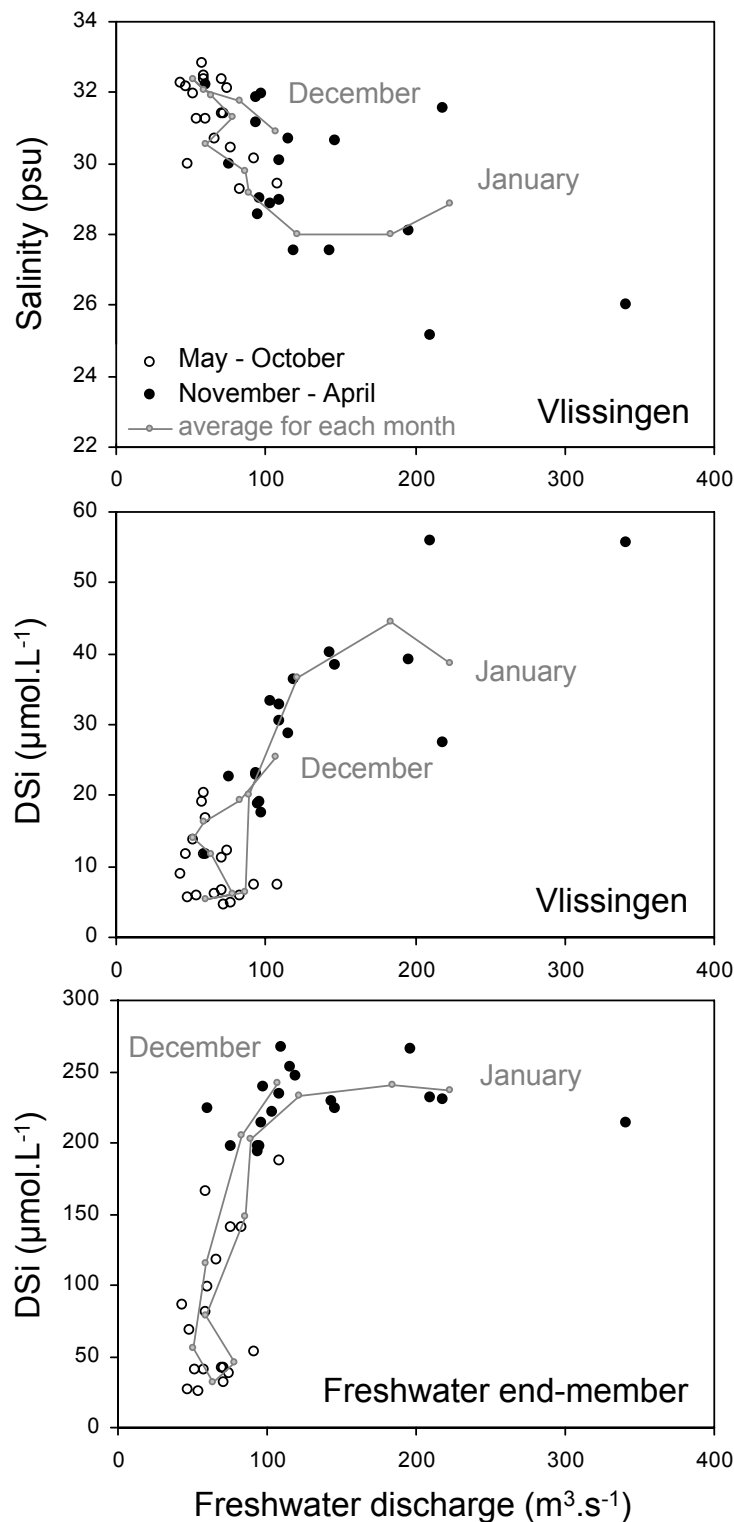
**Figure 22**. Monthly averages of the salinity at Vlissingen (high tide) and of the DSi concentrations at Vlissingen (high tide) and in the freshwater end-member plotted versus the monthly average freshwater discharge for the period 2003-2005 (black open and solid symbols). The grey line and symbols represent the evolution from the average January situation for 2003-2005 to the average December situation for 2003-2005.
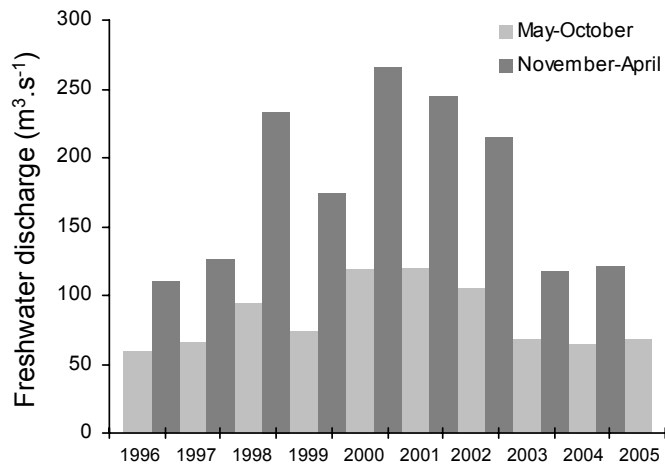
**Figure 23**. Average freshwater discharges for the periods from May to October and from November to April, from 1996 to 2005. Data were provided by the Flemish Community (Afdeling Maritieme Toegang).

Van der Zee and Chou (2005) found linear relationships between winter DSi concentrations and salinity. If extrapolated, the DSi concentration of a seawater mass of 35 psu would be near zero. Winter DSi concentrations were about 250 µM in the freshwater end-member (Figure 21b). If there was no DSi consumption, i.e. if the DSi concentrations in the freshwater and the seawater stayed at their winter values and if variations of DSi concentrations in Vlissingen were only due to mixing, the DSi concentrations would be expected to vary between about 20 µM to more than 70 µM at high tide in winter and late-summer respectively (Figure 24).
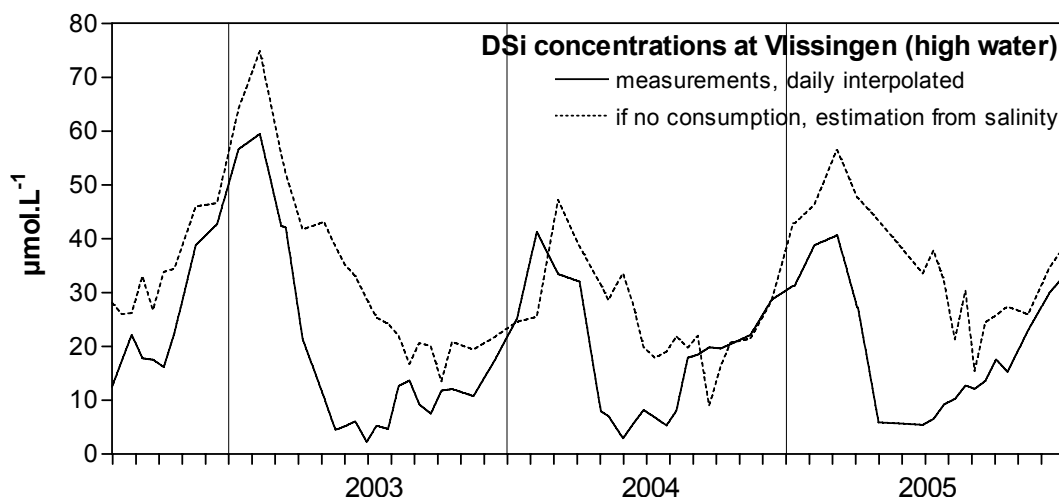


**Figure 24**. DSi concentrations at Vlissingen (high tide), measured (data from Figure 21c) or calculated from salinity data (Figure 21d), i.e. if there was no DSi consumption in the Scheldt estuary, nor in the coastal zone.

The maximum difference between the "mixing" and "measurement" curves (§4.4.3, Figure 26) was about 30 µM to 40 µM and occurred each year in April-June. As

spring diatom blooms are known to occur both in the coastal zone and in the estuary, this difference could be ascribed to diatom consumption. Our calculation does not provide a precise distribution of consumption in the coastal zone and in the estuary. However, it shows that freshwater discharge plays an important role in the dynamics of DSi concentrations at Vlissingen, and thus presumably in the coastal zone. When the "mixing" DSi concentrations are calculated from salinity, a hysteresis similar to the one for salinity can be observed for DSi (not shown). This stresses the importance of past hydraulic regime and of the transient phenomena for the estimation of the DSi transport in the Scheldt.

When plotted against freshwater discharge, DSi concentrations in the freshwater end-member also show a particular pattern (Figure 22). This could however be easily explained by DSi consumption during summer and constant DSi concentrations in winter. Although not illustrated in our dataset, discharge may play a role in regulating DSi consumption by controlling the residence time and thus the diatom growth. Additionally, it is interesting to note the tendency of winter DSi concentrations to decrease at high discharge (Figure 22). This could be better observed in the temporal patter shown in Figure 25. This might be due to dilution by runoff water which would have not have been in contact with DSi-rich groundwater due to soil saturation.
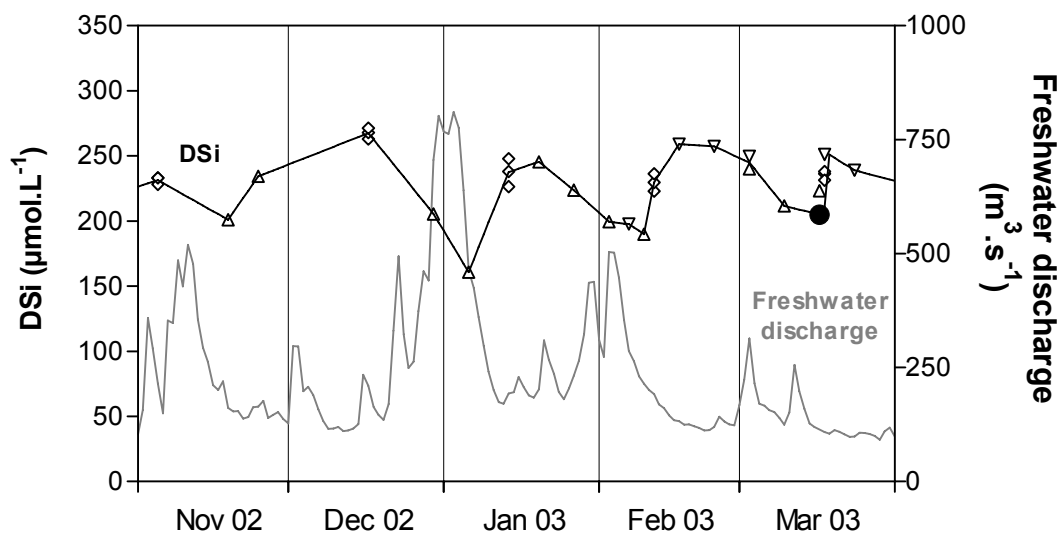


**Figure 25**. DSi concentrations and freshwater discharge in the freshwater end-member. Data and symbols for DSi concentrations are the same as those in Figure 21.

### 4.4.2 Procedure for estimation of conservative transport

In order to examine and evaluate the DSi consumption/remineralisation in the brackish estuary, DSi concentrations versus salinity profiles can be compared with the theoretical ones that would have been obtained if there was only mixing of the waters from the freshwater and the seawater end-members. This has been often performed in several estuaries using the "apparent zero end-member" method (Regnier et al., 1998 and reference therein). The method consists of plotting the concentration of the investigated element against the concentration of a conservative element (generally salinity). If the graph shows a straight line, the behaviour of the investigated element is estimated as conservative. Convex and concave curves are interpreted respectively as indicative of production and consumption within the estuary. However, this method requires the system to be at steady-state. Thus, interpreting the salinity plot with the "apparent zero end-member" method in the Scheldt estuary would lead to errors due to transient phenomena (Regnier et al., 1998). We used instead the 1D-CONTRASTE model (Regnier et al., 1998; Vanderborght et al., 2002) to simulate the conservative mixing of DSi, from the freshwater and the seawater end-members, in the brackish estuary. Data from Figure 21 were used as boundary conditions.

### 4.4.3 Comparison between measured and simulated DSi – salinity profiles

Each sample was taken at different times, irrespectively of the state of the tide. To eliminate the effect of the displacement of the water masses due to the tide, DSi concentrations are presented as a function of salinity (Figure 26). Except for one or two samples, measured DSi concentrations decreased from the freshwater end-member to the seawater end-member. Additionally, DSi concentrations along the brackish estuary were high in spring, in late autumn and winter, when there was no significant DSi consumption in the freshwater estuary (see §4.3).

Because sampling campaigns lasted generally from one to several days, it was then chosen to compare the measured profiles with the model output corresponding to the date of high tide at Vlissingen which was the closest to the mean sampling date (Figure 26). The variation within the sampling period of the simulated DSi concentrations for a given salinity was indeed small: the standard deviation was generally below 2% of the average and always below 4%, except for salinities below 5 psu during the campaigns of March 2003, July 2003 and May 2004 due to high frequency variations in DSi concentrations in the freshwater end-member. The profiles obtained by interpolation between neap and spring profiles are also shown in Figure 26. These interpolated profiles did not differ significantly from the instantaneous ones.
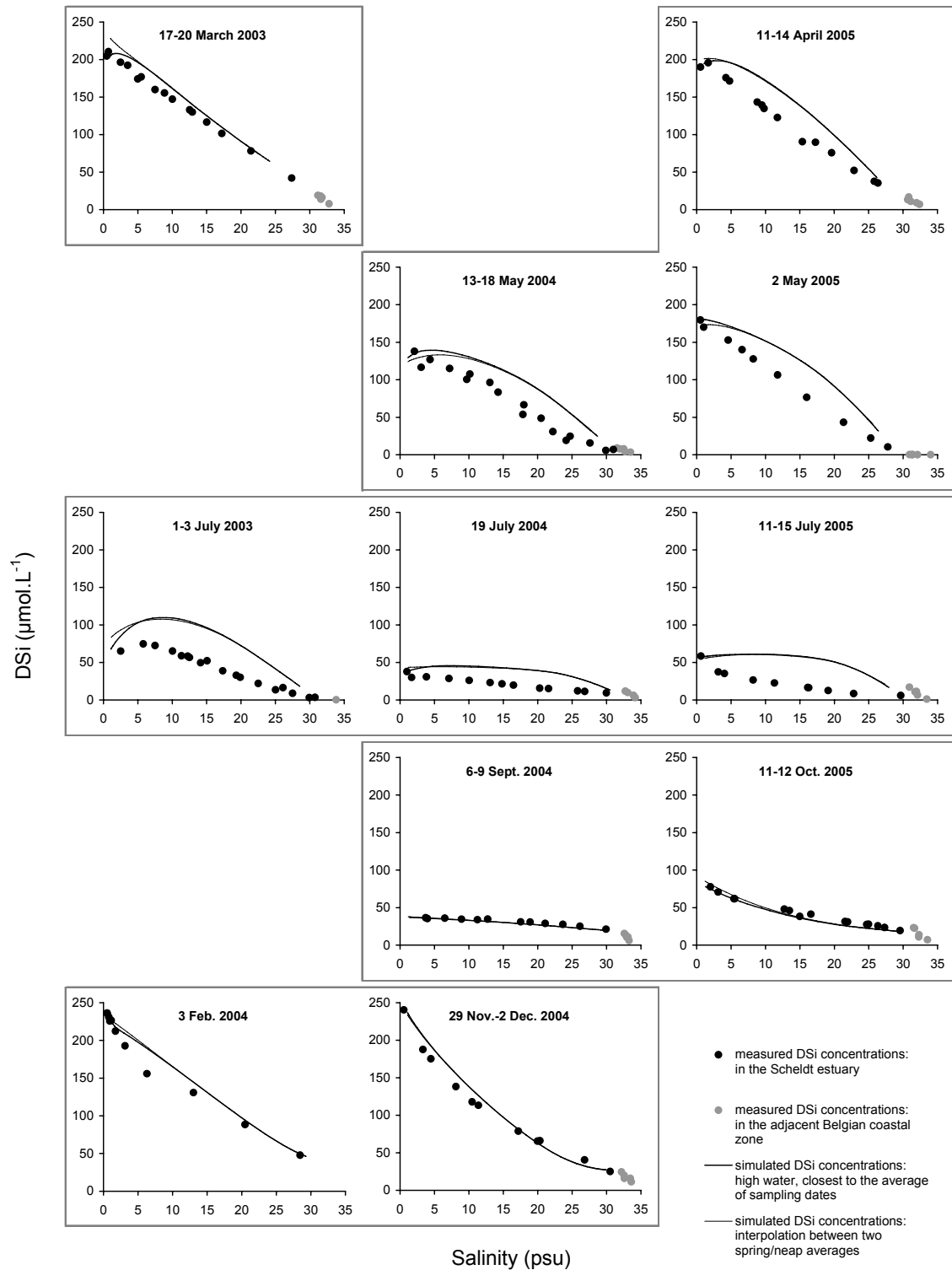
**Figure 26**. Measured (dots) and simulated (lines) DSi concentrations in the brackish estuary plotted against salinity. The sampling periods indicated correspond to the range of sampling dates only in the estuary (i.e. not in the sea).

DSi profiles obtained by simulation of purely conservative transport were generally strongly convex in spring and summer, but concave in winter (Figure 26). This was explained by transient phenomena due to the fact that DSi concentrations in the freshwater end-member varied faster than the residence time of the water in the estuary. In spring and summer, DSi concentrations in the freshwater end-member decrease at a rate of about 100 µM per month (Figure 21b). However it takes one to two months for the estuary to re-equilibrate due to the residence time of the water (1 to 3 months). Thus, when DSi in the freshwater end-member is decreasing, DSi concentrations may be higher in the middle estuary than in the upper estuary. The opposite happens in winter when DSi increases again. The application of the "apparent zero end-member" method on such profiles would have led to the erroneous conclusion of a DSi production in spring-summer and DSi consumption in winter.

The difference between the simulated and measured DSi profiles demonstrates also that a nearly linear profile of measured concentrations plotted versus salinity could not be interpreted as conservative transport of DSi in the estuary: the end-member concentrations being identical for the measured and simulated profiles as they have been set as boundary conditions, a difference between the two profiles indicates the occurrence of DSi consumption (or remineralisation) in the brackish estuary. The comparison showed a conservative transport in winter, but a consumption of DSi in the brackish estuary in spring-summer as the simulated DSi profiles were always higher than measured ones. The seasonal behaviour of DSi in the estuary was found to be identical in 2003, 2004 and 2005. Four to five periods could be observed as illustrated by the five groups of graphs on Figure 26.

In late-winter early-spring (March), there was not yet significant DSi consumption in the freshwater estuary (Figure 21b) and the estuary had re-equilibrated after 3 months of (nearly) constant DSi concentrations in the freshwater end-member. The measured DSi profile did not differ much from the simulated one indicating that there was hardly any DSi consumption in the estuary.

In spring (April-May) however, DSi was still barely altered in the freshwater estuary, but it was consumed in the brackish estuary with a maximum difference of 40 µM in the zone from 10 psu to 20 psu. Interestingly, the maximum relative estuarine consumption was around 30% at 17 psu in April and DSi was not yet consumed in the coastal zone. But in May, DSi was depleted in the coastal zone and the relative DSi consumption increased almost linearly with salinity, reaching 70% and 50% in the most seaward part of the estuary in May 2004 and May 2005 respectively. This suggests that the early-spring diatom development was not only of marine origin, a hypothesis supported by the fact that phytoplankton analysis revealed the presence of a typical estuarine phytoplankton community. But later in May, DSi might be

consumed in the downstream part of the estuary by intrusion into the estuary of the marine diatoms, which could eventually develop better in the estuary than in the coastal zone (as in May 2004, see Figure 27 in §4.4.4) presumably due to nutrient availability.

In July, DSi was consumed in the freshwater estuary (but not depleted). However, due to transient phenomena, even higher concentrations would be expected at around 5 psu or 10 psu if there was only conservative mixing. DSi was consumed in the estuary with maximum consumption ranging from 20 µM to 50 µM at around 15 psu to 20 psu. DSi concentrations started to increase again in the coastal zone (in 2004 and 2005) and, compared to May, the maximum relative consumption was shifted upstream to the 20-25 psu zone (60% to 80% consumption). The DSi concentrations increased in the sea while they were low in the estuary, especially towards the mouth, suggesting that there was a source of DSi in the coastal zone other than the Scheldt.

In early autumn (September-October), DSi was still at low levels in the freshwater end-member, but was not consumed anymore in the brackish estuary. This was coherent with the fact that DiatChla concentrations were nearly zero above 10 psu (see Figure 27 in §4.4.4). Although the residence time in the estuary is about three months in summer, the estuary re-equilibrated quickly from "consumption" to "conservative transport" situations. To allow enough time for this re-equilibration, DSi consumption might have already stopped in mid-summer. Indeed, even if there was DSi consumption in July, DiatChla concentrations were already low. The DSi consumption might have then happened earlier and its effect would have been still present in July due to the residence time of water. This decrease in diatom (and phytoplankton) biomass may appear as a paradox since the summer weather and the presence of nutrients in not-limiting levels provide ideal conditions for phytoplankton growth. Indeed, diatom blooms reach their maximum in summer in the freshwater estuary even if they may be limited by DSi availability (see Figure 17 in §4.3.1). However, the functional difference in the two parts of the estuary may be due to the presence of different zooplankton species with different grazing efficiencies. The phytoplankton biomass may be controlled by grazing in the brackish estuary as the zooplankton community is dominated by copepods, while in freshwater estuary the zooplankton community is dominated by rotifers (Muylaert et al., 2005).

DSi concentration in the freshwater end-member was back to high levels in winter. No DSi consumption was expected in the brackish estuary and the difference between the simulated and the measured profiles was indeed small. In February however, the highest difference at 6.3 psu might be ascribed to transient phenomena which were not simulated due to under-sampling for DSi in the freshwater-end

member. Indeed, a peak of discharge occurred between 12/01/2004 and 21/01/2004, whereas DSi was sampled on 12/01/2004 and on 27/01/2004 (Figure 21).

### 4.4.4  Longitudinal profiles of SPM and BSi

In estuaries, the dynamics of suspended particulate matter (SPM) and of dissolved components can be uncoupled as the particulate matter does not necessarily follow a water mass because of settling and resuspension processes. However, combined DSi and BSi mass-balances could be performed in the freshwater estuary where there was a net downstream transport of SPM (Chen et al., 2005). But this is not the case for the brackish estuary where, below 10 psu, there is a net upstream SPM transport. Additionally, the brackish estuary receives fluvial SPM, originating from the freshwater estuary, as well as marine SPM. Van Maldegem et al. (1993) estimated indeed that, in the brackish estuary, there was a 50% retention of the $300 \times 10^6$ to $400 \times 10^6$ kg yr$^{-1}$ of fluvial SPM, and a complete settling at a salinity lower than 5 psu of the $200 \times 10^6$ kg yr$^{-1}$ SPM of marine origin. The estuary acts thus as a sink for SPM. This is the reason for dredging activities, which maintain navigation channels.

However the SPM does not settle uniformly along the estuary. The deposition sites are mainly the intertidal areas, and in particular Saeftinge corresponding roughly to the 10 psu zone under average freshwater discharge (Van Maldegem et al., 1993). Upstream of this zone, a maximum of turbidity is generally observed, indicating an accumulation of SPM in this area (around 5 psu) and a higher residence time for the particulate matter than for the dissolved elements (Chen et al., 2005). Several explanations were put forward for this accumulation (Chen et al., 2005): 1) the salinity change in this zone induces flocculation/deflocculation processes which affect the incoming fluvial SPM, 2) this zone is the meeting area of two opposite residual bottom currents: the one from the brackish estuary orientated landwards, and the one of the freshwater estuary orientated seaward, and 3) the water energy (mainly tidal in this area) is maximum in this zone. Additionally, the SPM concentration was found to be highly dependant of the state of the tide, as a significant amount of particulate matter settles and is resuspended at each tide cycle: SPM concentrations could vary by a factor 4 within one tidal cycle (Chen et al., 2005). Downstream of 10 psu, the SPM concentrations remain constant during a tidal cycle.

The SPM dynamics could not be investigated based on our data (Figure 27) as samples were taken irrespective to the tidal phase. However, features such as turbidity maximum events above 5 psu but lower SPM concentrations at 10 psu and downstream could be observed. The particular SPM dynamics described above are nevertheless important for the phytoplankton dynamics and can explain the behaviour of BSi in this part of the estuary (Figure 27).

Highest Chla concentrations were found in most freshwater parts of the estuary from May to September (Figure 27). They are due to the upstream summer blooms in the freshwater estuary. However, the concentrations quickly dropped before reaching 5 psu and, except during the late-spring bloom, Chla and DiatChla concentrations were low (below 5-10 µg l$^{-1}$) in the brackish estuary with salinity > 5 psu, reaching a few µg l$^{-1}$ from September onwards. More than the result of an osmotic stress, this sudden mortality of freshwater diatoms at around 5 psu was attributed to light limitation because of high SPM concentrations and the deepening of the channel (Desmit et al., 2005).

BSi concentrations were always at a level around 10 µM to 40 µM except during summer (mid-July to September) when higher concentrations were reached, however only above 5 psu. In contrast to DiatChla and Chla concentrations, there was no significant seasonal variation in BSi concentration. Even if, as for the freshwater estuary, the phytoplankton community in the brackish estuary was dominated by diatoms, BSi concentrations did not follow the DiatChla concentrations (nor the Chla concentrations). Indeed, comparing DiatChla and BSi concentrations with Si:C ratios found for the freshwater estuary (see §4.3.4) or in the coastal zone (Rousseau et al., 2002), most of the BSi did not correspond to living diatoms. Rather, it seemed more linked to the SPM dynamics. During summer, high BSi content of the suspended matter (expressed as $SiO_2$ containing 10% of water) could be observed upstream of salinity 5 psu due to the bloom that occurred in the freshwater reaches. The rest of the year below 5 psu, and year-round between 5 psu and 15 psu, the BSi content was relatively constant at around 3% but increased towards the sea reaching values ranging from 6% to 10% in the coastal zone.

The close link between BSi and the bulk SPM suggests that, as for the SPM, 1) there is a transport of BSi of marine origin from the coastal zone upstream to 5 psu (thus the increasing BSi content could be explained by mixing between fluvial and marine SPM of different BSi contents), 2) the brackish estuary is a sink for BSi, 3) BSi deposition should occur in intertidal areas, and 4) there is an extended retention time of the BSi at around 5 psu with significant settling and resuspension.

left scales:

—— SPM (mg/L)
- ● BSi (estuary, µmol/L)
- ○ BSi (coastal zone, µmol/L)

right scales:

—— Chla (µg/L)
- - - DiatChla (µg/L)
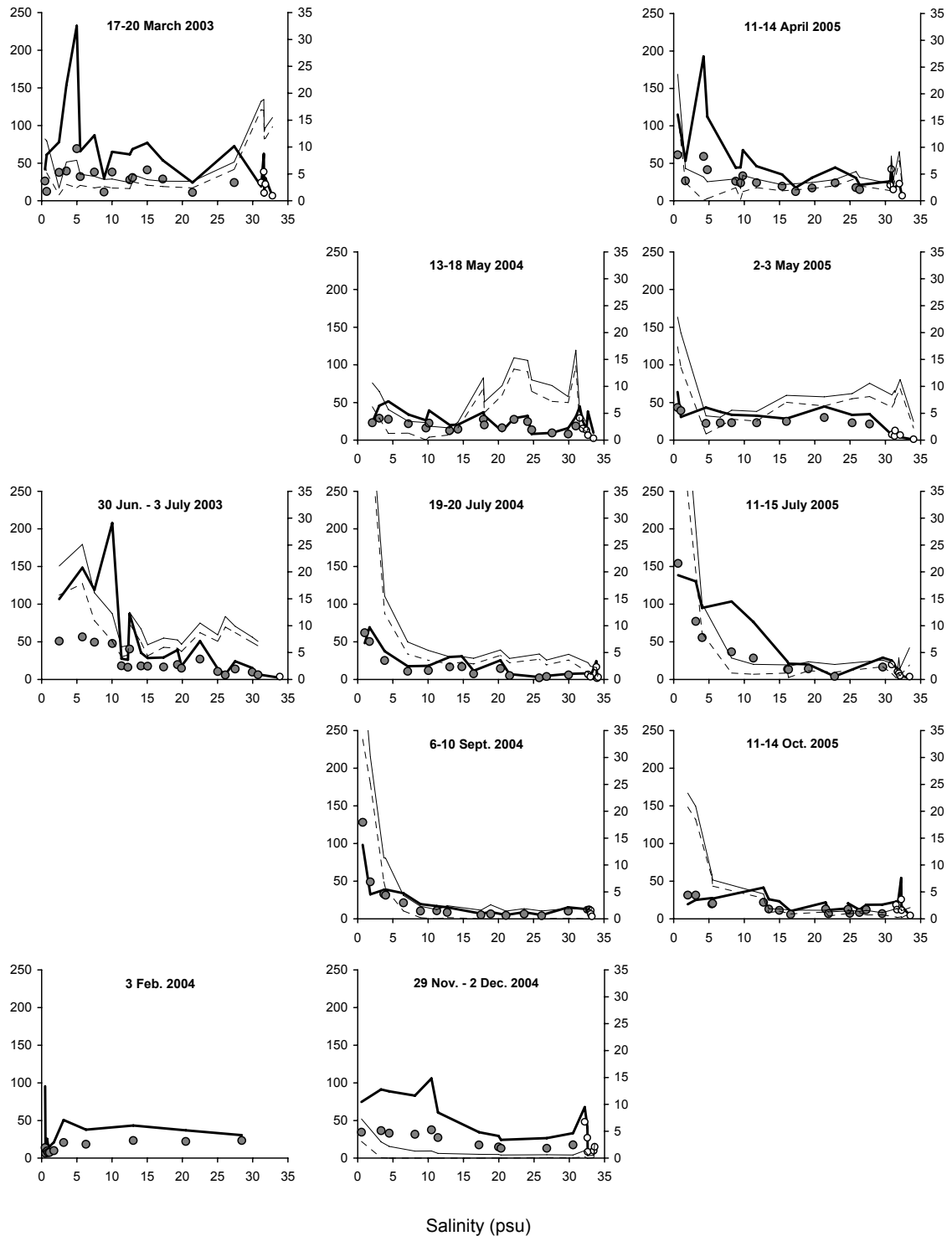


**Figure 27**. BSi and SPM (left scales), and Chla and DiatChla (right scales) concentrations plotted versus salinity in the brackish estuary and in the coastal zone.

## 4.5 Benthic fluxes and regeneration of silica in the sediments of the Scheldt continuum

### 4.5.1 Distribution of BSi in surface sediments

Surface sediments collected along a salinity transect across the Scheldt continuum during the 2004 cruises were analysed for their BSi contents. The measured values were relatively low and the longitudinal distribution showed no clear tendency (Figure 28). BSi contents were higher during September and November, which could be explained by the sedimentation of diatoms following the summer/early autumn blooms. During winter, the biogenic silica accumulated in the surface layer either dissolved and was released to the water column, or was further incorporated into the sediments where dissolution probably continued along with other diagenetic processes, such as metallic ions (Al, Fe…) incorporation into the frustule.
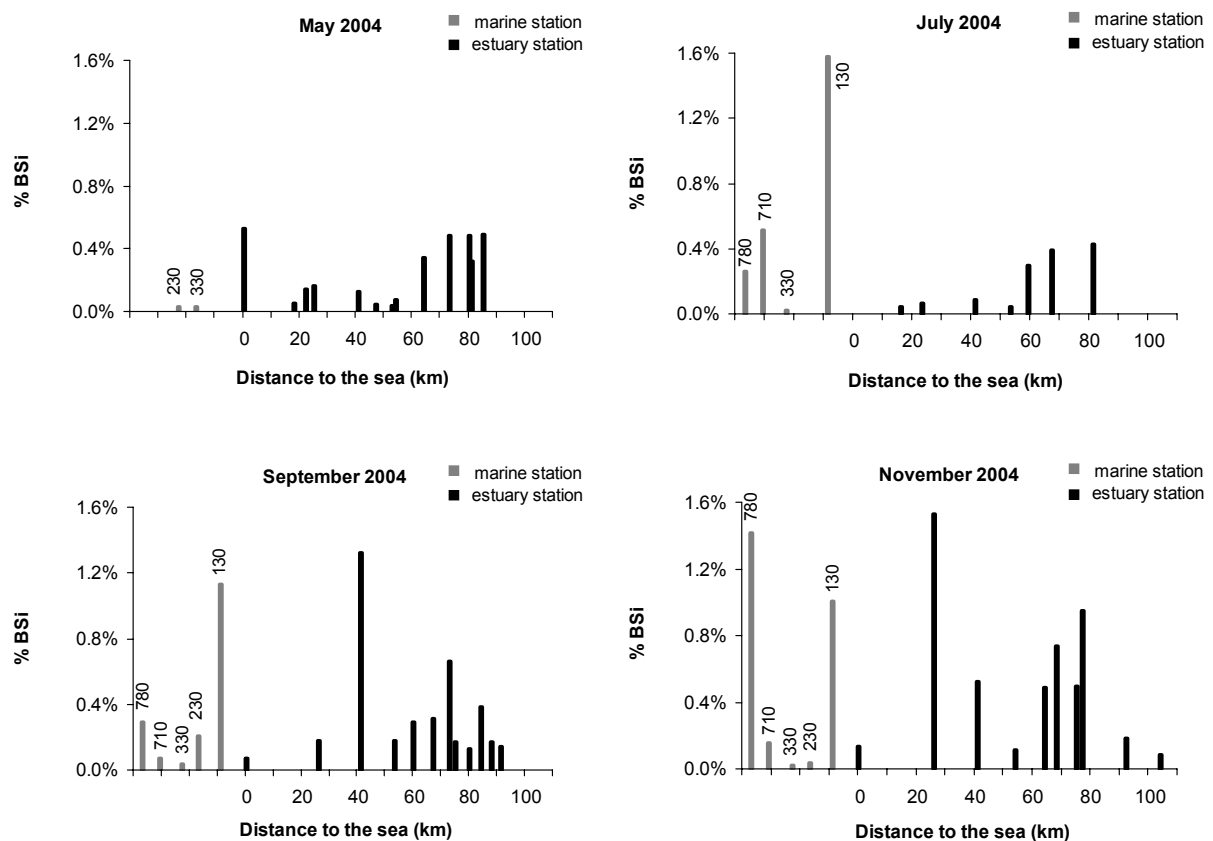


**Figure 28**. Longitudinal distribution of BSi content in the surface sediments of the Scheldt continuum.

Sediments were generally characterised by their heterogeneity. Sandy, rough sediments (stations 230 and 330, coastal zone) exhibited very low BSi contents,

while fine-grained material (stations 130 and 780, coastal zone) was more enriched in BSi. This suggests a strong influence of the hydrodynamic transport of particles on the BSi content of the sediments.

### 4.5.2 Vertical profiles of DSi and BSi in the sedimentary column

A few of the obtained profiles for the four stations where cores were taken for both sampling years are shown in Figures 29 and 30. The overall BSi content was very low and the maxima, generally reached at depth, did not exceed 5%, mainly due to the important dilution of biogenic matter by the lithogenic material. In general, BSi content and DSi concentration increased with depth, suggesting a rapid incorporation of biogenic material downcore and its relatively rapid dissolution in the first 15 cm of the sedimentary column. As a general feature, values were lower for the year 2005 than for 2004.

Station 230, located in the coastal zone, with an average salinity of 32.5 psu, was characterised by sandy, coarse sediments, and an important benthic biological activity. BSi contents of the sediments and pore water DSi concentrations in this area were globally about 10 times smaller than those observed for the estuarine sediments (Figure 29). This could be partly explained by the fact that diatoms were the dominant species in the estuary throughout the year, which was not the case in the coastal zone where they were the prevailing group only during certain periods. Also, the important benthic activity in this area could enhance the diagenetic processes, leading to an important dissolution of the BSi, and increase the transfer of the DSi to the water column. Furthermore, the fluxes through the sediment–water interface were facilitated by the permeable nature of the sediments. However, both the BSi and DSi values in October 2005 were much higher, suggesting that a relatively recent deposition event could have occurred.

Station S01, situated at the mouth of the estuary, had an average salinity of 30 psu and was characterised by a mixture of sandy and muddy sediments (Figure 29). Typical cores from 2004 exhibited a first sandy layer, with rather coarse material, followed by a compact, black mud layer. However, in 2005, the sandy layer was thicker, and the sediments had a general rougher granulometry. The BSi contents and the DSi concentrations were generally low in the first centimetres, but increased downcore, with the exception of the core taken in May, which exhibited high values near the surface, probably due to a recent deposition event of a diatom spring bloom.
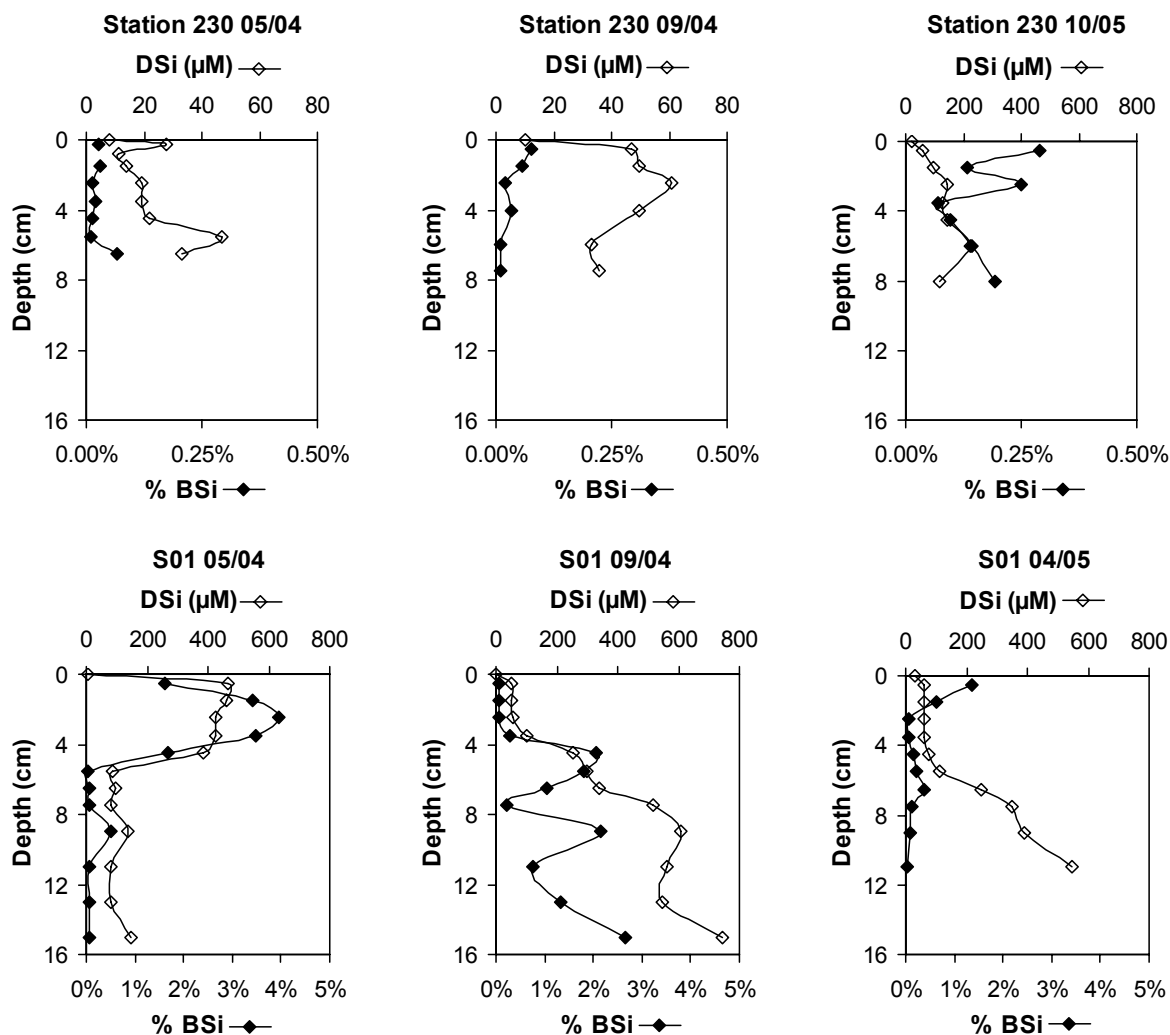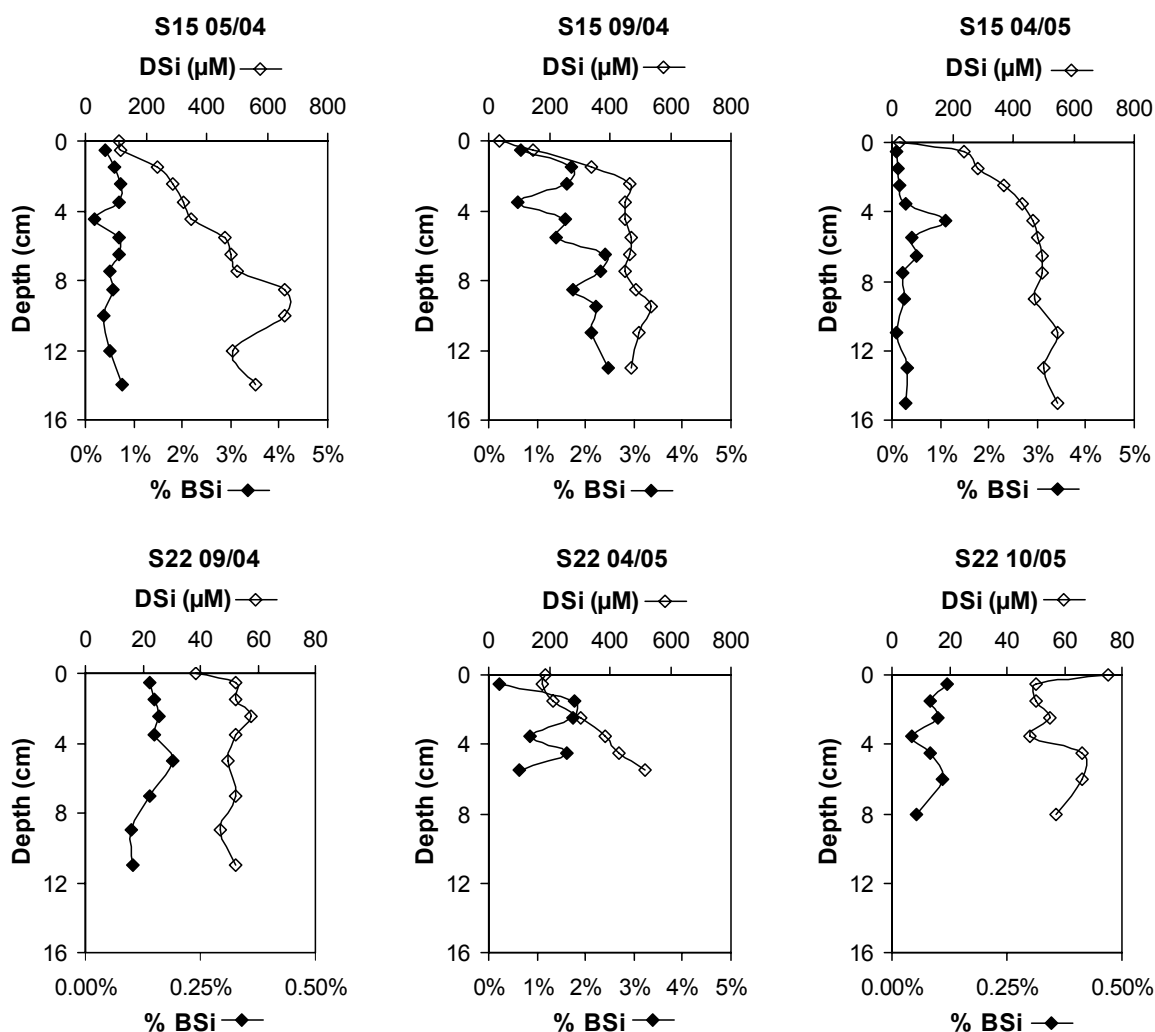
**Figure 29**. Vertical profiles of DSi in interstitial waters and of BSi contents in sediments for stations 230 (coastal zone) and S01 (mouth of the estuary).

Station S15, situated in the maximum turbidity zone, had a salinity varying between 5 psu and 15 psu (Figure 30). Sediments collected during 2004 were muddy, with a very fine grain size, while those collected in 2005 were rather consolidated, sandy, and with a coarser grain size. The observed BSi contents and DSi concentrations were higher for 2004 than for 2005, but for both years they exhibited a general increase with depth.

Station S22, also located in the maximum turbidity zone, had a salinity varying between 2 psu and 10 psu (Figure 30). Sediments in this area were mostly sandy, very compact, and with rather rough granulometry. The BSi content and the DSi concentration were about 10 times lower than those in sediments from the other estuarine stations (S15, S01) with the exception of April 2005, when they were slightly higher. This could be explained by the deposition or transport of deposited

biogenic material from the upper reaches, where the diatom bloom could have occurred as early as March.



**Figure 30**. Vertical profiles of DSi in interstitial waters and of BSi in sediments for stations S15 (maximum turbidity zone) and S22 (maximum turbidity zone, low salinity).

There is no clear tendency in the vertical distributions of BSi contents in the sediments and of DSi concentrations in the interstitial waters. Values for both parameters generally increased with depth and showed that although dissolution was important in the first centimetres, part of the biogenic material was incorporated in the sediments, where dissolution continued. As for the surface sediments, these results also suggest a correlation between the sediment type (sandy or muddy) and the BSi content. Based on these profiles, one can also note that the first centimetres of the sedimentary column were probably subject to different transient processes such as vertical mixing of the superficial layers, re-suspension and re-sedimentation. The Scheldt estuary is indeed a very heterogenic environment, with strong hydrodynamic

forcings and numerous human activities (navigation, dredging…) which could influence the transport of particles.

The vertical profiles of DSi in the interstitial waters can also be used to calculate the fluxes across the sediment–water interface and thus to estimate the contribution of sediments as a source of DSi for the water column. These calculated fluxes are presented in the following section, and are compared to the values obtained by direct measurement via incubation experiments of sediment cores.

### 4.5.3 Benthic fluxes of DSi across the sediment–water interface

In order to measure the fluxes of DSi across the sediment–water interface several incubation experiments of sediment cores were performed on board the RV Belgica, as well as in the laboratory during the years of 2005 and 2006.

On board incubation experiments were generally carried out for 36 to 72 hours using sediment cores freshly collected. Figure 31 shows as an example the amount of DSi released as a function of time for cores sampled at stations S01 (mouth of the estuary) and S15 (maximum turbidity zone), for the months of July and October 2005 and April 2006.



Figure 31. Evolution with time of the amount of DSi released to overlying waters for on board incubation experiments of sediment cores collected at stations S01 and S15, for the months of July 2005, October 2005 and April 2006.

It can be noted that the amount of DSi released from the sediments to the overlying water column was higher for station S01 than for station S15. This could be explained mainly by the lower DSi concentration in the overlying water column at the mouth of the estuary. Therefore, the initial concentration gradient across the

sediment-water interface would be more important for station S01 than S15, leading to higher fluxes as well as rates of dissolution of the biogenic material at station S01.

The increase in DSi in the water column was the lowest during springtime, and the highest in summer, with intermediate values during autumn, although for station S15 the differences between October and April were less noticeable. This could be attributed to the presence of fresh BSi that settled following the spring diatom blooms. BSi was dissolving throughout the year, but dissolution was enhanced during the summer period due to the higher water temperatures. This biogenic material could also be incorporated into the sedimentary column and altered by various early diagenetic processes modifying its solubility, which is probably the reason for the low values of released DSi observed during spring.

Longer incubation experiments (up to 3 months) were also carried out in the laboratory on frozen cores. The results for samples collected in October 2005 are shown in Figure 32. For all stations a very rapid release of DSi was observed at the beginning of the experiment, which then decreased, probably mainly due to the build-up of DSi in the water column, but also to a decrease of the concentration of reactive silica present in the sediments. In the example presented here, the highest increase in DSi was obtained for the marine station, and the observed values decrease upstream.

Assuming that the release of silica as function of time follows a linear rate law, the fluxes can be easily obtained by dividing the slope by the core area (Aller et al., 1996). This technique is generally better adapted to experiments carried out during relatively long periods of time, where the influence of initial processes such as the establishment of a new equilibrium between sediments and overlying water is less important than for shorter experiments. Nevertheless, we used this approach to determine the fluxes as it represented a good first approximation; the results are presented in Table 2.

The values obtained were relatively high but, as expected, they decreased from the coastal zone towards the upper part of the estuary, with the exception of April 2006. The fluxes measured during the laboratory experiments were generally higher than those obtained on board, which might be due to the precipitation of dissolved silica as the cores were frozen. However, station S22 exhibited atypical values for April 2006, which could be explained by the difficulties encountered during sampling, due to the presence of gravel and consolidated sediments.
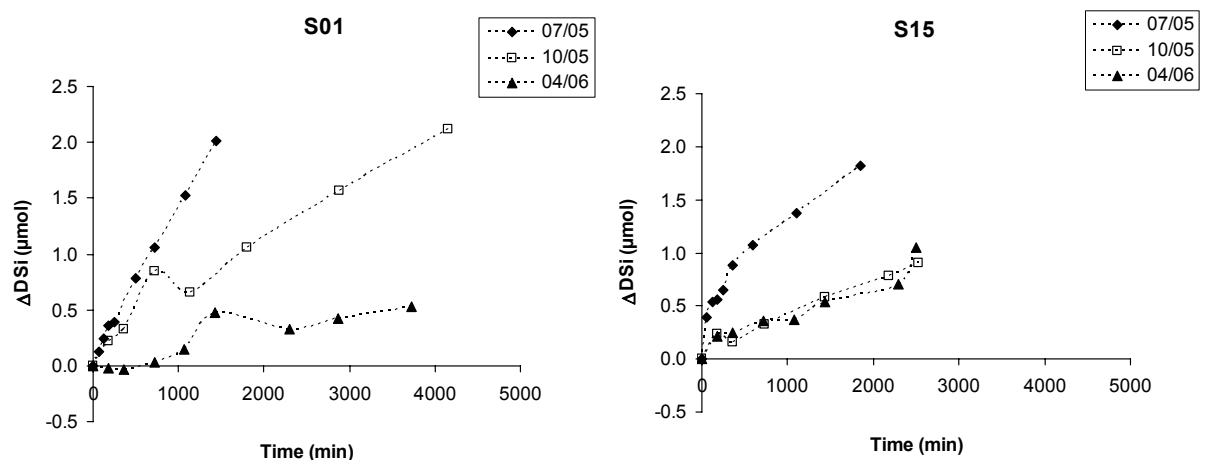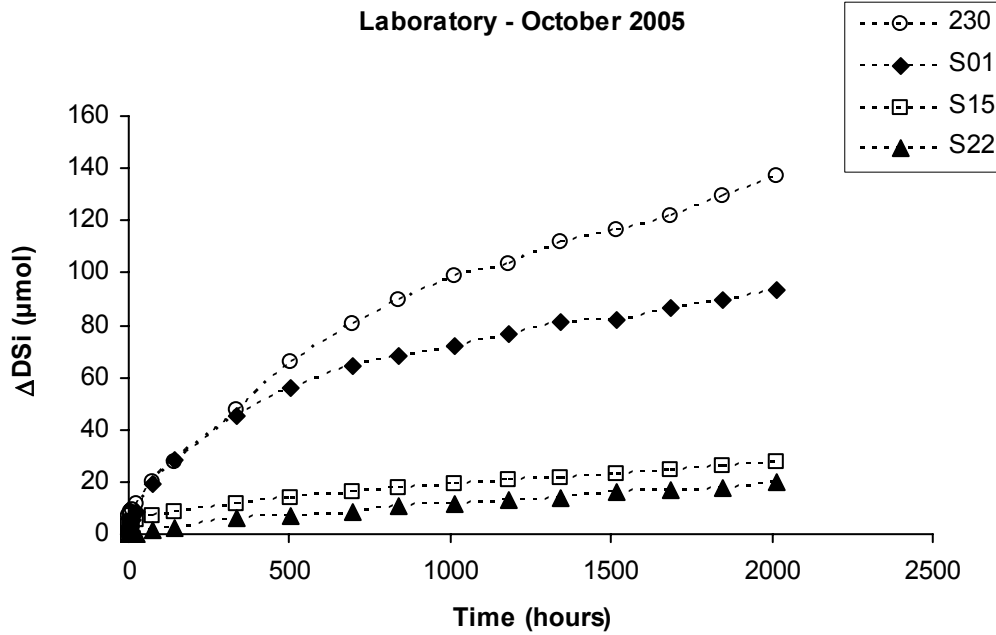
**Figure 32**. Evolution with time of the amount of DSi released to overlying waters for laboratory incubation experiments of sediment cores collected in October 2005 at stations 230, S01, S15, S22 (Clip, 2006).

**Table 2**. DSi fluxes (F, in mmol m$^{-2}$ day$^{-1}$) across the sediment–water interface as measured via incubation experiments. Positive values indicate fluxes from the sediments to the water column. The initial DSi concentration of the overlying water is also shown (DSi$_0$).

|  |  | 230 | | S01 | | S15 | | S22 | |
|---|---|---|---|---|---|---|---|---|---|
|  |  | F | DSi$_0$ ($\mu$M) | F | DSi$_0$ ($\mu$M) | F | DSi$_0$ ($\mu$M) | F | DSi$_0$ ($\mu$M) |
| July 05 | 72 h | 23.09 | 21 | 1.24 | 7 | 0.77 | 33 | 0.30 | 26 |
| Oct. 05 | 72 h | – | – | 1.58 | 16 | 0.30 | 88 | -0.023 | 53 |
| Oct. 05 Lab. | 72 h | 3.23 | 12 | 3.63 | 17 | 1.04 | 25 | 0.23 | 53 |
|  | 3 months | 1.03 | – | 0.71 | – | 0.18 | – | 0.15 | – |
| April 06 | 72 h | 0.22 | 6 | 0.14 | 4 | 0.30 | 16 | 6.48 | 196 |
| April 06 Lab. | 72 h | – | – | 0.40 | 19 | – | – | 2.27 | 100 |
|  | 2 months | – | – | 0.22 | – | – | – | 0.15 | – |

Fluxes can also be calculated from the vertical profiles of DSi in the interstitial waters by means of the first Fick's law of diffusion applied to sediments:

$$F_d = -\Phi * D_s * \left( \frac{\partial C}{\partial x} \right) \qquad \text{(Eqn. 4)}$$

where $F_d$ is the diffusive flux, $\Phi$ is the sediment porosity, $D_s$ is the whole sediment molecular diffusion coefficient for silicic acid (DSi), C is the DSi concentration, and x is the depth. $D_s$ is actually the molecular diffusion coefficient of silicic acid, $D_m$, corrected for tortuosity (Berner, 1980), with $D_{m,36} = 10^{-5}$ $cm^2$ $s^{-1}$ for seawater of salinity 36 psu at 25°C (Wollast and Garrels, 1971). A supplementary correction for $D_m$ is needed in order to use it for different salinity values, and it is based on the relation:

$$D_{m,\,36} \,/\, D_{m,\,a} = \eta_a \,/\, \eta_{36} \qquad\qquad \text{(Eqn. 5)}$$

where $\eta_{36}$ and $\eta_a$ are the viscosities for salinity 36 psu and a given salinity a, respectively (Li and Gregory, 1974). As a first approximation of the DSi concentration gradient with depth we used the difference in concentration between the pore water of the first or second centimetre of sediment and the overlying water.

The values obtained (Table 3) are, in general, much lower than those measured via incubation experiments, but comparisons are quite difficult given the inherent differences in methodology. Indeed, the incubation experiments give an insight on the diffusion of DSi from the sediments to the water column, but probably limited to the superficial layers. They also take into account the dissolution of reactive silica, particularly those carried out on longer periods of time. In contrast, the fluxes based on the vertical DSi profiles are purely diffusive and take into account the sediment nature and structure. These calculated values are almost in the same range as the one obtained using a similar procedure by Beckers and Wollast (1976), that is 43.2 µmol $m^{-2}$ $d^{-1}$, which is one of the very few, if not the only, available data concerning the DSi fluxes across the sediment–water interface in the Scheldt estuary.

**Table 3**. Calculated DSi fluxes from the vertical profiles of DSi in interstitial waters, in µmol m$^{-2}$ d$^{-1}$. The salinity of the time of sampling is also shown.

| | 230 | | S01 | | S15 | | S22 | |
|---|---|---|---|---|---|---|---|---|
| | Salinity | Flux | Salinity | Flux | Salinity | Flux | Salinity | Flux |
| **2004** | | | | | | | | |
| May | 31.97 | 39.7 | 30.02 | 467.0 | 10.92 | 9.2 | – | – |
| Sept. | 32.65 | 37.2 | 29.62 | 48.3 | 11.19 | 207.9 | 5.12 | 26.0 |
| Nov. | 33.59 | 25.2 | 30.62 | 79.4 | 12.09 | 265.5 | 2.86 | 225.2 |
| **2005** | | | | | | | | |
| April | – | – | 28.89 | 29.6 | 4.27 | 399.1 | 11.17 | 15.7 |
| July | – | – | 29.73 | 66.6 | 7.92 | 386.9 | – | – |
| Oct. | 31.59 | 35.1 | 29.55 | 14.7 | 12.58 | 0.71 | 7.07 | 16.0 |

We did not observe, as it was the case for the measured fluxes, a decrease in benthic DSi fluxed from the coastal area upstream. The highest values were obtained for station S15, located in the maximum turbidity zone, with the exception of station S01 in May 2004, when a very recent deposition event of fresh biogenic material probably ocurred, as mentioned previously. In the coastal zone, fluxes vary very little throughout the two years, with an average value of about 34 µmol m$^{-2}$ d$^{-1}$. In the estuary, on the contrary, they vary widely and not only among the different stations, but also from season to season and from year to year, illustrating once again the extreme heterogeneity of this very hydrodynamic system.

The above dataset suggests that probably the very first centimetres of the sedimentary column are the most active layer in the recycling of biogenic and other forms of reactive silica. They are in contact with the water column, and phenomena other than diffusive ones can affect the DSi transport across the sediment–water interface, such as the benthic biological activity or the bottom currents. Yet, in order to better asses the role of sediments as a source of DSi for the water column, more information is needed on the dissolution rates of BSi in this complex environment. The following section presents the main results of different dissolution experiments.

### 4.5.4  Regeneration of silica in the sediments

The dissolution kinetics of biogenic silica plays an important role in understanding the biogeochemical silica cycle not only in the sediments, but also in the water column. Indeed, dissolution of the diatom frustules begins already in the water column and can continue after deposition. If the dissolution rate is high, the frustules will rapidly dissolve in the superficial sediment layer, and the fluxes of DSi to the water column will be important. If, on the contrary, the dissolution rate is low, the DSi fluxes will also be low, and part of the settling biogenic material will be incorporated in the sedimentary column, where early diagenetic processes will transform it, modifying its solubility. In this environment, the DSi released can also be trapped and consumed by different diagenetic reactions, such as the precipitation of authigenic clays. Thus, the regeneration of DSi in the sedimentary column could constitute a source for the water column (House et al., 2000), but there is still little information available for the Scheldt continuum. In the present study, we report the results of dissolution experiments carried out on sediments collected from various locations and depths, at different salinities in order to better assess the role of the sedimentary column as a source of DSi.

#### 4.5.4.1  Influence of salinity

The first experiments were carried on diatomaceous earth, which is used as reference material for pure biogenic silica (95% BSi), and the influence of salinity on the dissolution rate was investigated. The results showed a fast initial release of silica, followed by a rapid decrease (Figure 33a). The DSi concentration seemed to approach an asymptotic value, suggesting that an apparent solubility was reached. The dissolution was enhanced by increasing salinity, which could be attributed to the formation of Na surface complexes (Plettinck et al., 1994). However, only a very small percentage of the total biogenic silica present in the sample dissolved even after more than a month, showing that the dissolution was a very slow processes.

The effect of salinity was also studied for the dissolution of natural samples. We chose to examine the dissolution behaviour of sediments collected at station S15, located in an area where salinity could vary significantly within a tidal cycle. The working salinities were 0 psu, 5 psu and 15 psu, values characteristic of the sampling area. The results of the experiments carried out during 10 months (Figure 33b) showed again a fast initial release of DSi, followed by a slow-down while an asymptotic concentration was approached. However, in this case, there was no clear influence of the salinity and for the three salinity values considered the apparent solubility remained very low, suggesting that only a small amount of the biogenic material present was dissolved. These results are not surprising, as the BSi content in these samples is inferior to 5% weight, against 95% for the diatomaceous earth,

and the opal might have already been altered by various diagenetic processes such as adsorption and inclusion in the lattice of metallic ions (Fe, Al…) which can strongly decrease its solubility.
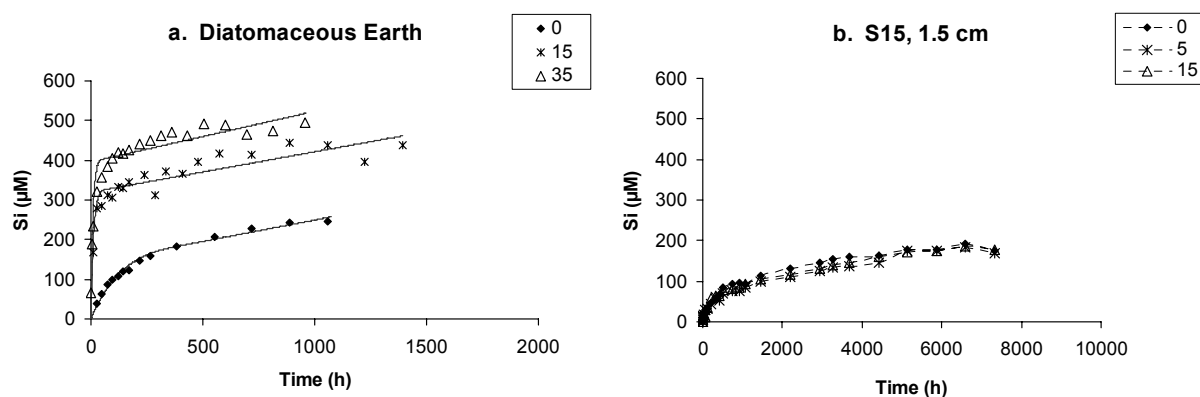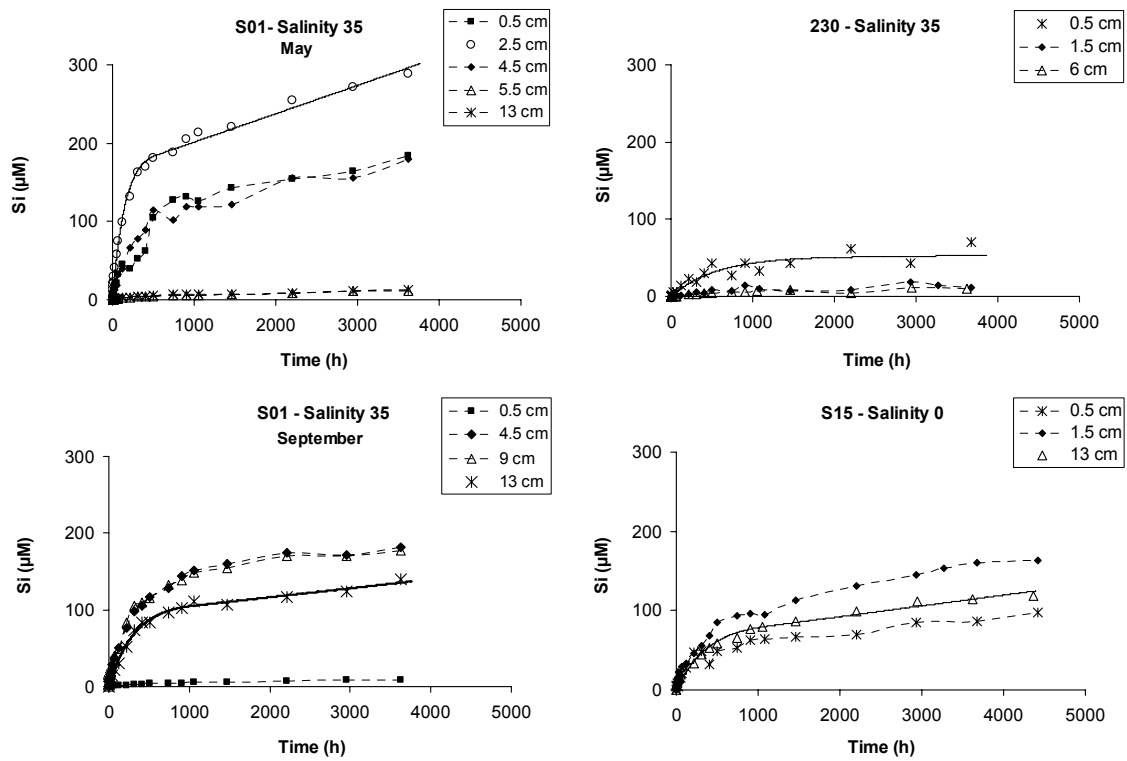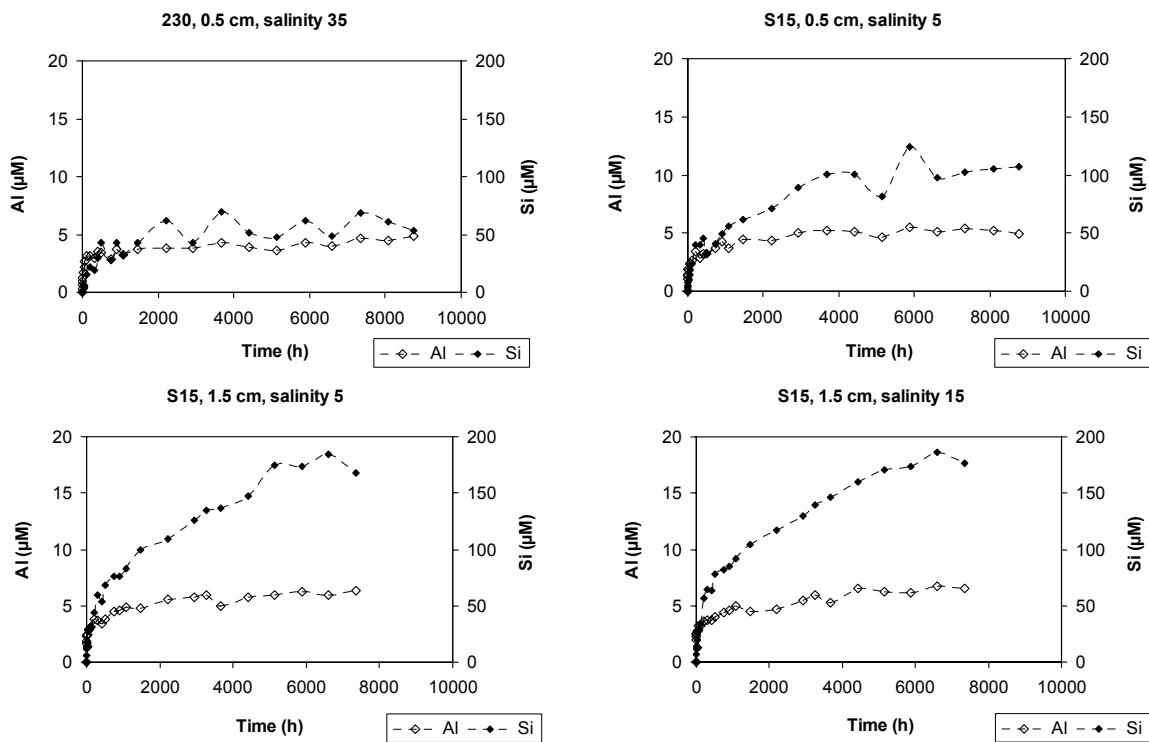


Figure 33. DSi released as a function of time for three different salinities, 0 psu, 15 psu and 35 psu. a. Diatomaceous earth, for an experiment time period of up to 2 months (De Bodt, 2005). Symbols represent the experimental data and curves the best fits using the model described in §4.5.4.3 (Eqns. 6 and 7). b. Sediments from station S15, September 2005, at 1.5 cm depth, for a duration of around 10 months. Only the experimental data are shown.

## 4.5.4.2 DSi released as a function of time – Variation with depth

The lowest DSi release values are observed for station 230 (Belgian coastal zone) characterised by sandy, coarse sediments with a low BSi content (Figure 34). Furthermore, the released DSi decreases downcore. On the contrary, for the May samples from station S01 (situated at the mouth of the estuary) high dissolution rates for the upper part of the cores and very low values at depth were obtained, in agreement with the measurements of BSi contents. For the September samples, the highest dissolution rates were found deeper in the core where the sediment was rather muddy and fine-grained, and the lowest at the surface where coarser material and low BSi levels were observed. Station S15, located in the maximum turbidity zone, exhibited intermediate dissolution rates; while lower values were observed at depth, the differences remained relatively small. As a general feature for both S01 and S15 stations, low dissolution rates were measured in the first centimetre and at depth, except for station 230. The dissolution rates appeared to be higher in the first centimetres under the surface, in good agreement with the vertical BSi profiles shown previously.

**Figure 34**. DSi released as a function of time – variation with the sampling depth. Symbols represent the experimental data and curves (—) the best fit using the model described in §4.5.4.3 (Eqns. 6 and 7).



**Figure 35**. Al and DSi released as a function of time.

Biogenic silica is not the only source of dissolved silica for interstitial waters, and lithogenic material such as alumino-silicates can also contribute to the DSi build-up in sediments. In order to assess the importance of the contribution of the lithogenic fraction, the release of Al was also measured as a function of time and some of the results obtained are shown in Figure 35. As for silica, there is a fast release of Al at the beginning of the experiment, which then slowed down very rapidly. The concentrations of Al reached quickly a relatively constant value, and whatever the sample considered this value did not exceed 5 µM. This suggests that the dissolution of lithogenic material was rather limited for the periods of time considered here. The almost constant concentrations observed could be attributed to the precipitation of Al(OH)$_3$ which has a low solubility at our working pH value (close to 8).

### 4.5.4.3 Modelling of dissolution kinetics

Pure BSi dissolution is generally modelled by a first-order kinetic rate law (Barker et al., 1994), but this cannot be applied to natural sediments characterised by many different physico-chemical phases. The simplest approach in this case is to consider the dissolution as a two-step reaction of samples composed of two phases: 1) a labile fraction, the so–called "biogenic material" (BSi), including all amorphous phases, as well as very fine grains, which dissolve rapidly and completely following a first-order kinetic law, and 2) a more refractory phase, the "lithogenic silica" (LSi), composed of the lithogenic phases and the coarser granulometry fractions, which follows zeroth-order dissolution kinetics (DeMaster, 1981). Although we use the term "biogenic" for the labile phase, "reactive silica" would be a more appropriate term, given its above definition.

During a first stage we have concomitant dissolution of the BSi and the LSi; in a second one, only the dissolution of the latter continues, as all the biogenic material would have been dissolved. Therefore we have:

$$\frac{dC}{dt} = k_B(C_{as} - C) + k_L \quad \text{for } C < C_{as} \tag{Eqn. 6}$$

$$\frac{dC}{dt} = k_L \quad \text{for } C > C_{as} \tag{Eqn. 7}$$

where C is the DSi concentration (μM), $k_B$ is the BSi dissolution rate constant ($h^{-1}$), $C_{as}$ is the asymptotic concentration reached when all the BSi is dissolved, and $k_L$ is the LSi dissolution rate constant ($\mu M\ h^{-1}$). By solving the above equations, we obtain:

$$C = (C_{as} + k_L/k_B)*(1 - \exp(k_B*t)) \quad \text{for } C < C_{as} \quad \text{(Eqn. 8)}$$

$$C = C_{as} - (k_L/k_B)*\ln[1 + C_{as}*(k_L/k_B)] + k_L*t \quad \text{for } C > C_{as} \quad \text{(Eqn. 9)}$$

$$t* = (1/k_B)*\ln[1 + C_{as}*(k_L/k_B)] \quad \text{for } C = C_{as} \quad \text{(Eqn. 10)}$$

where t is the time (h) and t* denotes the time at which BSi dissolution is complete. The values obtained for these parameters for a number of samples are summarised in Table 4, where the BSi contents in sediments are also indicated.

**Table 4**. Model parameters for dissolution of sediments taken at the three locations, for different depths and salinity values.

| Site | Depth (cm) | Salinity (psu) | $C_{as}$ (μM) | $k_B$ ($10^{-3}\ h^{-1}$) | $k_L$ ($10^{-3}\ \mu M\ h^{-1}$) | t* (h) | %BSi$_{sed}$ | %BSi $C_{as}$ |
|------|-----------|----------------|---------------|---------------------------|----------------------------------|--------|--------------|---------------|
| 230 | 0.5 | 35 | 51 | 1.8 | 1.4 | 2361 | 0.08% | 0.14% |
| S15 | 0.5 | 15 | 89 | 1.5 | 4.4 | 2346 | 0.66% | 0.24% |
|  | 0.5 | 5 | 78 | 1.4 | 5.4 | 2181 | 0.66% | 0.21% |
|  | 0.5 | 0 | 59 | 4.6 | 7.8 | 780 | 0.66% | 0.16% |
| S01 | 0.5 | 35 | 5 | 2.5 | 1.7 | 831 | 0.07% | 0.01% |
| September | 4.5 | 35 | 150 | 3.1 | 14.1 | 1132 | 2.04% | 0.40% |
|  | 9.0 | 35 | 142 | 3.8 | 14.9 | 948 | 2.14% | 0.38% |
|  | 13.0 | 35 | 106 | 3.2 | 11.7 | 1067 | 1.33% | 0.28% |

## 4.6 Modelling of silica input, reaction and transport in the Scheldt continuum

### 4.6.1 Hydrodynamics, transport and SPM

Hydrodynamic validation has been performed on the amplitude and travel time of the tidal wave. Relative deviations over the whole domain are <10%. A detailed analysis of the tidal distortion, which is essential for SPM transport, has also been carried out. Solute transport has been calibrated using a large set of salinity data in the Scheldt estuary (Arndt et al., 2007). The hydrodynamic model indicates that energy dissipation reaches its maximum 90 km upstream from the mouth, closely followed by a minimum further upstream (Figure 36). SPM dynamics is simulated to provide the transient light conditions in the water column. Figure 36 shows that the spatial distribution of SPM mirrors closely the profile of energy dissipation. The temporal SPM dynamics is highly sensitive to tidal fluctuations, but also to variations in river discharge, whose influence decreases downstream. Peaks in SPM are triggered by high discharges and can be recorded as far as 50 km seaward of the upstream model boundary (not shown).
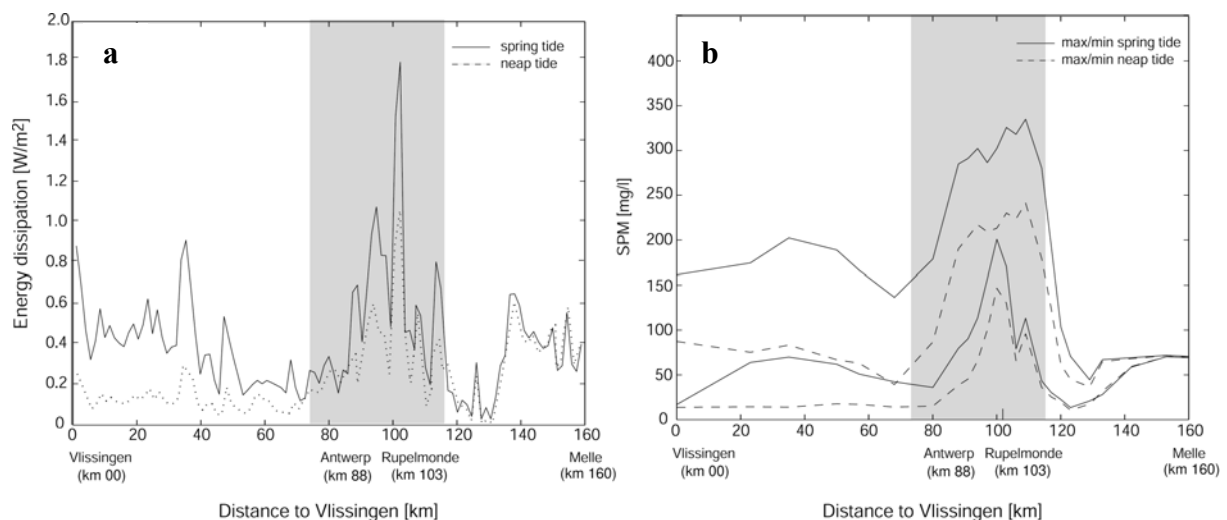


**Figure 36**. (a) Energy dissipation along the estuarine gradient for a spring and a neap tidal cycle and a constant river discharge (Q=100 $m^3 s^{-1}$). (b) Longitudinal distribution of maximum/minimum SPM concentrations during spring-neap tidal cycle. (The area of maximum turbidity is shaded.). From Arndt et al. (2007).

### 4.6.2 *Pelagic silica and diatom dynamics*

Model results show that primary production dynamics are mainly linked to variabilities in the physical forcing conditions. Monthly observations of diatom carbon and pelagic dissolved silica (PDSI$\equiv$H$_4$SiO$_4$) in summer 2003 reveal a characteristic spatial pattern which is well captured by the pelagic model (Figure 37). During a seasonal cycle, diatom biomass reaches maximum values of 200–1200 µM C in the upstream reaches of the Scheldt river (>km 100) where shallow water depths (average h=2.6 m), low turbidities (<50–100 mg l$^{-1}$) and a constant riverine supply of PDSI create a favourable environment for diatom growth. Within this zone, the area around km 120 provides the most favourable physical conditions for diatom development (balance point with lowest total energy dissipation and, thus, low SPM concentrations). Downstream of km 100, diatom carbon concentrations abruptly decrease as a consequence of the rapid increase in SPM concentrations, from <50 mg l$^{-1}$ around km 120 to 60–340 mg l$^{-1}$ in the estuarine turbidity maximum between km 80 and km 114. Despite local shallow water depths, these high SPM concentrations result in a strong light-limitation of photosynthesis. Downstream of the turbidity maximum, the widening and deepening of the estuary lead to dilution. Besides, the increase in water depth result in a negative net phytoplankton growth (Desmit et al., 2005) and thus maintains low diatom biomass (<200 µM C). Weekly PDSI measurements indicate that during most of the simulation period, the Scheldt River and its tributaries provide an almost constant supply of PDSI to the tidal river-estuarine continuum. This riverine silica input is mostly consumed in the upstream zones of the Scheldt, where net primary production reaches maximum values.

Results from the phytoplankton model demonstrate the fast response of diatom growth to changes in the physical environment, especially those due to daily variations in river discharge which continuously modify the SPM concentrations and residence times. Figure 38 shows how episodes of persistent low flow conditions lead to a shift of the area of maximum primary production, away from the balance point. Figure 39 illustrates the concomitant, progressive depletion of dissolved silica. In this case, diatom growth becomes increasingly controlled by silica availability, until primary production finally collapses. Further details on the diatom growth response to physical forcings can be found in Arndt et al. (2007).
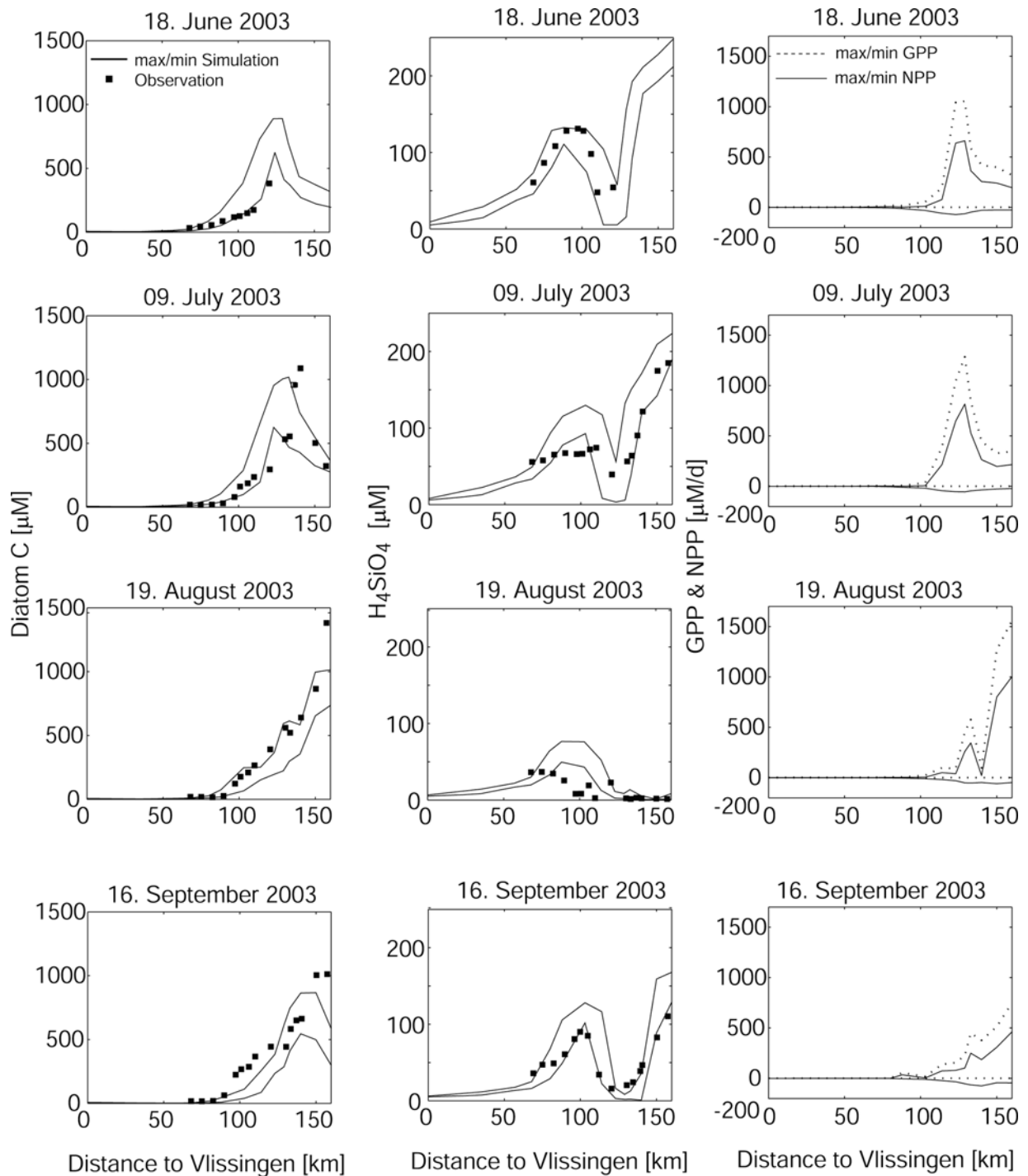
**Figure 37**. Spatio-temporal distribution of observed (squares) and simulated daily maximum and minimum (lines) diatom carbon and dissolved silica concentrations, net primary production NPP (solid line) and gross primary production GPP (dashed line). From Arndt et al. (2007).
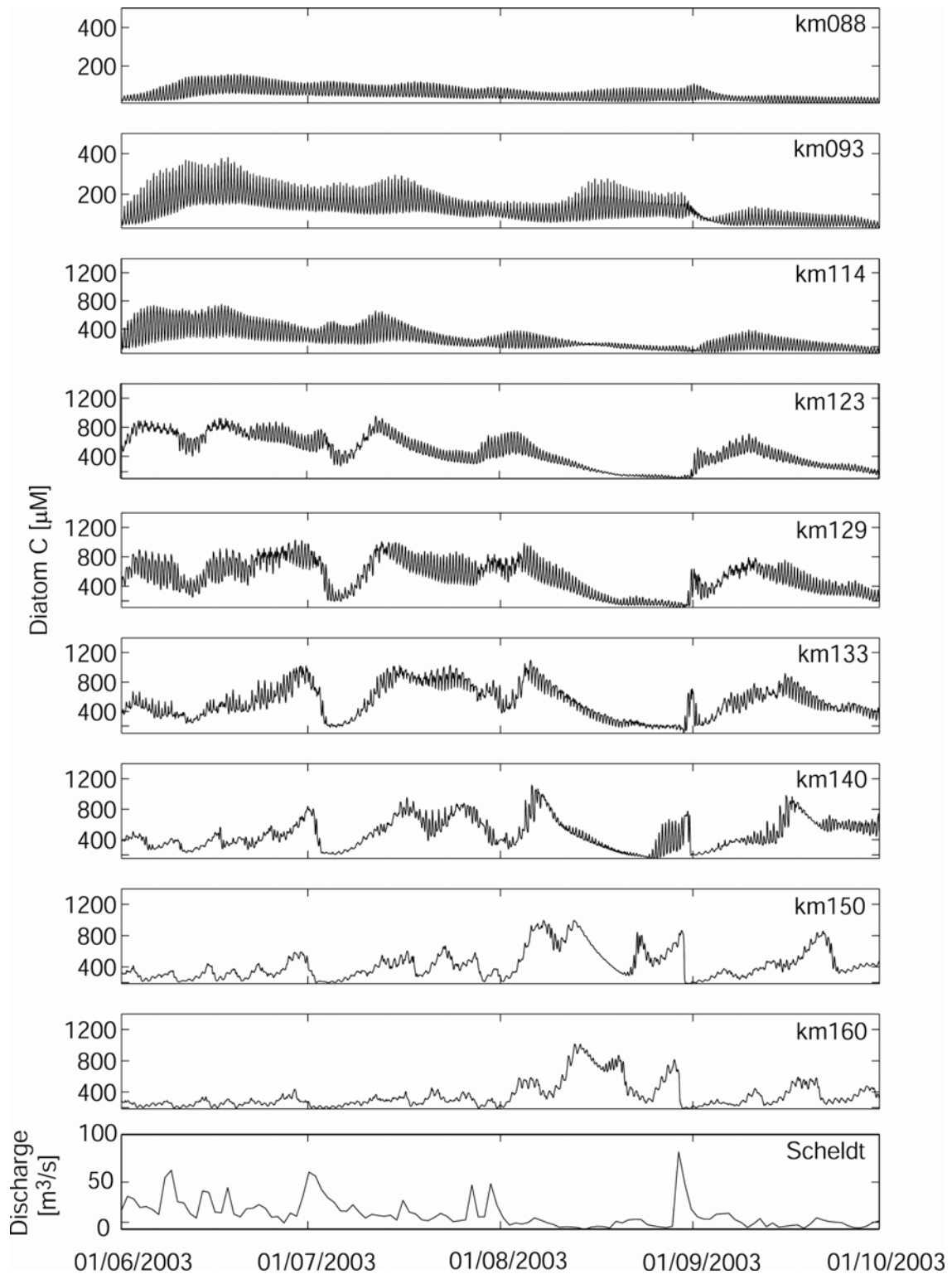
**Figure 38**. Temporal evolution of diatom carbon concentrations and Scheldt discharge at selected points in the tidal freshwater reaches from June-September.
Note the different axis scaling at km 88 and km 93. From Arndt et al. (2007).
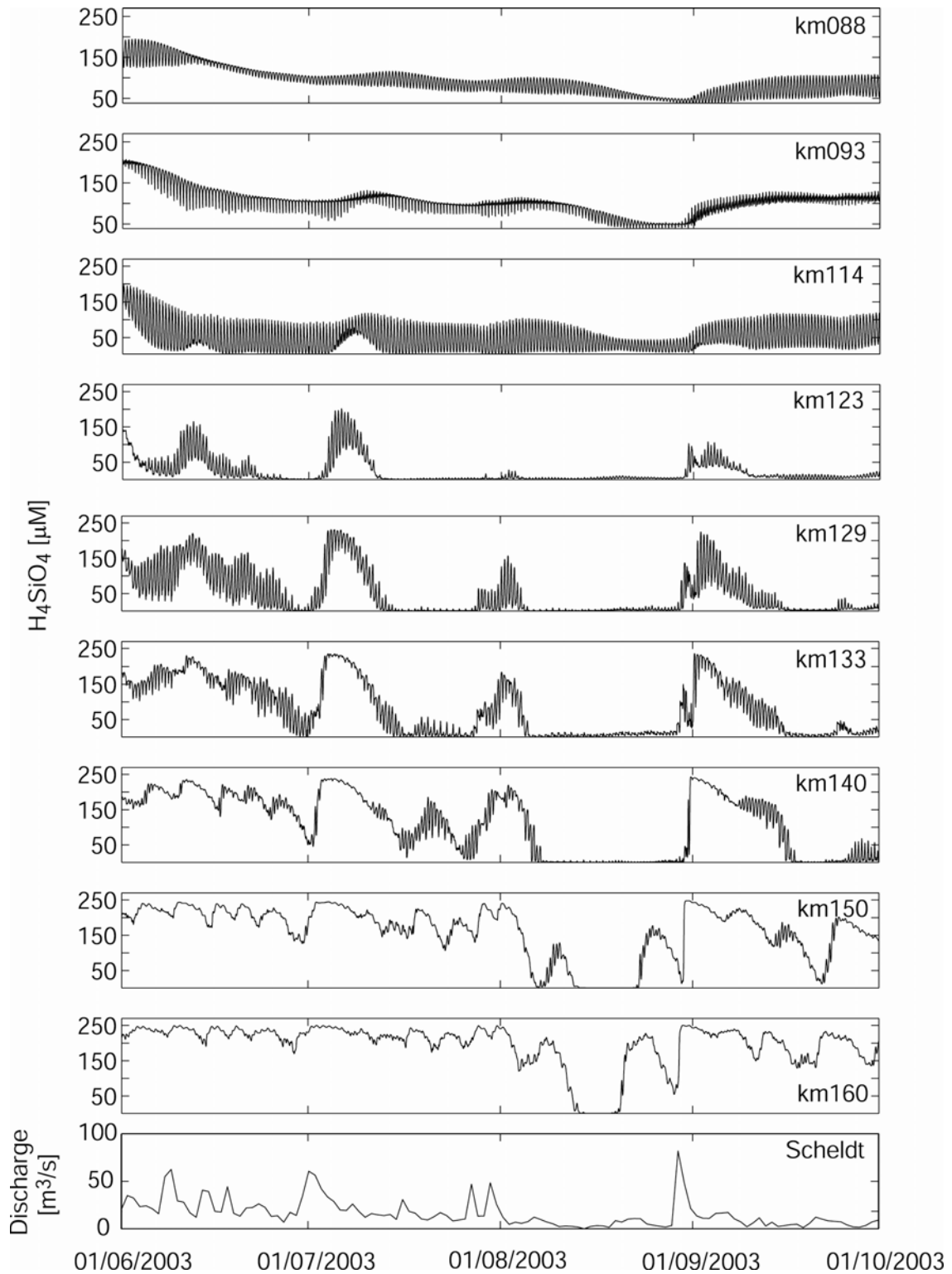
**Figure 39**. Temporal evolution of dissolved silica concentrations at selected points in the tidal freshwater reaches and Scheldt discharge from June-September. From Arndt et al. (2007).

### 4.6.3 Benthic silica dynamics

A sensitivity analysis based on Monte-Carlo simulations has been carried out to assess the intensity and timing of benthic diffusive fluxes in response to a pelagic diatom bloom. The diffusive flux dynamics are analyzed over a realistic range of dissolution rate constants (max $k_{Si}$: $6.0 \times 10^{-3} - 3.6 \times 10^{-1}$ $d^{-1}$), diffusion coefficients of dissolved silica ($D_{Si}$: $35 \times 10^{-6} - 35 \times 10^{-5}$ $m^2$ $d^{-1}$) and duration of dissolved silica depletion in the water column ($w_{PDSI}$: 1–3 month). Results show that the diffusive silica flux responds with a time delay of 20 to 120 days to the biogenic silica deposition pulse (Figure 40a). For high max $k_{Si}$, simulated time lags are the shortest and completely determined by the dissolution kinetics. However, decreasing max $k_{Si}$ leads to a slower benthic flux response. In addition, the variability increases due to the increasing importance of transport processes. Figure 40b shows as an example the preservation of BBSI after one year of simulation over the logarithm of maximum dissolution rate constant.
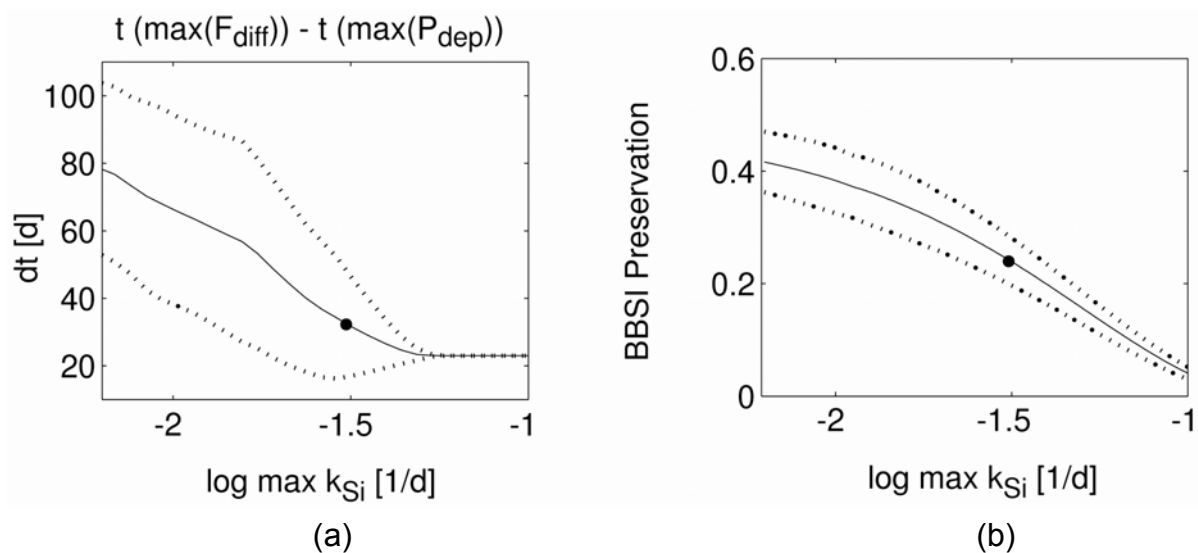


**Figure 40.** Distribution of benthic processes over the logarithm of maximum dissolution rate constants (max $k_{Si}$). a: Time lags between maximum diffusive flux t(max $F_{diff}$) and maximum deposition rate t(max $P_{dep}$). b: preservation of BBSI after one year of simulation. From Arndt and Regnier (2007).

The results of the sensitivity analysis over the entire parameter space are described in details in Arndt and Regnier (2007). This sensitivity study allows us to constrain the uncertainties of benthic silica fluxes in the system-scale simulations (see below).

### 4.6.4 Benthic-pelagic coupling

Figure 41 illustrates the temporal evolution of processes and fluxes of the Si cycle, integrated over the freshwater tidal reaches of the estuary (km 170–100). The area-integrated deposition of biogenic silica in the tidal freshwater reaches of the Scheldt estuary ($\int P_{dep}$) is driven by the combined influence of pelagic production and river discharge (Figure 41a). Deposition is high throughout the whole growth season and a total of $1.2 \times 10^7$ mol (=742 mmol m$^{-2}$) PBSI are deposited over the simulated period in the tidal freshwater reaches. However, $\int P_{dep}$ reveals variabilities which are induced by variations in river discharge. Low river discharges reduce the hydrodynamic energy and thus favour deposition and potentially pelagic primary production (Arndt et al., 2007).
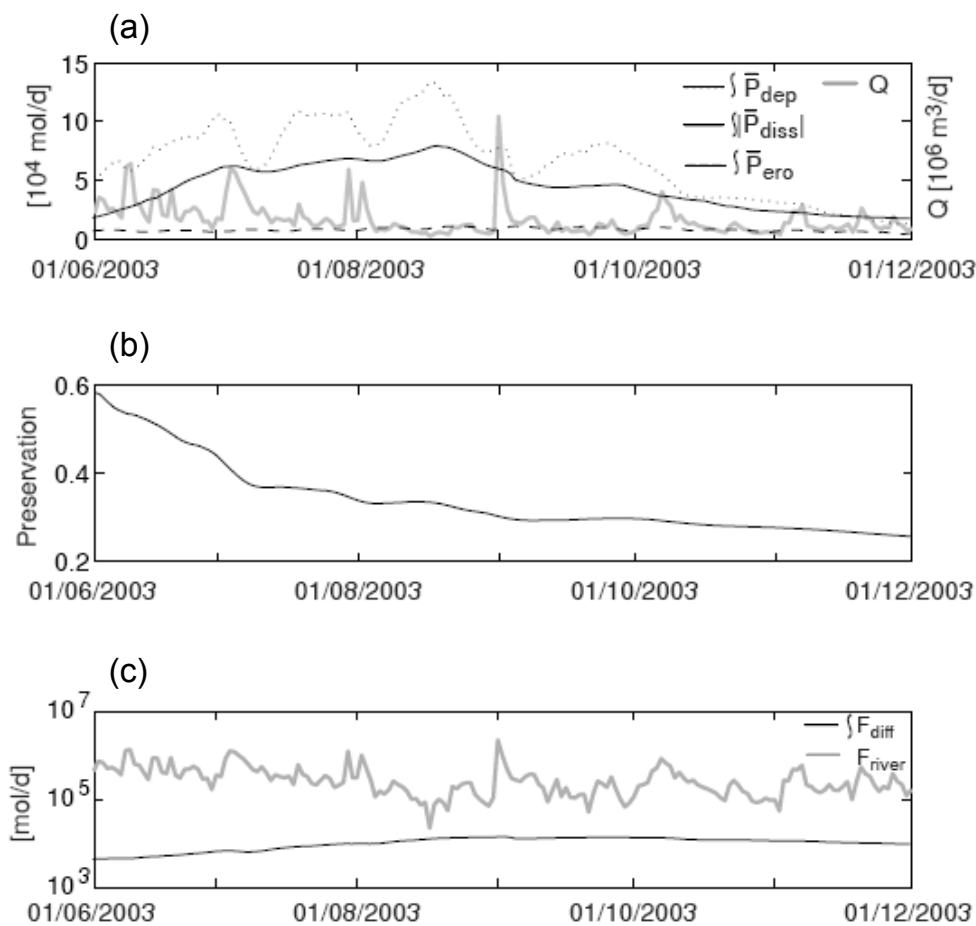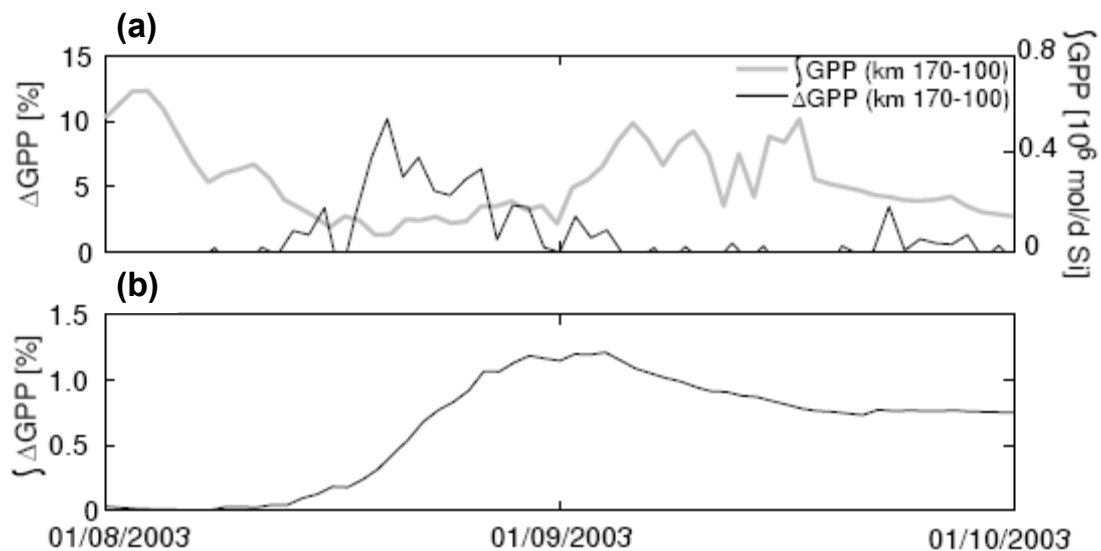


**Figure 41**. Temporal evolution of (a) area-integrated depositional flux $\int P_{dep}$, dissolution of biogenic silica $\int P_{diss}$ and erosion flux $\int P_{ero}$ in the freshwater tidal reaches (km 170–km 100) of the Scheldt estuary, as well as daily river discharge Q. (b) Preservation of deposited BBSI in the freshwater reaches. (c) Comparison of logarithmic, area-integrated (km 170–km 100) diffusive flux of silica and logarithmic, daily riverine (Scheldt+Dender) silica influx into the tidal freshwater reaches of the Scheldt. From Arndt and Regnier (2007).

High river discharge has an opposite effect and leads therefore to a reduction of biogenic silica deposition. A maximum in deposition flux ($1.3 \times 10^5$ mol d$^{-1}$) is reached in mid-August, even though silica depletion in the tidal river maintains low pelagic primary production at this time (Arndt et al., 2007). The high $\int P_{dep}$ must therefore originate from biogenic silica produced a few weeks before and which mainly settles in the upper tidal reaches due to extremely low river discharges (<5m$^3$ s$^{-1}$) during this period. The deposition of biogenic silica decreases in fall and dissolution becomes of similar magnitude in mid-October (Figure 41a). In general, dissolution rates respond with a significant dampening and a small delay (<7 d) to variations in $\int P_{dep}$ (Figure 41a). A total of $8.0 \times 10^6$ mol (=486 mmol m$^{-2}$) BBSI are dissolved in the freshwater reaches from June to December 2003. The magnitude of erosion fluxes ($10^4$ mol d$^{-1}$) is one to two orders of magnitude lower than those of $\int P_{dep}$ and $\int P_{diss}$ (Figure 41a). The total erosive flux removes $1.0 \times 10^6$ mol (=67 mmol m$^{-2}$) of BBSI from the sediments. Most of the biogenic silica deposited in the tidal freshwater reaches is consumed in this stretch during the simulated period (Figure 41b). A small fraction (ca. 27%) of the deposition flux is preserved in the estuarine sediments at the beginning of December.

The diffusive silica flux ($\int P_{diff}$) increases steadily during the first half of the simulated period and reaches its maximum value one month after the maximum in $\int P_{dep}$ and $\int P_{diss}$, at the end of the growth period (Figure 41c). However, compared to the riverine silica influx ($F_{riv}$), benthic recycling fluxes are of minor importance. Overall, the riverine input exceeds the diffusive silica flux by about two orders of magnitude. $F_{riv}$ and $\int P_{diff}$ are of the same order of magnitude only in mid-August, when extremely low river discharges reduce the riverine silica influx to minimum values. During the simulated period (June–November 2003) a total of $5.9 \times 10^7$ mol is supplied by the freshwater input, while the spatially integrated benthic diffusive flux only accounts for a total $2 \times 10^6$ mol. Thus, the benthic recycling fluxes account for a mere 3.6% of the total dissolved silica flux discharged into the tidal freshwater reaches of the Scheldt estuary. However, the sensitivity study showed that the uncertainty of the benthic flux response can be as high as 75% over a realistic range of internal parameter values for the estuarine environment. Nevertheless, a 75% increase of the diffusive flux would still only represent 5.9% of the riverine dissolved silica input. Thus, the conclusion also holds for the whole range of variability associated with the benthic flux.

The high riverine loads of dissolved silica decrease the relative importance of benthic-pelagic coupling for the system-scale pelagic primary production. Figure 42 illustrates the difference between the simulated GPP with and without benthic-pelagic coupling during August and September, when benthic recycling fluxes reach their annual maximum and the riverine silica influx is low. The difference in GPP between

these two simulations is the largest in mid-August, when the reduced riverine silica input leads to silica depletion in the freshwater reaches (Figure 39). However, the coupled benthic-pelagic model merely increases the gross primary production by 10% during this period. In addition, in mid-August, gross primary production rates are roughly one order of magnitude lower than during most of the growth period (Figure 42a). The difference in GPP between the beginning of August and September, when high GPP rates are reached again, is thus much lower (Figure 42b). The time-integrated difference in GPP increases to 1% at the end of August before it decreases again in September and reaches 0.7% at the end of September. Therefore, the benthic recycling of silica sustains only a small fraction (<1%) of the total pelagic primary production in the Scheldt estuary and the benthic-pelagic coupling is thus of minor importance on the system scale.



**Figure 42**. Temporal evolution of (a) area-integrated (km 170–km 100) gross primary production ∫GPP, simulated with the benthic-pelagic model and daily percentage increase of simulated GPP of the benthic-pelagic model compared to the pelagic model ΔGPP; (b) time-integrated percentage increase of simulated GPP of the benthic-pelagic model compared to the pelagic model ∫ΔGPP. From Arndt and Regnier (2007).

# 5. CONCLUSION AND RECOMMENDATIONS

By combing historical data analysis, field and laboratory investigations and modelling efforts, SISCO has contributed to an improved understanding of the phytoplankton dynamics and biogeochemical cycling of silica in the Scheldt continuum river-estuary-coastal zone. The major conclusions and achievements are presented. Perspectives for future research are also provided.

## 5.1 Phytoplankton dynamics

HPLC analysis of phytoplankton pigments in combination with the CHEMTAX software proved to be a useful method for estimating biomass of diatoms in the Scheldt estuary as well as in the Belgian Coastal Zone. HPLC-CHEMTAX was for the first time applied successfully to estimate biomass of the problematic alga Phaeocystis. Care should be taken when estimating biomass of chlorophytes using this method, as biomass of chlorophytes was overestimated in the estuarine as well as the coastal zone samples. It is hypothesized that this is due to pigments derived from terrestrial plant detritus, but further research is needed to confirm this.

Monitoring of phytoplankton in the Belgian coastal zone revealed pronounced spatio-temporal variability in the timing and magnitude of the spring bloom. Probably due to a more favourable mixing depth to photic depth ratio, the spring bloom started earlier in the western part of the Belgian coastal zone. The magnitude of the spring bloom was higher in the eastern part of the coastal zone, probably because of higher nutrient inputs (N and P) from the Scheldt estuary. It would be interesting to see whether this pattern recurs every year.

Before the onset of the Phaeocystis bloom, dissolved inorganic phosphate concentrations were much closer to the limiting level for Phaeocystis than dissolved nitrate levels. This would suggest that phosphorus rather than nitrogen is the limiting nutrient in Belgian coastal waters. Experimental studies are needed to confirm this.

In contrast to many previous monitoring studies in the Scheldt estuary, SISCO not only focused on the Scheldt branch of the estuary but also on the Rupel branch. It would be interesting to continue monitoring of the Rupel branch, especially given the recent efforts in water purification in Brussels, a major source of nutrients and organic matter to the Rupel branch.

Laboratory experiments with Cyclotella meneghiniana, one of the most common diatoms in the Scheldt estuary, revealed a large variability in the half-saturation constant (Ks) for Si-limited growth. In fact, the range in Ks values observed within this single species was comparable to the range reported for all freshwater diatoms in the

literature. This observation indicates that great care should be taken when using published Ks values for a given species for modelling Si uptake by diatoms.

This study focused on the upper, freshwater tidal reaches of the Scheldt estuary, where diatom biomass and Si consumption were maximal. Interannual variability in the diatom summer bloom was high in this part of the Scheldt estuary, with maximum summer chlorophyll a concentration ranging from about 100 to 700 μg l$^{-1}$. Chlorophyll a concentrations were higher when discharge was lower. This observation may be relevant for predicting phytoplankton primary production under a climate change scenario.

Although estuaries are generally considered to have a relatively low diversity, the Scheldt estuary harboured a diverse phytoplankton community. Comparison of abundances of phytoplankton species in the estuary with abundances in the tributary rivers and the coastal zone revealed that many of these species were imported from outside the estuary and did not survive well within the estuary. Relatively few of the species observed in the estuary were more successful in the estuary than in the coastal zone or in the tributary rivers.

## 5.2   Pelagic silica dynamics

The biogeochemical behaviour of DSi and BSi in the water column was investigated in the freshwater and brackish parts of the estuary. For the first time, a coherent high-frequency time-series dataset of simultaneous measurements of DSi and BSi concentrations in the freshwater tidal reaches was produced, which improved our knowledge of the pelagic cycling of Si in the continuum. Consumption of DSi by diatom growth would be the dominant factor controlling the Si biogeochemistry in the water column especially during the bloom period. In the freshwater estuary during summer, DSi was completely consumed and BSi concentration increased. Mass balance calculations showed that silica consumption and retention in the freshwater estuary were important at a seasonal time-scale: from May to September, one third of the total amount of riverine silica was retained.

In the context of the eutrophication study of the Belgian coastal zone, the goal of SISCO was also to estimate the retention of the different forms of silica in the estuary and their residual fluxes to the coastal zone. Fluxes could be easily determined in the freshwater estuary as the residual water discharge was known and as there was no mixing with seawater. However this would not be the case in the brackish estuary. At Vlissingen, due to tidal action the volume of water flowing through the estuarine mouth is three orders of magnitude higher than the residual discharge. To assess directly the fluxes at the outlet of the estuary would necessitate a quasi continuous recording of the DSi concentration. In addition, the analytical precision of the

measurements needs to be high enough to detect the minute changes in the instantaneous silica fluxes that would be due to residual fluxes. For practical reasons, this is not achievable. However, models can inter- and/or extrapolate the discrete measurements, and such silica fluxes could be estimated.

Accordingly, the 1D-CONTRASTE model could be used to estimate the fluxes of DSi if they were conservative. Comparison of the simulated and measured DSi concentrations allowed the estimation of DSi fluxes during the period of our sampling campaigns. A significant fraction of the average DSi flux (600 Mmol yr$^{-1}$) that entered the brackish estuary in 2003-2005 was retained in the brackish estuary. Retention of BSi could also be evaluated by comparing the BSi content in the SPM with the SPM budgets published in the literature by Van Maldegem et al. (1993) for example. As for SPM, in addition to the delivery of fluvial BSi, there was a significant input of BSi from marine origin in the brackish estuary. Most of these two BSi fractions were found to be highly retained in the brackish estuary, suggesting that the estuary is a sink for silica.

These estimations were however very crude and preliminary ones and were based on observations during specific years. They thus cannot reflect the situation in the case of higher discharge, or of changes that would affect the phytoplankton dynamics. This is however the aim of the development of such a 2D model as described in §3.4 and §4.6.

## 5.3    Benthic silica dynamics

The longitudinal distribution of BSi in surface sediments, as well as the vertical BSi and DSi profiles in sediments were determined for different seasons, and for sites chosen in order to have a general view of the Scheldt continuum. No clear tendencies could be observed, with the exception of a correlation between the type of sediment and the BSi content. This suggests a strong influence of the particle transport, which was to be expected in this very hydrodynamic system. Sediments are clearly subject to transient phenomena such as re-suspension and re-settling. As a general feature, biogenic material appeared to accumulate in the superficial layers of sediments following the spring/summer diatom blooms.

The vertical DSi profiles in the interstitial waters allowed us to evaluate the DSi fluxes across the sediment–water interface. The values obtained were generally low, but remained in agreement with the published results. Laboratory incubation experiments of sediment cores provided, via direct measurements, a second set of DSi flux estimates, which are in general higher than the calculated ones based on pore water DSi profiles. The measured values took into account the diffusive processes as well as the dissolution of BSi, which could explain partly the observed differences.

The rate of Si dissolution was relatively low for surface sediments and at depth, but increased in the first few centimetres. Only the sediments from the coastal zone, extremely poor in BSi, exhibited a constant decrease in DSi release with depth. The results are coherent with the BSi contents measured and with the microscopic observations, showing low BSi contents in the first centimetre, while higher deeper in the core. This indicates that the biogenic material reaching the benthic layer was rapidly consumed either by rapid dissolution or by incorporation in the sedimentary column. In the first centimetres dissolution continued, with decreasing rates at depth as the amorphous material was probably affected quite rapidly by different diagenetic processes such as adsorption or incorporation of metallic ions (Al, Fe…). Our data showed that only a small fraction of the total BSi present in the sediments dissolved even after several months.

In conclusion, most of the BSi incorporated in the sedimentary column was retained in the sediments. The DSi released by dissolution was either removed by diagenetic processes, such as precipitation of authigenic minerals, or transferred to the water column, which was probably the case in coarser sediments, but also in highly hydrodynamic environments. Although this is a characteristic of the Scheldt Estuary, the sediments probably do not represent in general a very important source of DSi for the water column.

## 5.4 Improved modelling of silica input, reaction and transport in the Scheldt continuum

An improved fully coupled two-dimensional, hydrodynamic and reactive transport model was developed within the MIKE 21-ECOLab simulation environment to describe the pelagic silica dynamics along the Scheldt continuum. The model extended from the upper tidal river and its tributaries to the southern Bight of the North Sea. The hydrodynamic model included a fully-formulated suspended particulate matter (SPM) transport algorithm. Major improvements of the current biogeochemical model compared to the most recent version of the 1D-CONTRASTE model consisted of the incorporation of silica as an explicit model variable and the coupling between SPM dynamics, light penetration and primary production.

A transient, vertically resolved, analytical model for the early diagenesis of Si was in addition developed to deal with the full complexity of benthic processes. These included dissolution, bioturbation, deposition, erosion and burial of biogenic silica. The benthic model was then coupled to the two-dimensional pelagic model to quantify the importance of benthic-pelagic coupling in estuarine and coastal biogeochemical silica cycling.

Pelagic model results showed that primary production dynamics were mainly linked to variabilities in the physical forcing conditions. They demonstrated the fast response of diatom growth to changes in the physical environment, especially those due to daily variations in river discharge which continuously modify the SPM concentrations and residence times.

Sensitivity analyses of the benthic model showed that the diffusive silica flux responded with a time delay of 20 to 120 days to the biogenic silica deposition pulse. They allowed us to constrain the uncertainties of benthic silica fluxes in the system-scale simulations.

Model simulations of benthic-pelagic coupling during the August-September period showed that the area-integrated deposition of biogenic silica in the tidal freshwater reaches of the Scheldt estuary was driven by the combined influence of pelagic production and river discharge. Overall, the riverine input exceeded the diffusive silica flux by about two orders of magnitude. The benthic recycling of silica would sustain only a small fraction (<1%) of the total pelagic primary production in the Scheldt estuary and the benthic-pelagic coupling would thus be of minor importance on the system scale.

The model developed in the framework of the SISCO project will be extended to investigate carbon and nutrient (N, Si) dynamics within the entire land-ocean continuum, including the Belgian-Dutch coastal zone and the Southern Bight of the North Sea. This extension will be performed using an existing hydrodynamic and transport model of the continuum. The main aim will be to address the problem of coastal eutrophication by nutrient delivery from the Scheldt estuary and how it is controlled by man-made intervention. Figure 43 shows as an example that the proposed model is particularly suited to quantify fully transient nutrient fluxes along the river-estuary-coastal zone continuum.
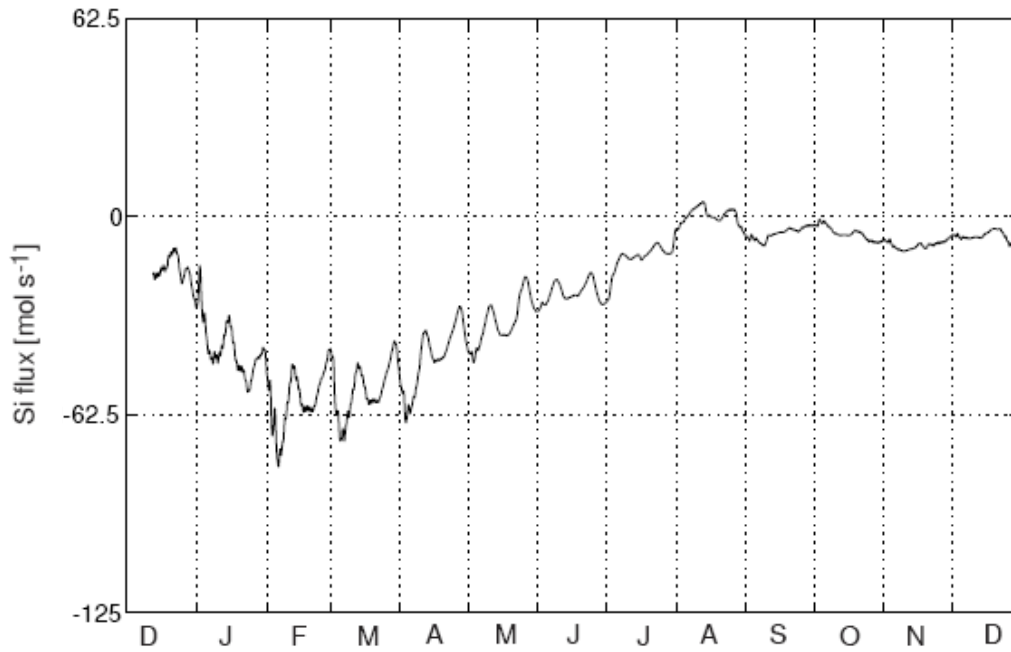
**Figure 43**. Si fluxes at the mouth of the Scheldt estuary
from December 2002 to December 2003.

## 6. ACKNOWLEDGEMENTS

## 7. REFERENCES

Admiraal W., P. Breugem, D.M.L.H.A. Jacobs and E.D. de Ruyter van Steveninck (1990) Fixation of dissolved silicate and sedimentation of biogenic silicate in the lower river Rhine during diatom blooms. Biogeochemistry, 9, 175-185.

Admiraal W., D.M.L.H.A. Jacobs, P. Breugem, and E.D. de Ruyter van Steveninck (1992) Effects of phytoplankton on the elemental composition (C, N, P) of suspended particulate material in the lower river Rhine. Hydrobiologia, 235/236, 479-489.

Aguilera D., P. Jourabchi, C. Meile, C. Spiteri and P. Regnier (2005) A knowledge-based reactive transport approach for the simulation of biogeochemical dynamics in Earth systems. Geochemistry, Geophysics, Geosystems, 6, Q07012.

Aller R.C., N.E. Blair, Q. Xia and P. Rude (1996) Remineralization rates, recycling and storage of Corg in Amazon shelf sediments. Continental Shelf Research, 16, 753-786.

Antajan E., M.J. Chretiennot-Dinet, C. Leblanc, M.H. Daro, C. Lancelot (2004) 19′–hexanoyloxyfucoxanthin may not be the appropriate pigment to trace occurrence and fate of Phaeocystis: the case of P. globosa in Belgian coastal waters. J. Sea Res., 52, 165–177.

Arndt S. and P. Regnier (2007) A model for the benthic-pelagic coupling of silica in estuarine ecosystems: sensitivity analysis and system scale simulation. Biogeosciences Discuss., 4, 747–796.

Arndt S., J.-P. Vanderborght and P. Regnier (2007) Diatom growth response to physical forcing in a macrotidal estuary: Coupling hydrodynamics, sediment transport, and biogeochemistry. J. Geophys. Res., 112, C05045, doi:10.1029/ 2006JC003581.

Ariathurai C.R. (1974) Finite element model for sediment transport in estuaries. Ph.D. thesis, University of California.

Baeyens W., B. Van Eck, C. Lambert, R. Wollast, and L. Goeyens (1998) General description of the Scheldt estuary. Hydrobiologia, 366, 1-14.

Barker P., J.-C. Fontes, F. Gasse, and J.-C. Druart (1994) Experimental dissolution of diatom silica in concentrated salt solutions and implications for paleoenvironmental reconstruction. Limnology and Oceanography, 39(1), 99 - 110.

Beckers O. and R. Wollast (1976) Comportement de la silice dissoute dans l'estuaire de l'Escaut. Projet Mer – Rapport Final, 10, 153 – 170.

Berner R.A. (1980) Early Diagenesis: A Theoretical Approach. Princeton, New Jersey, Princeton University Press.

Beszteri B., E. Acs, L.K. Medlin (2005) Ribosomal DNA sequence variation among sympatric strains of the Cyclotella meneghiniana complex (Bacillariophyceae) reveals cryptic diversity. Protist, 156, 317-333.

Bianchi, T.S., S. Findlay, D. Fontvieille (1991) Experimental degradation of plant materials in Hudson River sediments. 1. Heterotrophic transformations of plant pigments. Biogeochemistry, 12, 171-187.

Billen G., J. Garnier and V. Rousseau (2005) Nutrient fluxes and water quality in the drainage network of the Scheldt basin over the last 50 years. Hydrobiol., 540, 47-67.

Billen G., C. Lancelot, and M. Meybeck (1991) N, P, and Si retention along the aquatic continuum from land to ocean. In: Ocean Margin Processes in Global Change, R.F.C. Mantoura, J. M. Martin and R. Wollast (eds). Dahlem Workshop Reports, pp. 19-44. John Wiley & Sons, N.Y.

Bouezmarni M. and R. Wollast (2005) Geochemical composition of sediments in the Scheldt estuary with emphasis on trace metals. Hydrobiologia, 540, 155-168.

Cadée, G.C. and J. Hegeman (1991a) Historical phytoplankton data of the Marsdiep. Hydrobiol. Bull., 24(2), 111-188.

Cadée, G.C. and J. Hegeman (1991b) Phytoplankton primary production, chlorophyll and species composition, organic carbon and turbidity in the Marsdiep in 1990, compared with foregoing years. Hydrobiol. Bull., 25(1), 29-35.

Chen M.S., S. Wartel, B. Van Eck, and D. Van Maldegem (2005) Suspended matter in the Scheldt estuary. Hydrobiologia, 540, 79-104.

Chou L. and R. Wollast (2006) Estuarine silicon dynamics. In V. Ittekot, D. Unger, C. Humborg, and N. TacAn [eds.], The silicon cycle. Human perturbations and impacts on aquatic systems. SCOPE, 66, pp. 93-120. Island Press, Washington, Covelo, London.

Clip G (2006) Etude des processus diagénétiques de la silice dans l'estuaire de l'Escaut. Travail de fin d'études présenté en vue de l'obtention du grade de bioingénieur.

Conley D. J. and S. S. Kilham (1989) Differences in silica content between marine and freshwater diatoms. Limnol. Oceanogr., 34, 205-213.

Conley D.L., C. Schelske and E.F. Stoermer (1993) Modification of the biogeochemical cycle of silica with eutrophication. Mar. Ecol. Prog. Ser., 101, 179-192.

De Bodt C. (2005) Etude de la silice biogénique dans les sediments de l'estuaire de l'Escaut. Travail de fin d'études présenté en vue de l'obtention du grade de bioingénieur.

DeMaster D.J. (1981) The supply and accumulation of silica in the marine environment. Geochimica et Cosmochimica Acta, 45, 1715-1732.

Desmit X., J.-P. Vanderborght, P. Regnier and R. Wollast (2005) Control of phytoplankton production by physical forcing in a strongly tidal, well-mixed estuary. Biogeosciences, 2, 205-218.

Dougan W.K. and A.L. Wilson (1974) The absorptiometric determination of aluminium in water. A comparison of some chromogenic reagents and the development of an improved method. Analyst, 99, 413-430.

Einstein H.B. and R.B. Krone (1926) Experiments to determine modes of cohesive sediment transport in salt water. J. Geophys. Res., 67(4), 1451–1461.

Guillard R.R.L. and C.J. Lorenzen (1972) Yellow-green algae with chlorophyllide c. J. Phycol., 8, 10-14.

Garnier J., G. Billen and M. Coste (1995) Seasonal succession of diatoms and chlorophyceae in the drainage network of the Seine River: observation and modelling. Limnol. Oceanogr., 40, 750-765.

Geider R.J. (1987) Light and temperature dependence of the carbon to chlorophyll ratio in microalgae and cyanobacteria: implications for physiology and growth of phytoplankton. New Phytologist, 106, 1-34.

Grasshoff, K., M. Ehrhardt and K. Kremling (1983) Methods of Seawater Analysis. Verlag Chemie, Basel.

Hellings L., F. Dehairs, M. Tackx, E. Keppens and W. Baeyens (1999) Origin and fate of organic carbon in the freshwater part of the Scheldt Estuary as traced by stable carbon isotope composition. Biogeochemistry, 47, 167-186.

Hildebrand M. (2002) Lack of coupling between silicon and other elemental metabolisms in diatoms. J. Phycol., 38, 841-843.

House W. A., F.H. Denison, M.S. Warwick and B.V. Zhmud (2000) Dissolution of silica and the development of concentration profiles in freshwater sediments. Applied Geochemistry, 15 (4), 425 - 438.

Humborg C., D.J. Conley, L. Rahm, F. Wulff, A. Cociasu and V. Ittekot (2000) Silica retention in river basins: far reaching effects on biogeochemistry and aquatic food aquatic food webs. Ambio, 29, 45-50.

IRMB (Institut Royal Météorologique de Belgique). 2003-2004. Bulletins mensuels, Observations climatologiques, parties I et II. Institut Royal Météorologique de Belgique, Bruxelles (In French/Dutch).

Ittekkot V., C. Humborg and P. Schäfer (2000) Hydrological alterations and marine biogeochemistry: A silicate issue? BioScience, 50(9), 776-782.

Kamatani A. and O. Oku (2000) Measuring biogenic silica in marine sediments. Mar. Chem., 68, 219-229.

Köhler J., M.Bahnwart and K. Ockenfeld (2002) Growth and loss processes of riverine phytoplankton in relation to water depth. Int. Rev. Hydrobiol., 87, 241-254.

Lancelot C. (1995) The mucilage phenomenon in the continental coastal waters of the North Sea. Sci. Total Environ., 165, 83-102.

Lancelot, C., G. Billen, A. Sournia, T. Weisse, F. Colijn, M.J.W. Veldhuis, A. Davies and P. Wassman (1987) Phaeocystis blooms and nutrient enrichment in the continental coastal zones of the North Sea. Ambio, 16, 38–46.

Lancelot C., Y. Spitz, N. Gypens, S. Becquevort, V. Rousseau, G. Lacroix and G. Billen (2005) Modelling diatom and Phaeocystis blooms and nutrient cycles in the Southern Bight of the North Sea: the MIRO model. Marine Ecology Progress Series, 289, 63-78.

Li Y-H. and S.Gregory (1974) Diffusion of ions in sea water and deep-sea sediments. Geochimica et Cosmochimica Acta, 38, 703-714.

Lionard M., F. Azémar, S. Boulêtreau, K. Muylaert, M. Tackx and W. Vyverman (2005). Grazing by meso- and microzooplankton in the upper reaches of the Schelde estuary (Belgium/The Netherlands). Estuarine Coastal Shelf Sci., 64, 764-774.

Luo Y., M. Tackx, F.Y. Li, D.Q. Mao and & Q.X. Zhou (2002) Leaf litter ecological fate in the Schelde estuary in Belgium. J. Env. Sci.-China, 14, 563-567.

Mackey M., D.J. Mackey, H.W. Higgins and S.W. Wright (1996). CHEMTAX- a program for estimating class abundances from chemical markers: application to HPLC measurements of phytoplankton. Mar. Ecol. Progr. Ser., 144, 265-283.

Martin-Jézequel V., M. Hildebrand and M.A. Brzezinski (2000) Silicon metabolism in diatoms : implications for growth. J. Phycology, 36, 821-840.

Menden-Deuer S. and E.J. Lessard (2000) Carbon to volume relationships for dinoflagellates, diatoms, and other protist plankton. Limnol. Oceanogr., 45, 569-579.

Muylaert K., R. Gonzales, M. Franck, M. Lionard, C. van der Zee, A. Cattrijsse, K. Sabbe, L. Chou and W. Vyverman (2006) Spatial variation in phytoplankton dynamics in the Belgian coastal zone of the North Sea studied by microscopy, HPLC-CHEMTAX and underway fluorescence recordings. J. Sea Res., 55, 253-265.

Muylaert K., K. Sabbe and W. Vyverman (2000) Spatial and temporal dynamics of phytoplankton communities in a freshwater tidal estuary (Schelde, Belgium). Estuarine Coastal Shelf Sci., 50, 673-687.

Muylaert K., M. Tackx and W. Vyverman (2005) Phytoplankton growth rates in the freshwater tidal reaches of the Schelde estuary (Belgium) estimated using a simple light-limited primary production model. Hydrobiologia, 540, 127-140.

Muylaert K., A. Van Kerkvoorde, W. Vyverman and K. Sabbe (1997) Structural characteristics of phytoplankton assemblages in tidal and non-tidal freshwater systems: a case-study from the Schelde basin. Freshw. Biol., 38, 263-276.

Muylaert K., J. Van Wichelen, K. Sabbe, and W. Vyverman (2001) Effects of freshets on phytoplankton dynamics in a freshwater tidal estuary (Schelde, Belgium). Arch. Hydrobiol., 150, 269-288.

Partheniades E. (1962) A study of erosion and deposition of cohesive soils in salt water. Ph.D. thesis, University of California.

Plettinck S., L. Chou and R. Wollast (1994) Kinetics and mechanisms of dissolution of silica at room temperature and pressure. Mineralogical Magazine, 58A, 728-729.

Philippart C.J.M., G.C. Cadée, W. Van Raaphorst and R. Riegman (2000) Long-term phytoplankton-nutrient interactions in a shallow coastal sea: algal community structure, nutrient budgets, and denitrification potential. Limnol. Oceanogr., 45, 131–144.

Ragueneau O., P. Tréguer, A. Leynaert, R.F. Anderson, M.A. Brzezinski, D.J. DeMaster, R.C. Dugdale, J. Dymond, G. Fischer, R. Francois, C. Heinze, E. Maier-Reimer, V. Martin-Jézéquel, D. M. Nelson and B. Quéguiner (2000) A review of the Si cycle in the modern ocean: recent progress and missing gaps in the application of biogenic opal as a paleoproductivity proxy. Glob. Planet. Change, 26, 317-365.

Ragueneau O., N. Savoye, Y. Del Amo, J. Cotten, B. Tardiveau, and A. Leynaert (2005) A new method for the measurement of biogenic silica in suspended matter of coastal waters: using Si:Al ratios to correct for the mineral interference. Cont. Shelf Res., 25, 697-710.

Redfield A.C, B.H. Ketchum and F.A. Richards (1963) The influence of organisms on the composition of sea water. In: The Sea, M.N. Hill ed., Vol. 2, pp. 26-77. Interscience, N.Y.

Regnier P., A. Mouchet, R. Wollast and F. Ronday (1998) A discussion of methods for estimating residual fluxes in strong tidal estuaries. Continental Shelf Research, 18, 1543–1571.

Regnier P. and C. I. Steefel (1999) A high resolution estimate of the inorganic nitrogen flux from the Scheldt estuary to the coastal North Sea during a nitrogen-limited algal bloom, spring 1995. Geochimica et Cosmochimica Acta, 63(9), 1359–1374.

Regnier P., R. Wollast and C.I. Steefel (1997) Long-term fluxes of reactive species in macrotidal estuaries: Estimates from a fully transient, multicomponent reaction-transport model. Mar. Chem., 58, 127-145.

Rousseau V., A. Leynaert, N. Daoud, and C. Lancelot (2002) Diatom succession, silification and silicic acid availability in Belgian coastal waters (Southern North Sea). Marine Ecology Progress Series, 236, 61-73.

Schoemann V., S. Becquevort, J.Stefels, V.Rousseau and C. Lancelot (2005) Phaeocystis blooms in the global ocean and their controlling mechanisms: a review. J. Sea Res., 53, 43–66.

Sicko-Goad L.M., C.L. Schelske and E.F. Stoermer (1984) Estimation of intracellular carbon and silica content of diatoms from natural assemblages using morphometric techniques. Limnol. Oceanogr., 29, 1170-1178.

Smeteck V. (1998) Diatoms and the silicate factor. Nature, 391, 224-225.

Soetaert K., and P. M. J. Herman. 1995. Estimating estuarine residence times in the Westerschelde (The Netherlands) using a box model with fixed dispersion coefficients. Hydrobiologia, 311, 215-224.

Soetaert K., P.M.J. Herman and J. Kromkamp (1994) living in the twilight - estimating net phytoplankton growth in the Westerschelde estuary (The Netherlands) by means of an ecosystem model (MOSES). J. Plankton Res., 16, 1277-1301.

Soetaert K., M. Hoffmann, P. Meire, M. Starink, D. van Oevelen, S. Van Regenmortel and T. Cox (2004) Modeling growth and carbon allocation in two reed beds (Phragmites australis) in the Scheldt estuary. Aquat. Bot., 79, 211-234.

Soetaert K., J.J. Middelburg, C. Heip, P. Meire, S. Van Damme and T. Maris (2006) Long-term change in dissolved inorganic nutrients in the heterotrophic Scheldt estuary (Belgium, The Netherlands). Limnol. Oceanogr., 51, 409-423.

Struyf E., A. Dausse, S. Van Damme, K. Bal, B. Gribsholt, H.T.S. Boschker, J.J. Middelburg and P. Meire (2006) Tidal marshes and biogenic silica recycling at the land-sea interface. Limnol. Oceanogr., 51, 838-846.

Thompson P. (1999). Response of growth and biochemical composition to variations in daylenght, temperature, and irradiance in the marine diatom Thalassiosira pseudonana (Bacillariophyceae). J. Phycology, 35, 1215-1222.

Tréguer P. and P. Pondaven (2000) Global change silica control of carbon dioxide. Nature, 406, 358 359.

Van Damme S., E. Struyf, T. Maris, T. Ysebaert, F. Dehairs, M. Tackx, C. Heip, and P. Meire (2005) Spatial and temporal patterns of water quality along the estuarine salinity gradient of the Scheldt estuary (Belgium and The Netherlands): results of an integrated monitoring approach. Hydrobiologia, 540, 29-45.

Van der Zee C. and L. Chou (2005) Seasonal cycling of phosphorus in the Southern Bight of the North Sea. Biogeosciences, 2, 27-42.

Van Maldegem D.C., H.P.J. Mulder and A. Langerak (1993) A cohesive sediment balance for the Scheldt Estuary. Neth. J. Aquat. Ecol., 27, 247-256.

Vanderborght J.-P., R. Wollast, M. Loijens and P. Regnier (2002) Application of a transport-reaction model to the estimation of biogas fluxes in the Scheldt estuary. Biogeochemistry, 59, 207–237.

Vanderborght J.-P., I. Folmer, D.R. Aguilera, T. Uhrenholdt and P. Regnier (2007) Reactive-transport modelling of a river-estuarine-coastal zone system: application to the Scheldt estuary. Marine Chemistry, 106, 92-110.

Wirtz K.W. (1997) Modellierung von Anpassungsvorgängen in der belebten Natur. Ph.D. thesis, Universität Kassel.

Wirtz K.W. and B. Eckhardt (1996) Effective variables in ecosystem models with an application to phytoplankton succession. Ecological Modelling, 92, 33–53.

Wollast R. (1988) The Schelt estuary. In: Pollution of the North Sea: An Assessment. W. Salomon, B. Bayne, E.K. Duursma and U. Forstner (Eds.), pp. 183-193, Springer Verlag, Berlin.

Wollast R. and R.M. Garrels (1971) Diffusion coefficient of silica in seawater. Nature (Phys; Sci.), 229, 94.

Wright S.W., S.W. Jeffrey, R.F.C. Mantoura, C.A. Llewellyn, T. Bjornland, D. Repeat and N. Welshmeyer (1991) Improved HPLC method for the analysis of chlorophylls and carotenoids from marine phytoplankton. Mar. Ecol. Progr. Ser., 77, 183-196.